THESIS APPROVAL

GRADUATE SCHOOL, KASETSART UNIVERSITY

Master of Science (Chemistry)
DEGREE

Chemistry   Chemistry
FIELD   **DEPARTMENT**

TITLE: Magnetic and Mechanical Properites of Barium Ferrite-Natural Rubber Composites

NAME: Miss Lalita Kantiyong

THIS THESIS HAS BEEN ACCEPTED BY

_____ **THESIS ADVISOR**
(Assistant Professor Wirunya Keawwattana, Ph.D.   )

_____ **THESIS CO-ADVISOR**
(Assistant Professor Nattamon Koonsaeng, Ph.D.   )

_____ **THESIS CO-ADVISOR**
(Mr. Pongsakorn Jantaratana, Ph.D.   )

_____ **DEPARTMENT HEAD**
(Assistant Professor Noojaree Prasitpan, Ph.D.   )

APPROVED BY THE GRADUATE SCHOOL ON _____

_____ **DEAN**
(Associate Professor Gunjana Theeragool, D.Agr.   )

THESIS

MAGNETIC AND MECHANICAL PROPERTIES OF BARIUM
FERRITE-NATURAL RUBBER COMPOSITES

LALITA KANTIYONG

A Thesis Submitted in Partial Fulfillment of
the Requirements for the Degree of
Master of Science (Chemistry)
Graduate School, Kasetsart University
2009

Lalita Kantiyong 2009: Magnetic and Mechanical Properties of Barium
Ferrite-Natural Rubber Composites. Master of Science (Chemistry), Major
Field: Chemistry, Department of Chemistry. Thesis Advisor: Assistant
Professor Wirunya Keawwattana, Ph.D. 118 pages.

Barium ferrites ($BaFe_{12}O_{19}$) have been synthesized using the Oxide One Pot
Process (OOPS). These precursors were calcined at 600, 800, 1000 and 1200 ^{o} C for
2 hrs, during which time the precursor that calcined at 1000 ^{o} C was found both
hematite and hexagonal ferrite whereas the precursor calcined at 1200 ^{o} C was
transformed to the hexagonal ferrite. With increasing the calcination time of
precursors calcined at 1000 ^{o} C from 2 to 8 hrs, the ones calcined for 8 hrs became
hexagonal ferrite phase with high purity, resulting in high magnetic properties,
including the coercivity (H_c), saturation magnetization (M_s) and magnetic Remanence
(M_r). The effect of barium ferrite (commercial grade) on the cure characteristics,
mechanical and magnetic properties of RFCs was investigated. Commercial
hexagonal barium ferrite was incorporated with various loading in the natural rubber
matrix to produce rubber ferrite composites (RFCs). Tensile strength increased up to
100 phr and then decreased. Modulus and hardness increased, while elongation at
break decreased gradually with increasing barium ferrite loading. SEM was used to
determine the dispersion of filler in rubber matrix, the fine dispersion of barium ferrite
particles in the rubber matrix can be observed. The magnetic properties of these
composites were studied using a VSM at room temperature (25 ^{o} C). The results show
that the H_c of the composites increased with increasing filler content up to 140 phr.
Comparison of the magnetic and mechanical properties between RFCs with
commercial barium ferrite and barium ferrite synthesized by OOPS was undertaken.
RFCs with synthesized barium ferrite showed lower tensile properties and hardness,
while greater magnetic properties than those of RFCs with commercial barium ferrite.
The addition of 30 phr carbon black into RFCs improve mechanical properties was
conducted

| | | ___ / ___ / ___ |
| Student's signature | Thesis Advisor's signature | |

ACKNOWLEDGEMENTS

Lalita Kantiyong

April 2009

TABLE OF CONTENTS

Page

LIST OF TABLES

LIST OF TABLES (Continued)

Appendix Table

LIST OF FIGURES

LIST OF FIGURES (Continued)

LIST OF FIGURES (Continued)

LIST OF ABBREVIATIONS

BET   =   Brunauer-Emmett-Teller

CB   =   Carbon Black

FTIR   =   Fourier transform infrared spectroscopy

MDR   =   Moving-Die Rheometer

MPa   =   Mega Pascal

NR   =   Natural rubber

OOPS   =   Oxide One Pot Synthesized

phr   =   parts per hundred of rubber (resin)

RFC   =   Rubber Ferrite Composite

TMQ   =   2,2,4-trimethyl-1,2-dihydroquinoline

MAGNETIC AND MECHANICAL PROPERTIES OF BARIUM FERRITE-NATURAL RUBBER COMPOSITES

INTRODUCTION

Ferrites are ferromagnetic materials containing predominantly oxides of iron along with other oxides of barium, strontium, manganese, nickel, zinc, lithium and cadmium. Ferrites are ideally suited for making device like inductor cores, circulators, memory devices and also for various microwave application. Although the saturation magnetization of ferrites is less than that of ferromagnetic alloys, they have advantages such as applicability at higher frequency, lower price and greater electrical resistance. Ferrites are classified into two groups, namely magnetically soft and hard. Furthermore, depending on their crystal symmetry, they may be cubic, hexagonal or orthorhombic. Barium ferrites belong to the class of hexagonal ferrite. They are normally prepared by using ceramic technique. The methods comprised solid-solid reaction, co-precipitation and sol–gel combustion. Recently, the Oxide One Pot Synthesis (OOPS) process was successfully used to prepare the barium ferrite powder. This method also offers an easy, inexpensive, straightforward alternative to solid-solid reaction, co-precipitation and other chemical techniques of ceramics processing, and retains the advantages of purity, homogeneity, and low processing temperature.

Natural rubber (NR) is an unsaturated elastomer characterized by its crystallinity and has some good properties, such as high strength, hot tear resistance, retention of strength at elevated temperature, excellent dynamic properties and general fatigue resistance. However, NR is very sensitive to heat and oxidation because of the double bonds in its chain as shown in Scheme 1. Furthermore, NR can be vulcanized with sulfur compounds, which can crosslink the chain because of the presence of the reactive double bonds, so it has accounted for its use in many applications. The incorporation of magnetic fillers with NR leads to the formation of a composite with improvement mechanical, magnetic and electrical properties.

The development of natural rubber with hexagonal barium ferrite powders showing in Figure 1 has become an important material because of its potential novel applications as the media for magnetic and magneto-optical recording and for microwave devices, in addition to a wide range of applications and large amount of production as permanent magnets.

The hexaferrites, namely barium ferrite ($BaFe_{12}O_{19}$) has low cost and the excellent chemical stability make ferrite one of the important magnetic materials that cannot be easily replaced. Ferrites are usually employed in the ceramic form, and one of the drawbacks is that they are not flexible or moldable to complex shapes. It is well known that the incorporation of magnetic ferrites in various elastometer matrixes produces flexible magnets or elastomer magnets, known as Rubber Ferrite Composites (RFCs) as shown in Figure 2.

Figure 1 Barium ferrite powders: $BaFe_{12}O_{19}$

Figure 2 Elastomer magnet or Rubber Ferrite Composites (RFCs)

The advantages of Rubber Ferrite Composite include low weight and cost, resistance to corrosion, ease of machining and forming, and capability of high production rates. Each materials has unique properties that make it more suitable from selected applications than other magnet and mechanical option such as, magnetic strength, resistance to demagnetization, density, physical strength and flexibility. The impregnation of magnetic fillers in the matrix imparts magnetic properties and modifies the physical properties of the matrix considerably.

In this work, an attempt has been made for magnetic application in the form of a barium ferrite with natural rubber composite. Barium ferrite powders were synthesized by OOPS method in order to replace the commercial barium ferrite that import from aboard and our aim is produce Rubber Ferrite Composites having low weight, low cost, highly flexible bonded magnet and suitable stored energy, which is one of the most important magnetic properties of the composite. This will be achieved by selecting the recipe and high coercivity fillers with a low surface energy. It is reported in this article some magnetic and mechanical properties of RFCs, and it is expected the good magnetic properties and high mechanical properties for many applications, such as microwave absorbers, other electronic devices and anisotropic rubber magnet that influence the value of natural rubber.

OBJECTIVES

1. Study the effect of commercial barium ferrite loading on the magnetic and mechanical properties of RFCs.

2. Investigate the influence of calcined temperature of synthesized barium ferrite on the mechanical and magnetic properties of the composite materials.

3. Compare the mechanical and magnetic properties of RFCs filled with commercial and synthesized barium ferrites.

LITERATURE REVIEW

1. Natural Rubber (NR)

1.1 Introduction of natural rubber

Natural rubber (NR) is a polymer of isoprene. About 95% of isoprene production is used to produce cis-1,4-polyisoprene with a molecular weight of 100,000 to 1,000,000 as shown in Figure 1. Typically, a few percent of other materials, such as proteins, fatty acids, resins and inorganic materials are found in high quality natural rubber. Some natural rubber sources called gutta percha are composed of trans-1,4-polyisoprene, a structural isomer which has similar, but not identical properties. However, NR is very sensitive to heat and oxidation because of the double bonds in its chain as shown in Figure 1 (Jame *et al.*, 1994). Furthermore, NR is vulcanized with sulfur compounds, which can crosslink the chain because of the presence of the reactive double bonds. It has strain induced crystallization at low temperature that behave high strength, hot tear resistance, retention of strength at elevated temperature, excellent dynamic properties and general fatigue resistance (Morton., 1987), so it has accounted for its use in many applications.
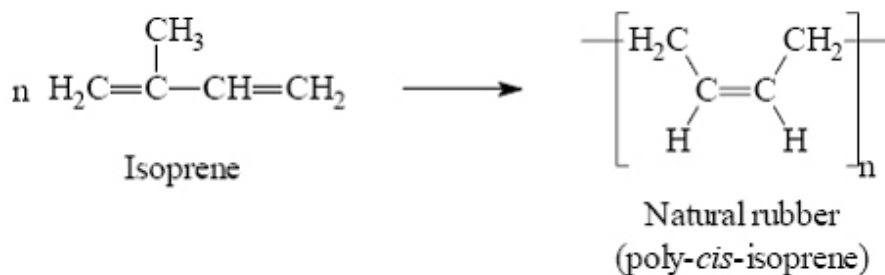
Figure 3 The structure of cis- 1,4 polyisoprene

1.2 Properties of natural rubber

Strength

The strength of a material refers to the material's ability to resist an applied force. Strength is considered in terms of compressive strength, tensile strength, and shear strength, respectively. The effects of dynamic loading is probably the most important practical part of the strength of materials. Natural rubber is well-known for the strength properties of its vulcanizates. The tensile strength of gum vulcanizates range from 17 to 24 MPa while those black filled vulcanizates range from 24 to 32 MPa. Strength can also be characterized as tear resistance, in both of which natural rubber is excellent. This high strength of natural rubber is certainly due to its ability to undergo strain-induced crystallization. The strength drops rapidly with increase in temperature but is still better than other elastomers.

Elongation at break

The elongation recorded at the moment of rupture of the specimen, often expressed as a percentage of the original length. It corresponds to the breaking or maximum load. The ultimate elongation depends, naturally, on the nature and amount of fillers in the compound, and on the degree of vulcanization. In general, it is about 500 to 1,000% or even greater.

Abrasion or wear resistance

Natural rubber has excellent abrasion resistance, especially under mild abrasive conditions. Below about 35 $^{\circ}$ C, natural rubber shows better wear than styrene butadiene rubber (SBR), while above 35 $^{\circ}$ C, SBR is better.

Dynamic properties

Natural rubber has high resilience, with values exceeding 90% in well cured gum vulcanizates. At large strain, the fatigue life of natural rubber is superior to that of SBR, there reverse is true for small strains. Good resistance to flexing and fatigue together with high resilience makes natural rubber useful in applications where cyclic stressing is involved.

Compression set

At ambient and slightly elevated temperature, the compression set of NR vulcanizates is relatively low. At lower temperatures the compression set appear to be poor. Heat resistance of NR vulcanizate has detrimental effect on the compression set.

Aging resistance

Natural rubber vulcanizates can be given adequate heating-aging resistance by suitable of vulcanization system and by use of amine or phenolic antioxidants. The heat-aging resistance of NR vulcanizates is insufficient for many technical applications.

2. Vulcanization

Vulcanization is generally applied to rubber or elastic materials. These materials forcibly retract to their approximately original shape after a rather large mechanically imposed deformation. Vulcanization can be defined as a process which increases the retractile force and reduces the amount of permanent deformation remaining after removal of the deforming force. Thus, vulcanization increases elasticity while it decreases plasticity. It is generally accomplished by the formation of a crosslinked molecular network (Jame et al., 1994).

According to the theory of rubber elasticity, the retractile force to resist a deformation is proportional to the number of network-supporting polymer chains per unit volume of elastomer. A supporting polymer chain is a linear polymer molecular segment between network junctures. An increase in the number of junctures or crosslinks give an increases in the number of supporting chains. In an unvulcanized linear high polymer (above its melting point) only molecular chain entanglements constitute junctures.

Vulcanization is a process of chemically producing network junctures by the insertion of crosslinks between polymer chains (Akiba *et al.*, 1997). The crosslink may be a group of sulfur atoms in a short chain, a single sulfur atom, carbon to carbon bond, a polyvalent organic radical, an inorganic cluster, or a polyvalent metal ion. The process is usually carried out by heating the rubber (mixed with vulcanizing agents) in a mold under pressure.

Usually, the actual chemical cross-linking is done with sulfur, but there are other technologies, including peroxide-based systems. The combined cure package in a typical rubber compound comprises the cure agent itself, (sulfur or peroxide), together with accelerators, activators like zinc oxide and stearic acid and antidegradants. Prevention of vulcanization starting too early is done by addition of retarding agents. Antidegradants are used to prevent degradation by heat, oxygen and ozone.
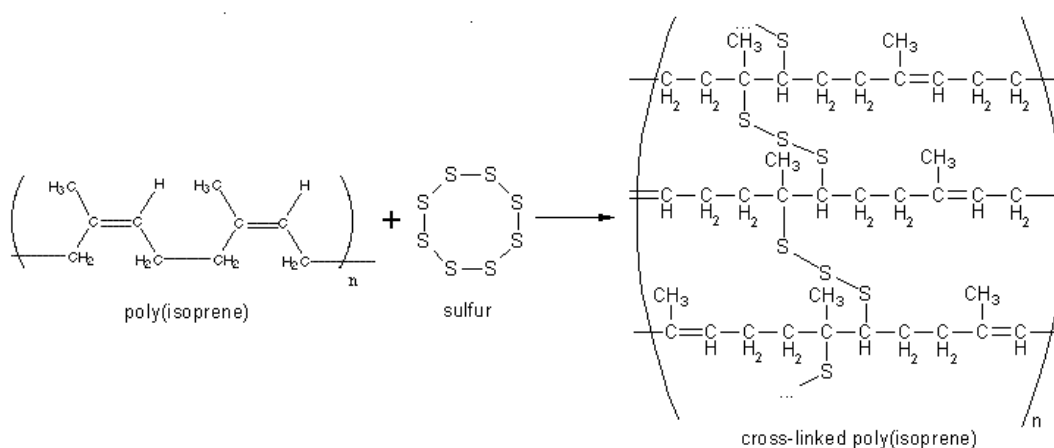
Figure 4 Sulfur vulcanization of polyisoprene

Along the rubber molecule, there are a number of sites which are attractive to sulfur atoms. These are called cure sites, and are generally sites with an unsaturated carbon-carbon bond, like in polyisoprene (Figure 3), the basic material of natural rubber. The active sites are allylic hydrogen atoms; that means they are hydrogen atoms connected to the first saturated carbon atom connected to the carbon-carbon double bond. During vulcanization the eight-membered ring of sulfur breaks down in smaller parts with one to eight sulfur atoms. These small sulfur chains are quite reactive. At each cure site on the rubber molecule, such short sulfur chain can attach itself, and eventually reacts with a cure site of another rubber molecule, and so forming a bond between two chains. These sulfur bridges are typically between two and eight atoms long. The number of sulfur atoms in a sulfur crosslink has a strong influence on the physical properties of the final rubber article. Short sulfur crosslinks, with just one or two sulfur atoms in the crosslink, give the rubber a very good heat resistance. Crosslinks with higher number of sulfur atoms, up to six or seven, give the rubber very good dynamic properties but with lesser heat resistance. Dynamic properties are important for flexing movements of the rubber article, e.g., the movement of a side-wall of a running tire. Without good flexing properties these movements will rapidly lead to formation of cracks and, ultimately, to failure of the rubber article.

2.1 Effects of vulcanization on vulcanizates properties.

At the molecular level, vulcanization causes profound chemical changes. The long rubber molecules usually between 100,000 to 500,000 which become linked together with crosslinks spaced along the polymeric chains. As a result of this network information, the rubber becomes essentially insoluble in any solvent and it cannot be processed by any means which requires it to flow in a mixer, an extruder, a mill, calender or during shaping, forming or molding. Thus, it is essential that vulcanization occur only after the rubber article is in its final form.

Uncured natural rubber is sticky and can easily deform when warm, and is brittle when cold. In this state it cannot be used to make article with a good level of elasticity. The reason of unvulcanized rubber can be found in the chemical nature which made of long polymer chains. These polymer chains can move independently relative to each other, and this will result in a change of shape. Vulcanization is a chemical process performed on rubber to strengthen it by causing polymer molecules to interlink with other polymer molecules. The vulcanized rubber is harder, more durable, and more resistant to chemicals and other damage. The surface becomes smoother and less likely to stick to metal or plastic. Rubber being vulcanized is usually exposed to sulfur or peroxide for curing; the sulfur atoms are released, and grow "bridges" from rubber molecule to rubber molecule, creating a tight network throughout the rubber structure. The resulting chemical reaction is irreversible, and the compounds created are thermoset, they do not melt on heating, unlike other thermoplastics (Hoffman *et al.,* 1965).

In order for a rubbery polymer to attain an effectively high elastic state, it is necessary to lightly crosslink the highly flexible polymer molecules to prevent them from slipping past each other on application of a stress. In the rubber industry this process is known as 'vulcanization'. Vulcanization increases the retractile force and reduces the amount of permanent deformation remaining after removal of the deforming force by the insertion of crosslinks between polymer chains forming a crosslinked molecular network. The crosslink may be a group of sulfur atoms in a

short chain, a single sulfur atom, carbon-to-carbon bond, a polyvalent organic radical, an ionic cluster, or a polyvalent metal ion. The process is usually carried out by heating the rubber (mixed with vulcanizing agents) in a mold under pressure.

More effect of vulcanization on use related properties are studied on the idealization. The dynamic modulus is a composite of viscous and elastic behavior, whereas modulus is largely a measure of only the elastic component of rheological behavior. Hysteresis is reduced with increasing crosslink formation. Hysteresis is the ratio of the rate-independent or viscous component to the elastic component of deformation resistance. It is also a measure of deformation energy which is not stored or borne by the elastic network but which is converted to heat. Vulcanization then cause the trade-off of elasticity for viscous or plastic behavior. Tear strength, fatigue life and toughness are related to the breaking energy. Values of these properties increase with small amounts of crosslinking but they are reduced by further crosslink formation. Properties related to the energy-to-break increase with increasing in both the number of network chain and hysteresis. When the hysteresis decreases as more network chains are developed, the energy-to-break related properties are maximized at some intermediate crosslink density.

Reversion is a general term that applied to the loss network structures by thermal aging. It is usually associated with isoprene rubbers vulcanized by sulfur. It can be the result of too long vulcanized time (post cure) or hot aging of thick section. It is almost severe at temperatures above about $155\,^{\circ}$ C. It occurs in vulcanizates containing a large number of polysulfidic crosslinks. Though its mechanism is complex, a good deal about the chemical changes which occur during the reversion of natural rubber has been deduced.

2.2 Vulcanization by sulfur without accelerator

Generally, vulcanization was accomplished by using sulfur at 8 part per hundred parts of rubber (phr). It requires 5 hours at 140 $^\circ$ C. The addition of zinc oxide reduced the time to 3 hours. The use of accelerators in concentration as low as 0.5 phr has since reduced the time to as short as $1 - 3$ minutes. As a result, elastomer vulcanization by sulfur without accelerator is no longer of much commercial significance. The chemistry of unaccelerated vulcanization is controversial. Many slow reactions occur over the long period of vulcanization. A proposed mechanism involving free radicals is given in Figure 5.
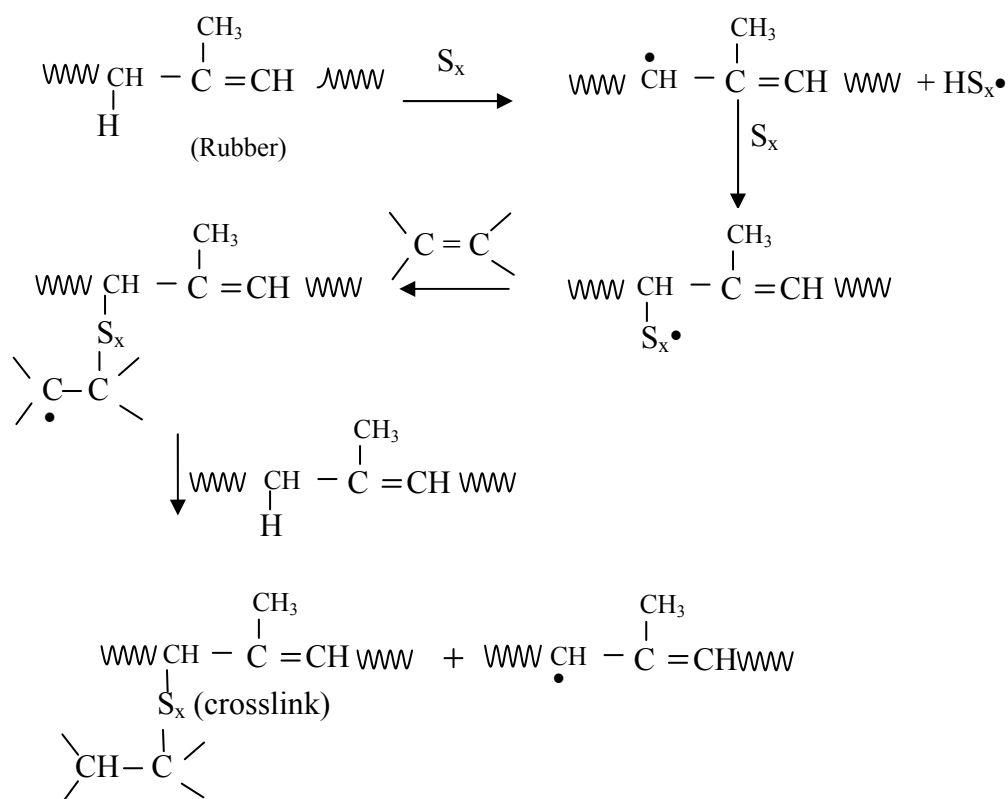
Figure 5 Unaccelerated vulcanization by sulfur, free radical mechanism

2.2.1 Metal Oxides

Carboxylated nitrile, butadiene, and styrene - butadiene rubbers may be crosslinked by the reaction of zinc oxide with the carboxylated groups on the polymer chains. This involves the formation of zinc salts. Other metal oxides are also capable of reacting in the same manner

In case of neoprenes, the double bond is 'hindered' by the neighbouring chlorine atoms, and so vulcanization with sulfur is not possible.

Neoprenes are generally vulcanized by reaction with metal oxides; zinc oxide is generally used along with magnesium oxide. Neoprenes can be vulcanized in the presence of zinc oxide alone; however, magnesium oxide is necessary to give scorch resistance. The reaction is supposed to involve the allylic chlorine atom (active chlorine) which is the result of the allylic shift of chlorine atom occurring during small amount of 1,2 polymerization. Figure 6 is given for the vulcanization of neoprene rubber by the action of zinc oxide and magnesium oxide.
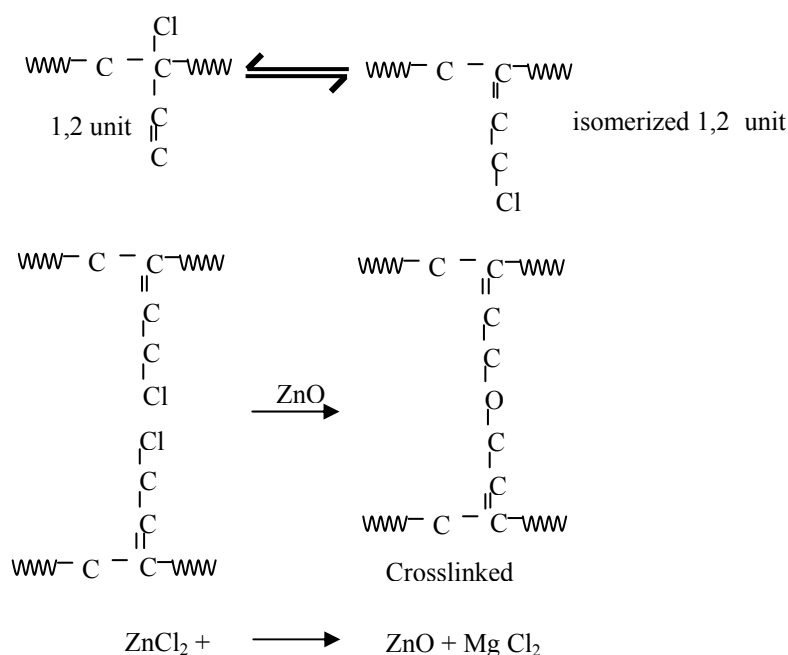
Figure 6 Mechanism of crosslinking of neoprenes by the action of metal oxide

2.3 Accelerated – sulfur vulcanization

Accelerated- sulfur formulation is the most common vulcanization system used in commercial and industrial application. Elemental sulfur is the predominant vulcanizing agent for general-purpose rubbers. It is used in combination with one or more accelerators and an activator system comprising zinc oxide and stearic acid. The most popular accelerators are delayed-action sulfenamides, thiazoles, thiuram sulfides, dithocarbamates and guanidines which are shown in Table 1. The accelerator determines the rate of vulcanization, whereas the accelerator to sulfur ratio dictates the efficiency of vulcanization.

Accelerator are grouped as follows:

1. Inorganic compounds (mainly metal oxides): Include zinc oxide, hydrated lime, litharge, red lead, white lead, magnesium oxide. Zinc oxide is the most common and is generally used in combination with a fatty acid to form a rubber soluble soap in the rubber matrix. The majority of metal oxide are used in coated or treated forms in order to disperse more readily in the rubber mixtures. Normal use level is 2 to 5 phr.

2. Organic acids: Normally used in combination with metal oxides such as zinc oxide; they are generally monobasic fatty acids or mixtures of the types, stearic, oleic, lauric, palmitic and myristic acids, and hydrogeneated oils from palm, castor, fish, and linseed oils. The usage of each particular type depends on the accelerator used and the amounts of compounding ingredients present. Normal use level is 1 to 3 phr.

It is believed that fatty acids with zinc oxide (or other metal oxides) give a salt that form intermediate complexes with the accelerators. The complex thus formed is more effective in activating the sulfur present in the mixture, thus increasing the reaction rate.

The reduction in the amount of time required for vulcanization is generally accomplished by changing the amounts and types of accelerators used. There are some common practice used by rubber compounders to arrive at suitable recipes for specific applications:

1. Single accelerator systems (primary accelerators) which are of sufficient activity to produce satisfactory cures within specified time.

2. Combinations of two or more accelertors, consisting of the primary accelerator which is used in the largest amount, and the secondary accelerator which is used in smaller amounts (10-20 % of the total) in order to activate and improve the properties of the vulcanizate. Combinations of this type usually produce a synergistic effect as the final properties are somewhat better than those produced by either accelerator separately. For example, when a mixture of a benzothiazole with smaller amounts of a dithiocarbamate or thiuram or amine is used, each accelerator activates the other and high crosslinking rates can be obtained.

3. Delayed action accelerators, not affected by processing temperatures (thus providing some protection against scorching) but produce satisfactory cures at ordinary vulcanization temperatures.

Table 1 Several common accelerators used in sulfur vulcanization

Compound	Abbreviation	Structure
Benzothiazoles		
2-Mercaptobenzothiazole	MBT	
2-2'-Dithiobisbenzothiazole	MBTS	
Benzothiazolesulfenamides		
N-Cyclohexylbenzothiazole-2-sulfenamide	CBS	
N-t-Butylbenzothiazole-2-sulfenamide	TBBS	
2- Morpholinothiobenzothiazole	MBS	
N-Dicyclohexabenzothiazole-2-sulfenamide	DCBS	
Dithiocarbamates		
Tetramethylthiuram monosulfide	TMTM	
Tetramethylthiuram disulfide	TMTD	
Zinc diethyldithiocarbamate	ZDEC	
Amines		
Diphenylguanidine	DPG	
Di-o-tolylguanidine	DOTG	

Source: Jame *et al.* (1994)

Table 2 Classe of accelerators used in sulfur vulcanization

Classe of accelerators	Compound	Speed of vulcanisation
Guanidines	DPG, DOTG	Medium
Thiazoles	MBT, MBTS	Semi-fast
Sulfenamides	CBS, TBBS, MBS	Fast, delayed action
Thiurams	TMTD, TETD, TMTM	Very fast
Dithiocarbamates	ZDMC, ZDEC	Super fast

2.3.1 The sulfur vulcanization system can be classified into three types (Hoffman *et al.,* 1965).

Conventional vulcanization (CV)

In rubber an accelerator to sulfur ratio typically of 1: 5 is called a conventional vulcanizing system and it gives a network in which about 20 sulfur atoms are combined with the rubber for each inserted chemical crosslink. Most of the crosslinks are polysulfidic (ie. with a bridge of not less than three sulfur atoms) and a high proportion of the sulfur is in the form of cyclic sulfide main chain modifications. This combination provides good mechanical properties and excellent low temperature resistance, but polysulfidic crosslinks are thermally unstable and reversion can occur at high vulcanizing temperatures and high service temperatures.

Efficient vulcanization (EV)

An accelerator to sulfur ratio of 5: 1 is typical of an efficient vulcanizing (EV) system where no more than 4 - 5 sulfur atoms are combined with the rubber for each chemical crosslink. Most of the crosslinks at optimum cure are monosulfidic or disulfidic and only a relatively small proportion of the sulfur is wasted in main chain modifications. This combination provides very much enhanced

heat stability and oxidation resistance, however, have a poor resistance to fatigue because of the presence of predominantly monosulfidic and disulfidic crosslinks.

Semi-efficient vulcanization (semi-EV)

An intermediate accelerator to sulphur ratio of 1: 1 is typical of a semi-efficient vulcanizing (semi-EV) system and provides properties between those of conventional and EV systems that are comprised between resistance to oxidation and required product fatigue performance because of the presence of predominantly disulfidic crosslinks.
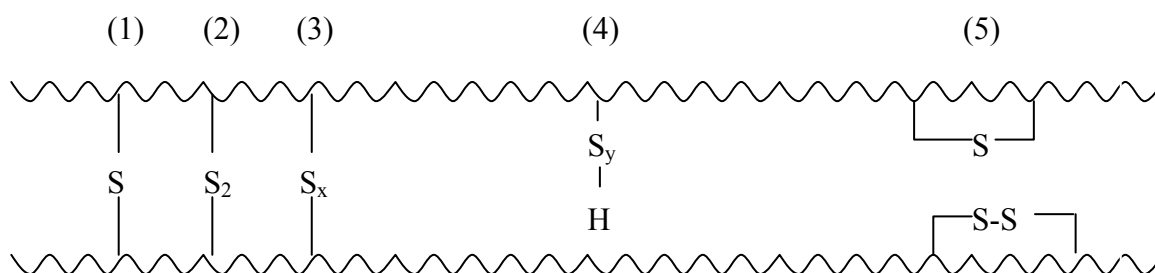
Figure 7 Different crosslink structures: (1) monosulfidic, (2) disulfidic,
 (3) polysulfidic, when $x \geq 3$, (4) thiol gruops, (5) cyclic sulfur structures

2.4 Cure time

Many of these substances, particularly rubbers and some high viscosity polymeric elastomers, are difficult to measure in conventional rheometers because of their high viscosity and the promotion of cross-linking, often through vulcanization, during processing at higher temperatures. After vulcanization, the viscoelastic mixture is converted to an elastic material, whose properties include high resistance to deformation and strength. These substances must be properly characteristic to ensure that they are not over-or under-processed.

The main equipment for assessing these properties in the rubber sector are the Mooney viscometer, the Oscillating Disc Rheometer (ODR) and the Moving Die Rheometer (MDR).

The ODR (Figure 8) is an oscillatory rheometer, consisting of an oscillating disc, enclosed in an unsealed, stationary cavity. The disc oscillates at a fixed frequency and amplitude (generally determined by international testing standards) and operates in the same range of temperatures and pressure as the Mooney viscometer.
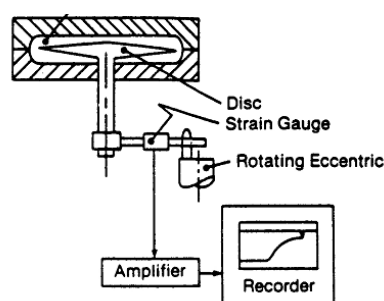
Figure 8 Oscillating disk rheometer

Vulcanization is measured by the increase in the torque required to maintain given amplitude (e.g. degree of arc) of oscillation at a given temperature. The torque is proportional to a low-strain modulus of elasticity. Since this torque is measured at the elevated temperature of vulcanization, the portion of it due to viscous effects is minimal. Thus, it has been assumed that the increase in torque unit volume of rubber, while the torque is automatically plotted against time to give a so-called rheometer chart, rheograph, or cure curve as shown in Figure 9.

The MDR which is a current generation cure-meter and is suitable for the rubber and elastomer industries. It helps overcome problems of thermal inertia, which has dogged the ODR. The MDR may be automated if necessary and continued use of volumetrically consistent samples, and good handling procedures, ensure repeatability.

MDR has a cavity rather than an internally oscillating fixture, which is filled with sample and enclosed by a biconical die. The sample is much smaller and heat transfer is faster. Also, because there is no rotor, the temperature of the cavity and sample can be changed more rapidly.
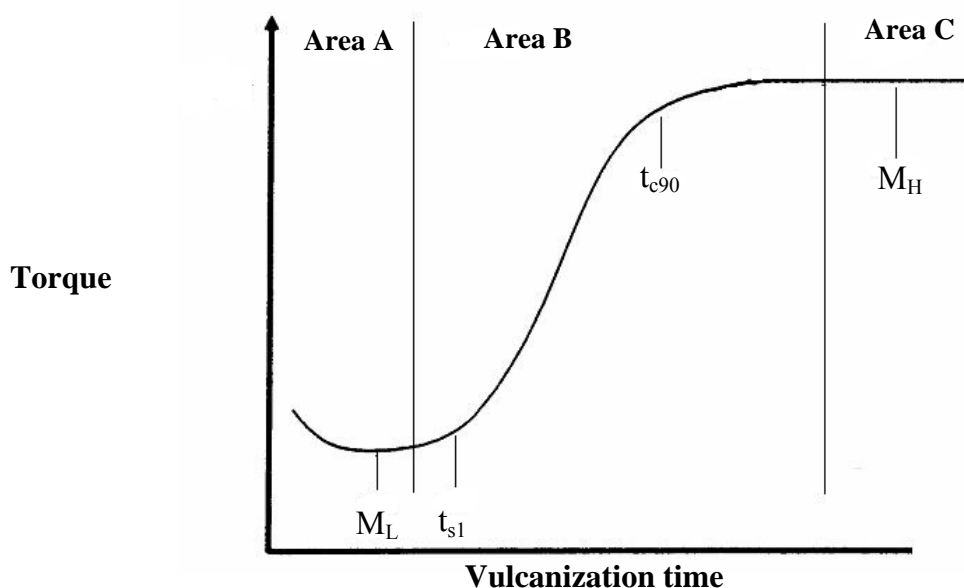
Figure 9 Rheometer cure curve

The measurements which can be made from this curve and the term used to describe them are:

Table 3 The measurement parameter of Rheometer cure curve

Parameter	Explanation
Area A	This gives an indication of compound viscosity before curing.
Area B	This indicates the rate of cure of the compound.
Area C	This indicates the state of cure of the vulcanizate.

Table 3 (continued)

Parameter	Explanation
t_{s1}	Time for torque to increase 1 dn.m (0.1 N.m) or 1 lb_f-in above M_L - a measure of scorch time or processing safety, some laboratories use t_{s2} (i.e., time for torque to increase 2 dN.m or 2 lb_f-in above M_L) instead of t_{s1}.
t_{c90}	Time needed for rubber compounds to reach maximum viscosity or elastic modulus at a given temperature. Cure time is conventionally considered complete at 90 percent of maximum torque.
M_L	Minimum torque - A measure of the viscosity of the uncured compound
M_H	Maximum torque - A measure of cure state during the specific period of time where no returning of cure, maximum torque can be related to vulcanizate modulus and hardness.
M_H-M_L	The difference between the maximum and the minimum torque, related to the crosslink density of the material although further detail for the evaluation will be given.

Note: t_{c50}, t_{c90} - Time for torque to reach M_L + 0.5 (M_H-M_L) or M_L + 0.9 (M_H-M_L)

3. Fillers

Fillers are used for improved materials that satify increasingly stringent requirement such as higher strength, modulus, thermal, electrical and magnetic properties, flame retardant, etc. For the manufacturers, fillers have been used for cheap diluents or additives. The fillers are classified as reinforcing filler and non-reinforcing (Harry *et al,*. 1987).

In spite of the fact that filler characteristic might be best in filler if one could control its properties completely is worthy of consideration. For the good ideal of filler should include in the following.

1. Low cost
2. Availability
3. Low oil absorption
4. Good surface wetting bonding
5. Good chemical resistance
6. High strength

The use of fillers in rubber is almost as old as the use of rubber itself. It has been observed since long that incorporation of particulate fillers such as carbon black increases the strength of vulcanized rubbers significantly, even more than tenfold by reinforcing it. Thus it is hardly surprising that relatively few applications of elastomers use the polymer in the unfilled state.

Reinforcement has been defined as the incorporation of small particles of materials, known as fillers, into rubber which improves the modulus and failure properties (tensile strength, tear resistance and abrasion resistance) of the final vulcanizate. In general, when a reinforcing agent is added to a base pure gum recipe, that agent imparts greater stiffness and higher ultimate tensile strength than would be obtained by using an equal volume of a common filler, e.g. coarse particle size whiting. The usual quantities of these materials are 10-50 parts per 100 parts by volume of rubber (Lee *et al.,* 2000).

The degree of reinforcement provided by a filler depends on a number of variables, the most important of which is the development of a large polymer-filler interface which can be furnished only by the particles of colloidal dimensions. Spherical particles 1 μm in diameter have a specific surface area of 6 m^2/cm^3. This constitutes roughly the lower limit of significant reinforcement. The upper limit of useful specific surface area is of the order of 300-400 m^2/cm^3, and is set by the

considerations of dispersibility, processability of the unvulcanized mix, and serious loss of rubbery characteristics of the composites. In general, the finer reinforcing agents require more energy for their dispersion into rubber and the plasticity of the resultant mix is lower. Therefore, it is more difficult to process in operations following mixing. This effect of reinforcing agents on the properties of the rubber - filler mixture is of great practical significance and, for the manufacture of some products, it may be a more important factor in the selection of reinforcing agents than their effect on the vulcanizate properties.
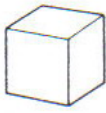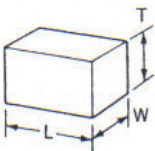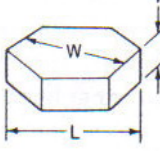
3.1 Principles of filler selection and use

Parameters affecting the performance of polymer or rubber composites functional filler are related to: the characteristics of the filler itself, including its geometry (particle shape, particle size and particle distribution, aspect ratio) its surface area and porosity affect to physical, mechanical, chemical, thermal, optical, electrical and magnetic properties or the other properties that dealing with specific fillers and surface modifiers, Harry *et al*., (1987) and Lee *et al*., (2000).

3.1.1 particle size and particle shape

Filler selection is primarily determined by the particle size distribution and the particle shapes which the particles pack together. This is fundamentally true whether or not a particular class of filler is indicated because of a systemic requirement such as electrical properties. A general classification of filler particles is presented in Figure 10. The classes are some what arbitrary, being based on the primary properties of particle size and surface area, both of which are directly measurable and serve as a basis for systematizing filler functions. There are many types of fillers that contain variously shaped particles having greater surface area to equivalent spherical diameter (esd) ratios than those indicated in Figure 12. An example of heterogeneity is shown in Figure 11, where is the smallest (thickness) to largest (diameter) dimensions of kaolinite were obtained by microscopic methods. It may be seen that at about 13 μm esd, the particles are stacks of bound platelets equal

in two dimensions. In effect then, the shapes of most real particles are too variable to be dealt with directly. Taken together, particle size and surface area provide the only means for classification of particles and their effects in composites (Xanthos *et al.*, 2005).

Particle Class	Sphere	Cube	Block	Flake	Fiber
Descriptor[a]	spheroidal[b]	cubic[c] prismatic rhombohedral	tabular prismatic pinacoid irregular	platy flaky[d]	acicular elongated fibrous
Shape ratios; length (L)	1	~1	1.4–4	1	1
width (W)	1	~1	1	<1	<1/10
thickness (T)	1	~1	1–<1	$\frac{1}{4}$–1/100	<1/10
Sedimentation diameter[e]	1	esd	esd	esd[f]	esd[f]
Surface area equivalence[g]	1	1.24[h]	1.26–1.5[i]	1.5–9.9[j]	1.87 for 1/10 2.3 for 1/20[k]
Examples	glass spheres microspheres	calcite[l] feldspar	calcite feldspar silica barite nephelite	kaolin mica talc graphite hydrous alumina	wollastonite tremolite wood flour

Figure 10 Particle characteristics

[a]Preferred to particle class since this is based on relative surface area. First descriptor
[b]In the sense that a spheroid approaches a true sphere.
[c]Generally distorted cubes; more nearly prismatic.
[d]Generally having the nature of hexagonal platelets, as illustrated.
[e]According to Stokes' law, esd = equivalent spherical diameter or the diameter of a sphere having the same volume as that of the particle.
[f]Must be modified for dissymmetry of greater than 4-1, maximum to minimum particle dimensions

[g]Equivalent to a spherical diameter of 1; an approximation of the area when the particle has a volume equivalent to an esd of 1

[h]About the same for cubic and prismatic shapes.

[i]For lengths of 1.4-4, respectively.

[j]Based on hexagonal platelets as follows:

length/thickness	area factor
4/1	1.47
6/1	1.78
8/1	2.09
10/1	2.34
100/1	9.88

[k]For a square cross-section

[l]There are more than 300 crystal shapes for calcite alone, but generally it is an irregular, low surface area particle

Diameter to thickness ratios
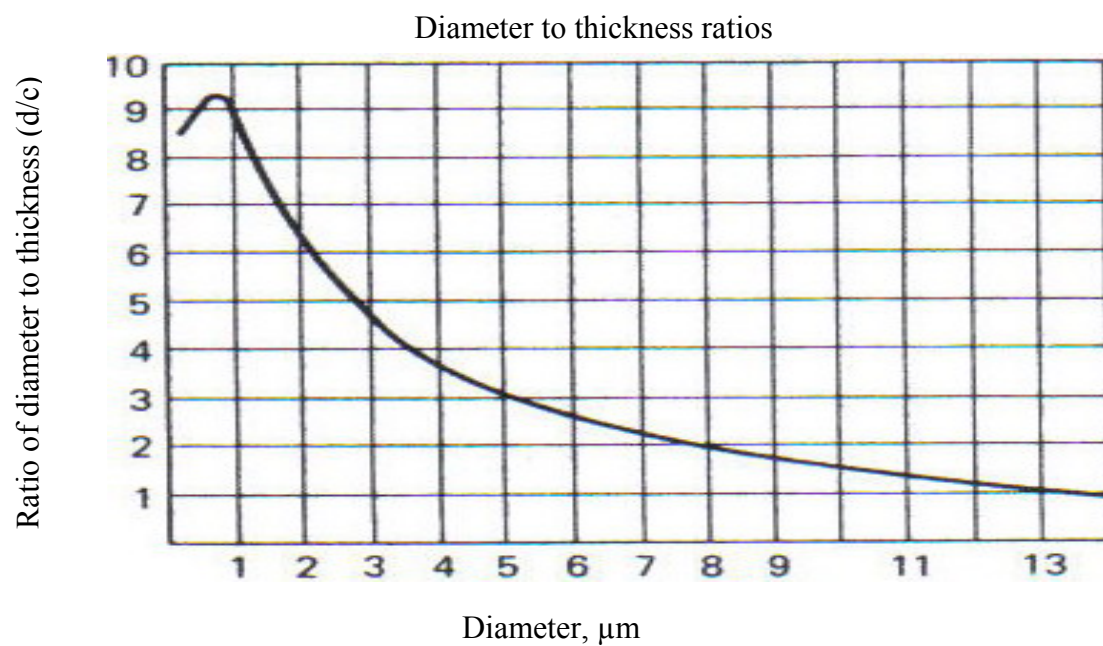
Figure 11 Comparison of diameter (largest dimension) to thickness (smallest dimension) of Kaolinite particle

3.1.2 Particle size distribution

Figure 12 illustrates the most common method of particle size graphing that describes a single species, because all particles have essentially the same density, the percent finer by weight and redundant volume are equal. Although a filler of very broad distribution was chosen and values approach zero, it is a common failing of supplier's literature that the entire distribution is not reported. It will be emphasized later that these missing data do not allow adequate assessment of the particle size distribution for surface area, packing values, and the true nature of the distribution.
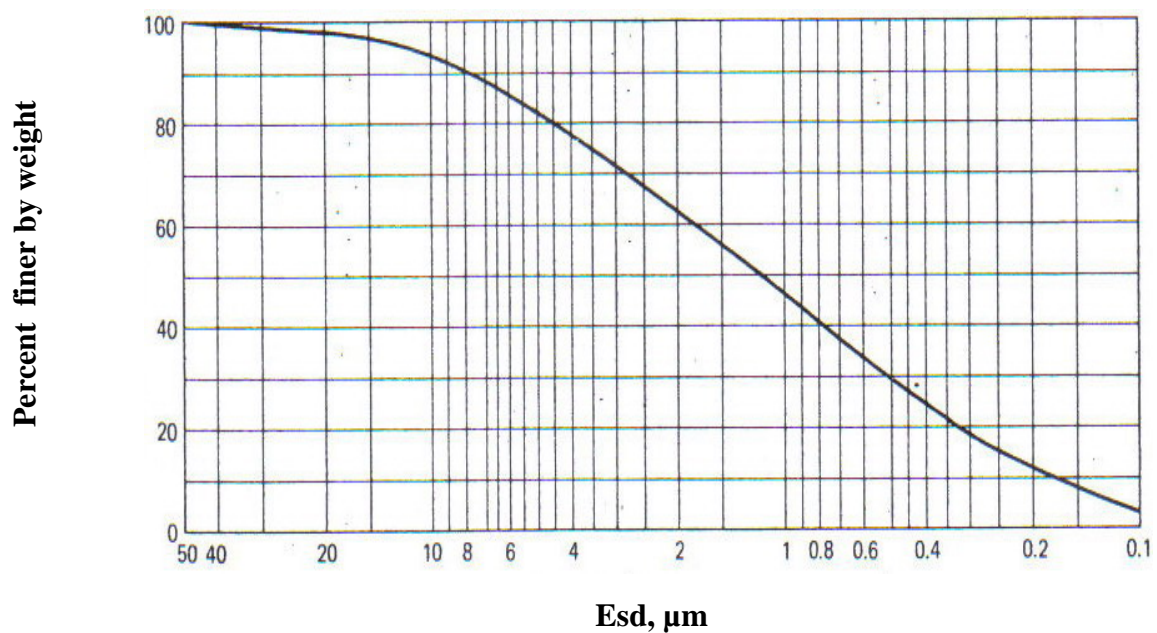
Figure 12 Particle size distribution of Huber 65A kaolin, semilog graph

3.1.3 Surface area

Surface area is one of the most important of filler properties. Surface area is generally the inverse of particle size. Many effects of fillers are surface-area-dependent, particularly where surfactants, dispersants, surfier, polar polymers, and so forth, are adsorbed or reacted with the filler surfaces. Fillers that have a high surface area have more contact area available, and therefore have a higher potential to reinforce the rubber chains. The chemistry and physics of solid surfaces are highly complex. Similar esd particle size distribution gives no indication of filler surface without considering shape factors.

3.1.4 Surface activity

A filler can offer high surface area and high structure, but still provide relatively poor reinforcement if it has low specific surface activity. The specific activity of the filler surface per cm^2 of filler-elastomer interface is determined by the physical and chemical nature of the filler surface in relation to that of the elastomer. Nonpolar fillers are best suited to nonpolar; polar fillers work best in polar elastomer. Beyond this general chemical compatibility is the potential for reaction between the elastomer and active sites on the filler surfaces.

3.1.5 Structure

The shape of an individual particle of reinforcing filler (e.g. carbon black or precipitated silica) is of less importance than the filler's effective shape once dispersed in elastomer. The blacks and precipitated inorganics used for reinforcement have generally round primary particles but function as anisometric acicular aggregates. The round particles clump together into chains or bundles that can be very dense or open and latticelike. These aggregate properties (shape, density, size) define their structure. High structure filler has aggregates favoring high particle count, with those particles jointed in chain-like clusters from which random branching of additional particle chains may occur. The more an aggregate deviates from a solid

spherical shape and the larger its size, the higher is its structure. The higher its structure, in turn, the greater its reinforce potential. For reinforcing fillers which exist as aggregates rather than discreet particles, a certain amount of structure that existed at manufacture is lost after compounding. The high shear forces encountered in rubber milling will break down the weaker aggregates and agglomerates of aggregates. The structure that exists in the rubber compound, the persistent structure, is what affects processability and properties.

3.2 Chemical composition

Chemical composition, a primary property of fillers, is an essential consideration for their use in many systems. As all reactivities proceed from the surface of the filler, it is easy to be misled by apparent equivalence. For example, all silicates contain silica and might be considered to have equivalent good acid and poor alkali resistance. This is not the case, as chemical composition does not indicate the relative positions of modifying elements in the crystal lattice or at the surface of the particle. Crystal structure and bond strength relationship are dealt with by Pauling.

3.3 Reinforcing fillers

The most common reinforcing fillers are carbon blacks and silicates. Silicates, clays, whiting (calcium carbonate) and other mineral fillers are used extensively where a high degree of reinforcement is not required. Carbon blacks represent the most important class of reinforcing fillers, both in tonnage and in variety of properties.

3.3.1   Carbon black

As has already been mentioned, carbon blacks constitute the most important class of reinforcing fillers for rubbers. They are prepared by incomplete combustion of hydrocarbons or by thermal cracking. Most of the carbon blacks used today is made by oil furnace process. In the thermal process, oil, or more

frequently, natural gas is cracked at 1300°C in absence of oxygen in a hot refractory surface. The recovery is about 40% - 50% of the available carbon and blacks thus obtained range in particle diameter from 120 nm to 500 nm. The five most important properties of carbon black are: (1) particle size, (2) structure, (3) physical nature of the surface, (4) chemical nature of surface and (5) particle porosity.

3.3.1.1 Particle Size

The particles of carbon black are not discrete but are fused "clusters" of individual particles. The fusion is especially pronounced with very fine carbon blacks. However, the reinforcement imparted by the black is not influenced by the size of the clusters but greatly by the size of the particles within it.

3.3.1.2 Structure

The term "structure" refers to the joining together of carbon particles into long chains and tangled three-dimensional aggregates. This aggregation of the particles takes place in the flame during carbon black manufacture. By virtue of their irregular morphology, the aggregates are bulky, and occupy an effective volume considerably larger than that of the carbon itself. 'High structure' refers to a high degree of bulkiness, manifested in low bulk density and a high capacity to absorb oil. In rubber technology it is customary to associate high structure of filler with high modulus of vulcanizate. The morphology of reinforcing silicas is similar to that of carbon blacks, except that fusion tends to be more extensive with precipitated silica. Clays and other mineral fillers exhibit essentially no structure in the sense considered here.

3.3.1.3 Physical nature of particle surface

The carbon atoms in a carbon black particle are present in layer planes which the layers are highly oriented. They are mainly parallel to the surface, have regular spacing and are quite large with very few defects in their network structure. On the contrary, blacks with high reinforcing potential, show less crystallite orientation (Godin *et al.,* 2009). Their particles are more irregular in shape, the layers are much smaller, less frequently parallel and have more defect; this may indicate the presence of significant amounts of 'non-graphitic' carbon.

It is possible that the nature of the carbon atoms at the surface of a particle may affect rubber reinforcement. The carbon atoms can be relatively un-reactive if they are an integral part of the layer plane, more reactive if attached to a hydrogen atom, and very reactive if present as a resonance stabilized free radical.

3.3.1.4 Chemical nature of particle surface

Carbon blacks consist of 90%-99% elemental carbon. The other major constituents are (combined) hydrogen and oxygen. The hydrogen comes from original hydrocarbon and is distributed throughout the carbon black particles, oxygen is confined to the surface as shown in Figure 13. The principal groups present are, phenolic, ketonic and carboxylic together with lactones which are chemically combined.
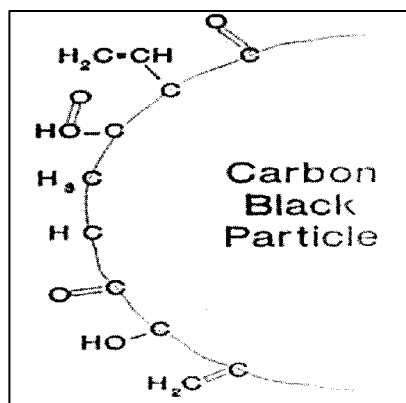
Figure 13 Chemical function on carbon black surface

3.3.1.5 Particle porosity

The surface of carbon black particles are not smooth owing to the attack on them by high-temperature oxidizing gases immediately after their formation. Oxidation takes place at the 'non-graphitic' atoms and can progress into the particle to give pores.

3.4 non reinforceing filler property

3.4.1 Optical

Color is an obvious property of fillers, but it is frequently misunderstood. The color of a dry powder is usually evaluated by pressing a disc shaped compact and obtained a reflectance value at a particular wavelength of light on the flat surface. When the full spectrum of visible light is used for the evaluation, subtle differences in the true color of the particles can be determined by calculation or by inspection of the reflectance graph, although such data are influenced by particle. Particles reflect, refract, or bend light according to their sizes.

3.4.2 Thermal

Thermochemical effects are of particular importance to fillers. Flammability of fillers is limited to organic types, with graphite again an exception for having oxidative stability to $1000\,^{\circ}C$. Hydrated alumina, which is actually aluminum hydroxide, begins to lose significant amounts of hydroxide, water at $230\,^{\circ}C$, continuing to do so endothermically until a total 35 % water loss at $900\,^{\circ}C$. Hydrous silicate filler also release hydroxyls as water, but at much higher temperatures. Limestone fillers liberate carbon dioxide beginning at about $900\,^{\circ}C$, and continuing at that temperature to leave a residue of calcium oxide or lime. Aluminum pigments will burn, and other metallic fillers are effective thermal conductors to promote heating and decomposition of plastics.

3.4.3 Physical

Density is the most important physical property of fillers because it affects the economics of composites. Densities for solid fillers vary from organics to metals in ascending order. Porous or cellular fillers fall into the lowest density range, depending on the voids contained in the fabricated part.

3.4.4 Electrical

It is necessary to consider the fundamental nature of filler particles in the absence of water when electrical properties are concerned. Virtually every surface at ambient conditions has a condensed layer of water molecules upon it, which are more or less tightly bonded depending on the nature of the surface. For the reason, the electrical properties of fillers may differ considerably on a fundamental versus a practical basis. As a generally valid statement, all metallic bonds produce excellent electrical conductivity, whereas ionic and covalent bonds produce nonconductors. Some materials have mixed bonds, ionic and metallic, and are semiconductors. Fillers having hydroxyl surfaces, adsorbed free ions, mixed

contaminants of polyvalent metal compounds, free salts, water, and water soluble matter all provide surface conductive paths for electricity.

3.3 Filler effects

Main effects of filler characterized on vulcanizate properties. Although rubber properties are interconnected and relate to the combination of all filler properties, a brief summary of the main influence of each of the four filler characteristics is given below:

1. Smaller particle size (larger external surface area) results in higher tensile strength, higher hysteresis, higher abrasion resistance, higher electrical conductivity and higher mooney viscosity, with minor effects on extrusion shrinkage and modulus (Lee *et al*., 2000).

2. An increase in surface activity (physical adsorption) results in modulus at the higher strain ($\geq 300\%$), higher abrasion resistance, higher adsorption properties, higher 'bound rubber' (discussed later) and lower hysteresis.

3. An increase in persistent structure (bulkiness) results in lower extrusion shrinkage, higher modulus at low and medium strains (upto 300%), higher mooney viscosity, higher hysteresis and longer incorporation time. Higher electrical conductivity and heat conductivity are found for higher structure blacks. This property is interrelated with surface activity, structure changes on fillers without surface activity (graphitized black) showing the effects indicated above only rather faintly. At constant high activity, the structure effects are most pronounced.

4. Porosity results in higher viscosity and higher electrical conductivity in the case of carbon blacks.

4. **Magnetic Material**

4.1 Types of magnetism

All magnetic materials contain magnetic moments, which behave in a way similar to microscopic bar magnetism. In order to define a ferromagnetism as a class of magnetism, it is easiest to compare the various properties of different possible types of magnetic material (Jung, n.d.). These are principally: dimagnetism, paramagnetism, ferromagnetism, antiferromagnetism and ferrimagnetism.

4.1.1 Diamangnetism

Diamagnetism is a very weak form of magnetism that is only exhibited in the presence of an external magnetic field. It is the result of changes in the orbital motion of electrons due to the external magnetic field. The induced magnetic moment is very small and in a direction opposite to that of the applied field. When placed between the poles of a strong electromagnet, diamagnetic materials are attracted towards regions where the magnetic field is weak. Diamagnetism is found in all materials; however, because it is so weak it can only be observed in materials that do not exhibit other forms of magnetism. Also, diamagnetism is found in elements with paired electrons. Oxygen was once thought to be diamagnetic, but a new revised molecular orbital (MO) model confirmed oxygen's paramagnetic nature.

Superconductors are perfect diamagnets that usually happens at lowered temperatures and when placed in an external magnetic field expel the field lines from their interiors (depending on field intensity and temperature). Superconductors also have zero electrical resistance, a consequence of their diamagnetism. Superconducting structures have been known to tear themselves apart with astonishing force in their attempt to escape an external field. Superconducting magnets are the major component of most magnetic resonance imaging systems, perhaps the only important application of diamagnetism. Diamagnetic materials have

a relative magnetic permeability that is less than 1, and a magnetic susceptibility that
is less than 0.

4.1.2 Paramagnetism

In a paramagnet, the magnetic moments tend to be randomly
orientated due to thermal fluctuations when there is no magnetic field. In an applied
magnetic field these moments start to align parallel to the field such that the
magnetization of the material is proportional to the applied field.
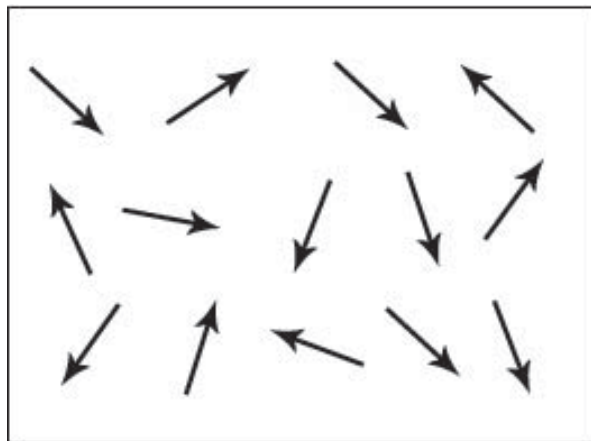
Figure 14 Schematic showing the magnetic dipole moments randomly aligned
in a paramagnetic sample.

Paramagnetism is a type of magnetism that occurs in substances
with a positive magnetic susceptibility. It results in these substances being weakly
attracted by a strong magnet. Paramagnetism is caused by the presence of at least one
unpaired electron orbital (i.e., an unpaired spin) in the atoms, molecules, or ions of the
paramagnetic material, which results in these particles having a dipole moment. An
applied magnetic field tends to align these dipoles in such a way that for small field
and high temperatures the induced field is proportional to the applied field; the
magnetization is in the same direction as the applied field. Paramagnetism is
normally stronger than diamagnetism, and the effect varies inversely with

temperature. Below the Curie temperature, certain paramagnetic materials exhibit ferromagnetism. Examples of paramagnetic materials at room temperature include aluminum (Al), manganese (Mn), platinum (Pt), oxygen (gas and liquid), and rare earth ions.

4.1.3 Superparamagnetism

There are materials that show induced magnetic behavior that follows a Curie type law but with exceptionally large values for the Curie constants. These materials are known as superparamagnets. They are characterized by a strong ferromagnetic or ferrimagnetic type of coupling into domains of a limited size that behave independently from one another. The bulk properties of such a system resembles that of a paramagnet, but on a microsopic level they are ordered. The materials do show an ordering temperature above which the behavior reverts to ordinary paramagnetism (with interaction). Ferrofluids are a good example, but the phenomenon can also occur inside solids, e.g. when dilute paramagnetic centers are introduced in a strong itinerant medium of ferromagnetic coupling such as when Fe is substituted in $TlCu_2Se_2$ or the alloy AuFe. Such systems contain ferromagnetically coupled clusters that freeze out at lower temperatures. A superparamagnetic material is composed of small ferromagnetic clusters (e.g. crystallites), but where the clusters are so small that they can randomly flip direction under thermal fluctuations. As a result, the material as a whole is not magnetized except in an externally applied magnetic field in that respect, it is like paramagnetism.

4.1.4 Ferromagnetism

The magnetic moments in a ferromagnet have the tendency to become aligned parallel to each other under the influence of a magnetic field. However, unlike the moments in a paramagnet, these moments will then remain parallel when a magnetic field is not applied (this will be discussed later). In a ferromagnet, they tend to align in the same direction because of the Pauli principle: two electrons with the same spin state cannot lie at the same position, and thus feel an

effective additional repulsion that lowers their electrostatic energy. This difference in energy is called the exchange energy and induces nearby electrons to align. At long distances (after many thousands of ions), the exchange energy advantage is overtaken by the classical tendency of dipoles to anti-align (Brannen *et al.*, 2006).
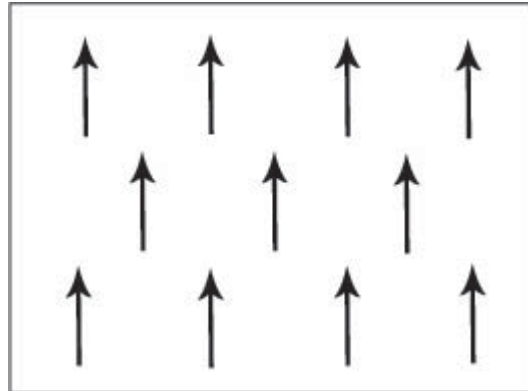
Figure 15 Schematic showing the magnetic dipole moments aligned parallel in a
            ferromagnetic material.

The net magnetization can be destroyed by heating and then cooling (annealing) the material without an external field. As the temperature increases, thermal oscillation, or entropy, competes with the ferromagnetic tendency for dipoles to align. When the temperature rises beyond a certain point, called the Curie temperature, there is a second-order phase transition and the system can no longer maintain a spontaneous magnetization, although it still responds paramagnetically to an external field. Below that temperature, there is a spontaneous symmetry breaking and random domains form (in the absence of an external field). The Curie temperature itself is a critical point, where the magnetic susceptibility is theoretically infinite and, although there is no net magnetization, domain-like spin correlations fluctuate at all lengthscales.

4.1.5 Antiferromagnetism

Adjacent magnetic moments from the magnetic ions tend to align anti-parallel to each other without an applied field. In the simplest case, adjacent magnetic moments are equal in magnitude and opposite therefore there is no overall magnetisation.
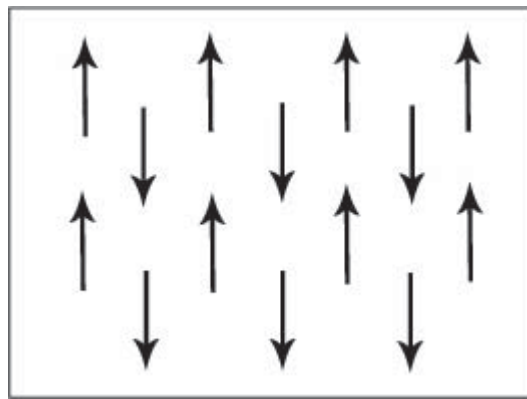
Figure 16 Schematic showing adjacent magnetic dipole moments with equal magnitude aligned anti-parallel in an antiferromagnetic material. This is only one of many possible antiferromagnetic arrangements of magnetic moments.

In materials that exhibit antiferromagnetism, the spins of magnetic electrons align in a regular pattern with neighboring spins pointing in opposite directions. This is the opposite of ferromagnetism. Generally, antiferromagnetic materials exhibit antiferromagnetism at a low temperature, and become disordered above a certain temperature; the transition temperature is called the Neel temperature. Above the Neel temperature, the material is typically paramagnetic. The antiferromagnetic behaviour at low temperature usually results in diamagnetic properties, but can sometimes display ferrimagnetic behaviour, which in many physically observable properties is more similar to ferromagnetic interactions. The magnetic susceptibility of an antiferromagnetic material will appear to go through a maximum as the temperature is lowered, in contrast, that of a paramagnet will

continually increase with decreasing temperature. Antiferromagnetic materials are relatively uncommon. An example is the heavy-fermion superconductor URu_2Si_2. More everyday examples include metals such as chromium, alloys such as Iron Manganese (FeMn), and oxides such as Nickel Oxide (El-Nashr *et al*., 2006). Antiferromagnets can also couple to ferromagnetic materials through a mechanism known as exchange anisotropy, in which the ferromagnetic film is either grown upon the antiferromagnet or annealed in an aligning magnetic field, causing the surface atoms of the ferromagnet to align with the surface atoms of the antiferromagnet.

4.1.6 Ferrimagnetism

The aligned magnetic moments are not of the same size; that is to say there is more than one type of magnetic ion. An overall magnetisation is produced but not all the magnetic moments may give a positive contribution to the overall magnetisation.
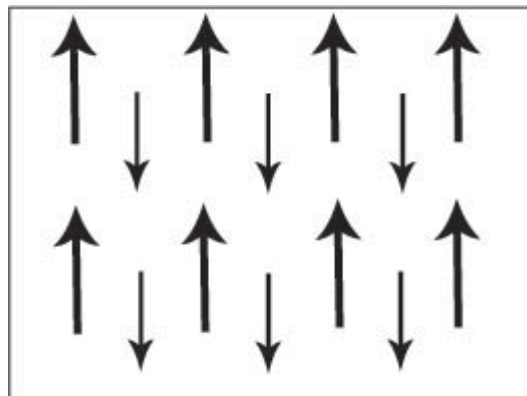
Figure 17 Schematic showing adjacent magnetic moments of different magnitudes aligned anti-parallel.

In physics, a ferrimagnetic material is one in which the magnetic moment of the atoms on different sublattices are opposed, as in antiferromagnetism; however, in ferrimagnetic materials, the opposing moments are unequal and a

spontaneous magnetization remains. This happens when the sublattices consist of different materials or ions (such as Fe^{2+} and Fe^{3+}). Ferrimagnetic materials are like ferromagnets in that they hold a spontaneous magnetization below the Curie temperature, and show no magnetic order (are paramagnetic) above this temperature. However, there is sometimes a temperature below the Curie temperature at which the two sublattices have equal moments, resulting in a net magnetic moment of zero; this is called the magnetization compensation point. This compensation point is observed easily in garnets and rare earth - transition metal alloys (RE-TM). Furthermore, ferrimagnets may also exhibit an angular momentum compensation point at which the angular momentum of the magnetic sublattices is compensated. This compensation point is a crucial point for achieving high speed magnetization reversal in magnetic memory devices. Ferrimagnetism is exhibited by ferrites and magnetic garnets. The oldest-known magnetic substance, magnetite (iron(II,III) oxide; Fe_3O_4), is a ferrimagnet. Some ferrimagnetic materials are YIG (yttrium iron garnet) and ferrites composed of iron oxides and other elements such as aluminum, cobalt, nickel, manganese and zinc.

Ferrimagnetic materials have high resistivity and have anisotropic properties. The anisotropy is actually induced by an external applied field. When this applied field aligns with the magnetic dipoles it causes a net magnetic dipole moment and causes the magnetic dipoles to precess at a frequency controlled by the applied field, called Larmor or precession frequency. As a particular example, a microwave signal circularly polarized in the same direction as this precession strongly interacts with the magnetic dipole moments; when it is polarized in the opposite direction theinteraction is very low. When the interaction is strong the microwave signal can pass through the material. This directional property is used in the construction of microwave devices like isolators, circulators and gyrators. Ferrimagnetic materials are also used to produce optical isolators and circulator.

The most important category for magnetic applications are ceramic hard ferrite, $BaO_6(Fe_2O_3)$ or $SrO_6(Fe_2O_3)$, and ceramic soft ferrite, $MOFe_2O_3$, where M is a metal such as Ni, Fe, Mn, Mg or Zn (Kingery *et al.*, 1975).

4.2 Hysteresis Loop

Hysteresis is well known in ferromagnetic materials (Sung *et al.*, n.d.). When an external magnetic field is applied to a ferromagnet, the atomic dipoles align themselves with the external field. Even when the external field is removed. A part of the alignment will be retained, so the material has become magnetized. The relationship between magnetic field strength (H) and magnetic flux density (B) is not linear in such materials that shows in Figure18 (b). The relationship between the two is plotted for increasing levels of field strength, it will follow a curve up to a point where further increases in magnetic field strength will result in no further change in flux density. This condition is called magnetic saturation.

(a)

(b)
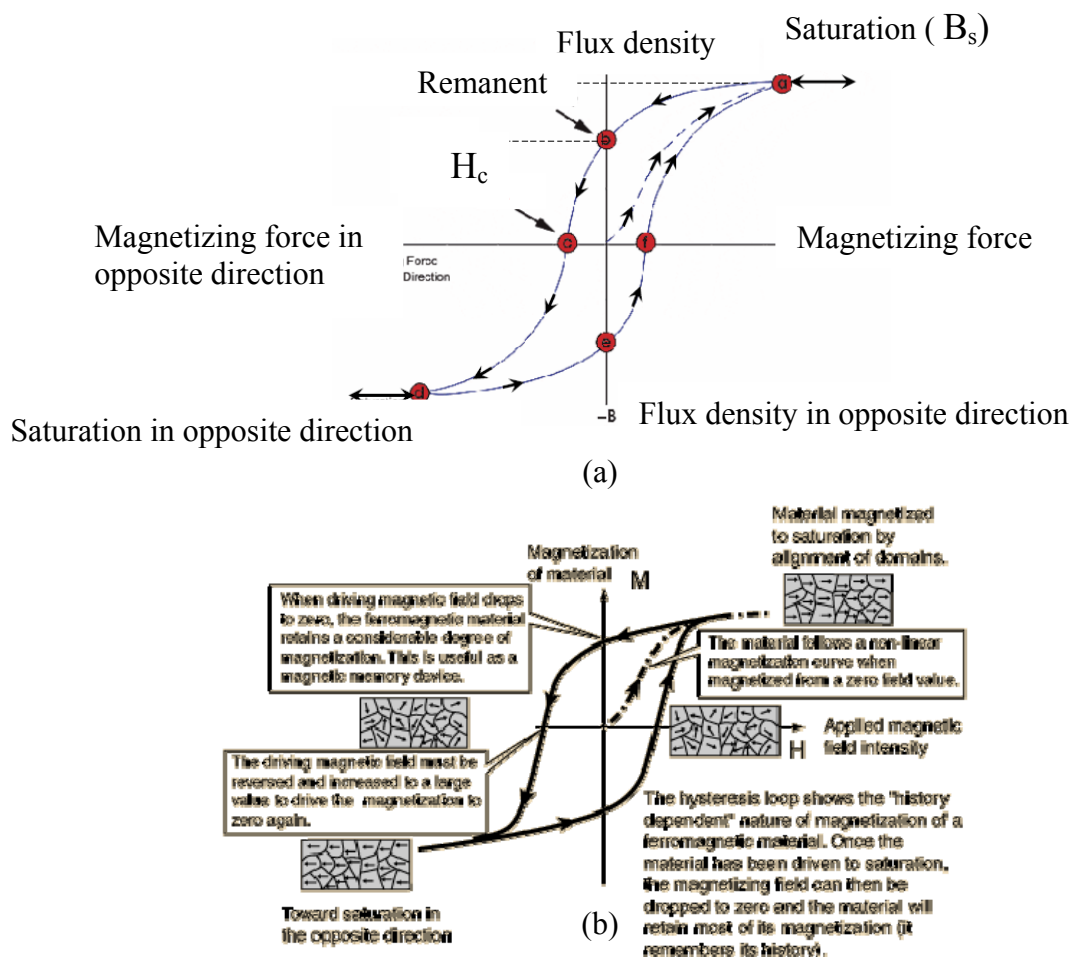
Figure 18 Hysteresis loop for a solenoid's ferromagnetic core

From figure 18 (a) represent the hysteresis loop of magnetism material the point magnetizing force (H =0), that a magnetic material is not magnetised. As the current in the coil is increases, magnetizing force (H) also increases until the material is saturated at point (a) that material has reached saturation and Magnetic flux density can not increase any more. When the material start to reduce the current in the coil so that we can demagnetise the material, as stated before the graph will not following the same path it did when the current increased but instead goes from point a, through point b then down to point (c).

At point (b), H=0, therefore the current has reached zero but there is still some remanant flux density so that the material is still partially magnetised. The current is now reversed so that H is in the opposite direction. When the current is increased, the value of H reduces and then H has a negative value at point (c). At point c the material is finally demagnetised and the value of H at this point is called the coercive force.

The hysteresis loop that was shown in Figure 18 (a) The material saturates so that the magnetic poles of the domains face in the opposite direction to those at point (b). The reversed current is now reduced and reaches zero at the point (f) however, once again, some flux remains. If the current is now increased in the original direction all the flux has gone at point (g) and saturation is reached once more at point (b).

4.3 Permanent magnets

The general classification of ferromagnetic materials, according to IEC standards, is based on the coercivity force. Magnetic materials are classified as: Soft material, when coercivity is lower than 1000 A/m and Hard material, when coercivity is higher than 1000 A/m. The coercive force is of fundamental importance in the technical applications. In soft magnetic materials, the coercivity is due mostly to structural defects (impurity atoms, elastic tensions, dislocations) that hinder the walls motions.

Hysteresis loses will always be a problem in AC transformers where the current is constantly changing direction and thus the magnetic poles in the core will cause losses because they constantly reverse direction. Rotating coils in DC machines will also incur hysteresis losses as they are alternately passing north the south magnetic poles. If you wish to create a permanent magnet you should use a material with a very fat hysteresis loop (figure 19 a). Such as materials, once magnetised, are very difficult to demagnetise and when the magnetising force is removed a substantial magnetic flux density remains. These materials are known as hard magnetic materials. Since the coercive force must be applied to overcome the remanent magnetism, work is done in completing the hysteresis loop and the energy concerned appears as heat in the magnetic material. This heat is known as hysteresis loss, the amount of loss depends on the material's value of coercive force. By adding silicon to iron a material with a very small coercive force can be made, such materials typically contain 5% silicon and have very narrow hysteresis loop (figure 19 b). Materials with narrow hysteresis loops are easily magnetised and demagnetised and known as soft magnetic materials (Saito, 1988).
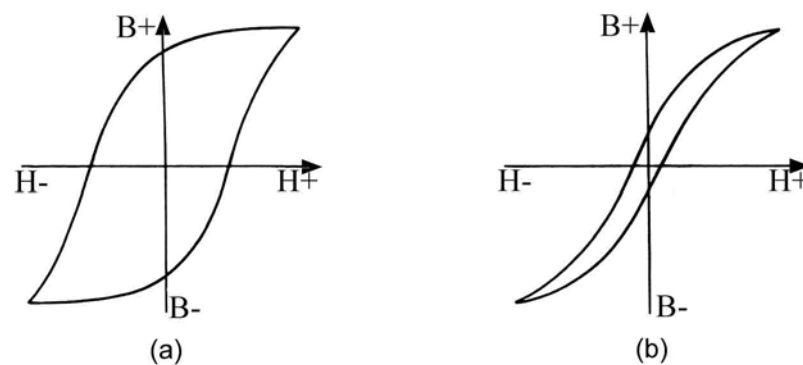
Figure 19 (a) the hysteresis loop for hard magnetic material

(b) the hysteresis loop for soft magnetic material

4.4 The high coercive fields of permanent magnets are obtained with other principles:

1. Crystalline anisotropy of the material, that makes difficult the rotating of the magnetization in directions different than the anisotropic one

2. Monodomain grains, which change their magnetization only when all the dipoles inside the grain rotate at the H_{cJ} field (for example, ferrite)

3. Shape anisotropy that makes difficult the rotation of the magnetization in directions other than the extended one. It is the case of alnico magnets, formed by of a magnetic monodomain phase (Fe-Co) with elongated shape, blocked in a non-magnetic phase (Fe-Ni-Al). In rare earth materials, that are all crystalline anisotropic, the mechanism of coercive force is of two types.

4. Nucleation mechanism in single phase magnets (NdFeB), the domain walls are locked at the grain boundaries, so the coercivity is the field at which a reverse domain nucleate inside a grain (Flavio et al., n.d.).

5. Pinning mechanism in multi phase magnets, such as the precipitation hardened alloy (Sm_2Co_{17} family) the domain wall are locked in a lot of pinning sites inside the grain. So, the coercivity is the field at which the walls are released from the pinning sites.

Nucleation mechanism   Pinning mechanism
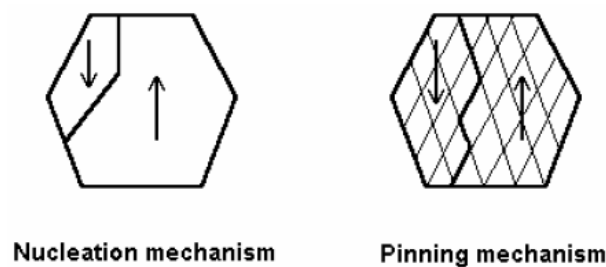
Figure 20 (a) Nucleation mechanism and (b) Pinning mechanism

4.5 Temperature behaviour

The change of the magnetic characteristics related to the temperature has a primary position in the evaluation of a permanent magnet. The characteristics of the magnets generally decay with the increase of temperature, except for coercive force of ferrite magnets (Olkhovik *et al.*, 2000). We can distinguish the temperature losses in reversible and irreversible, according to the necessity to remagnetize or not the sample after the temperature decay. If the magnet overcomes the irreversible temperature limit it must be remagnetized. Being the working point of a magnet the intercepts between the demagnetization curve and the load line (that depends on geometry of the magnetic circuit only), it is clear that it hanges regard to the variation of the demagnetization curve. If the intercept at temperature T is in the linear region of the demagnetization curve, the value of J_P will be fully recovered returning the temperature to the room temperature value T_0. If the intercept is under the knee, only a partial recover is possible.

The temperature variations of Br and HcJ are defined by two coefficients, αB_r and αH_{cJ}, given in % / ° C

$$\alpha B_r \quad = \quad \frac{1}{B_r(T_0)} \bullet \frac{B_r(T) - B_r(T_0)}{T - T_0} \quad \frac{1}{B_r(T_0)} \bullet \frac{B_r(T) - B_r(T_0)}{T - T_0}$$

Where: (T_0 is room temperature) IEC standards state that the measurements on hard materials (as well as soft materials) should be performed at 23 ± 5 ° C.

5. **Rubber Ferrite Composite**

All of standard permanent magnet materials can be utilized to produce bonded type magnets when fine particles are embedded in elastomer matrices (Lopez *et al.,* 2007). The major permanent magnet materials in use are hard ferrite, alnico and rare earths. Most of the bonded magnet products use a flexible matrix, but rigid-type bonded magnet are also made. The flexible type can be manufactured in cut pieces or continuous lengths. They can be drilled, cut, bent and machined into complex shapes. These unique features offer the designer a wide range of design possibility and opportunities for cost saving. The rigid boned magnets offer close magnetic and dimension tolerances. They can be produced with a variety of magnetic orientations in sample and instricate shapes (Flavio *et al.*, n.d.).

Saito *et al.,* (1988) studied hard ferrites are characterized by the general formula $MFe_{12}O_{19}$ (figure 21), where M is a divalent metal ion or combination of divalent metal ions such as barium or strontium. The crystal structure is hexagonal and is the same as the mineral magnetoplumbite.
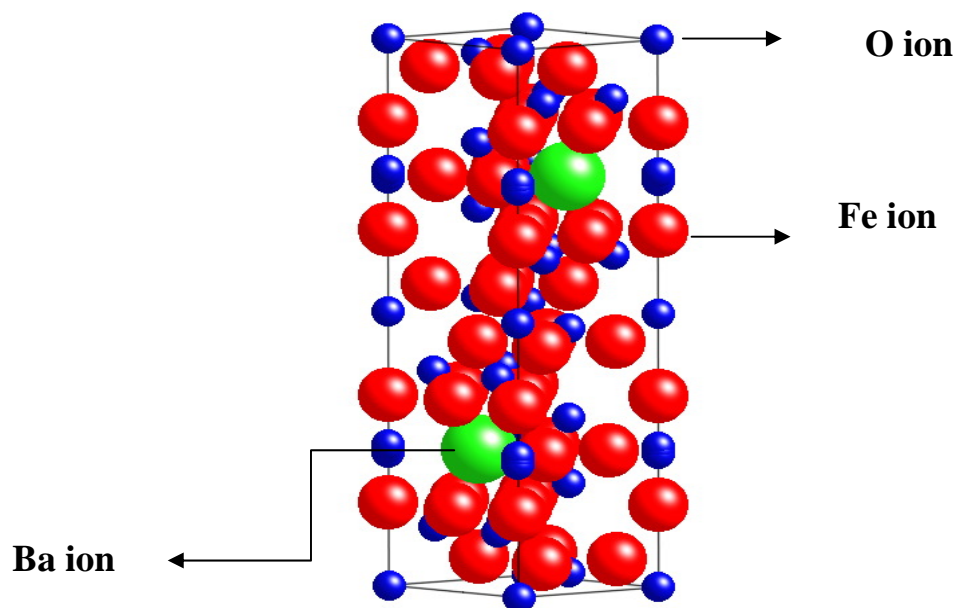
Figure 21 Hexagonal barium ferrite structure

A hard ferrite has a hexagonal crystal structure with the uni axial c axis being the one along which the magnetization prefers to align (Nowoseielski *et al*., 2007). Technical requirements for ferrite magnets are high residue flux density and high corecive force. Representative hard ferrite such as strontium ferrite and barium ferrite (figure 21). Barium ferrite is lower in cost than strontium ferrite that contain plate-shaped particle having two relatively parallel surfaces and either the regular or and irregular edge parameter, depending on the method of manufacture. There are several methods for producing hard ferrite powders: solid state reaction, co-precipitation (Mallick *et al*., 2001), for example. The solid-state method is the most widely used Mali *et al*., (2005) and Mozaffari *et al*., (2009). A typical solid state process uses starting materials of barium or strontium carbonate and iron oxide. A high degree of consistency in the raw material is critical natural or amount of impurities or the particle size of raw materials can result in the considerable variation in the end product (Brannen *et al*., 2006). Ball mill or ribbon blenders are among the many different types of equipment used for mixing raw materials. The homogeneous mixture is formed into pellets or large slabs and reacted at temperature ranging from 1000 ° C to 1300 ° C. Milling, which is the next step in the process, determines the final magnetic and physical properties of a hard powder of a hard ferrite powder, ideally would produce single crystals as close to the critical magnetic domain size as possible. Vibratory, attrition and ball mills, either wet or dry are used to produce the required particle size. Particle size distribution has a major effect, not only on the magnetic properties but also on the loading characteristics when the powder is embedded in a polymer for bonded magnets.

Mali *et al*., (2005) synthesized nano-crystalline particles of barium hexaferrite by using the sol-gel combustion method. The formation of the barium hexaferrite was found to comprise two steps: formation of monoferrite ($BaFe_2O_4$), followed by reaction between monoferrite and iron oxide which was completed at 900 ^{o}C. The results revealed that the average particle size derived from SEM measurement is larger than the average crystallite size measured by XRD. However, the particle and crystallite growth rate increased with increasing temperature.

Radwan *et al.*, (2006) studied the preparation of nanocrystalline barium hexaferrite ($BaFe_{12}O_{19}$) powders by the co-precipitation specimen on route. The ferrite precursor were obtained from aqueous mixtures of barium and ferric chlorides by co-precipitation of barium and iron ion using 5 M sodium hydroxide solution. These precursors were calcined at temperature of 800-1200 ^{o}C at 2 h. The effect of Fe^{3+}/Ba^{2+} mole ratio and addition of surface active agent on the structural and magnetic properties were studied. Barium Ferrite powder was achieved by decreasing the Fe^{3+}/Ba^{2+} molar ratio value 12-8 and increasing the calcinations temperature upper 1000 ^{o}C. In addition, the molar ratio of Fe^{3+}/Ba^{2+} was 8 at a low temperature of 800 ^{o}C exhibited the good magnetic saturation and wide instrinsic coercivities.

The hard ferrite or ceramic magnetic powders used in boned magnets. They are dark-colored and have a high specific gravity, in the range of 5.00 to 5.25 with average particle sizes ranging from 1.5 to 2.0 μm. They are abrasive and generally require hardened surfaces on equipment used in processing them into bonded magnets. The low cost of hard ferrite material qualifies it for use in two major markets, automotive and appliances. The loading of hard ferrite in polymer matrices range from 85 to 95 wt% and the maximum energy product approaches 2.00 megagauss oersteds (MGO). This compares with sintered hard ferrite magnets having a range of 1 to 4 MGO, Xanthos, M. (2005) and Xiang *et al.*, (1999).

Hard ferrite powders can be formed into flexible or rigid bonded magnets. The magnetic field strength obtained is determined by two major factors: the degree of orientation and the loading. The first can be obtained either magnetically or mechanically. The second depends on the type of polymer and the processing equipment used. The use of magnetic orientation requires that the hard ferrite particles be as mobile as possible during the forming process. These particle will align themselves in the reaction of magnetic field, which is applied during forming. Mechanical orientation can be attained by extruding or squeezing the particles, in a suitable flexible matrix, through a narrow slot. A certain number of the particles will align themselves to keep their largest dimension parallel to the largest dimension of

the slot opening. It is also possible to use a combination of magnetic and mechanical orientation (Yang *et al*., 2006).

Flexible bond magnets are fabricated using compounds containing up to 90% wt of hard ferrite powder. Various polymers are used depend on the chemical, physical and thermal requirement. Polymers include polyethylene, nitrile rubber, vinyl compounds, polyisoprene and the others. Mixing is done with two roll mill or Ban-bury mixer. The compound is then extrude or calendered. Manetizing is accomplished with conventional equipment using field on the order of 10,000 oersteds.

Malini *et al*., (2001) prepared rubber ferrite composites (RFC) containing Ni_{1-x} Zn_x Fe_2O_4 in natural rubber. The cure characteristics revealed that the processability and flexibility of the matrix was not much affected even up to a maximum loading of 120. Magnetic properties were studied the saturation magnetization (M_s) and magnetic field strength (H_c). The study also suggested that there was no possible interaction between the filler and the matrix at least at the macroscopic level.

Mohammed *et al.,* (2001) found that composite materials of manganese zinc ferrite with natural rubber can modify the electrical properties of ferrite. Mixed ferrites belonging to the series $Mn_{(1-x)}Zn_xFe_2O_4$ (MZF) were synthesized for different 'x' values in step of 0.2. These pre-characterized ceramic ferrites were incorporated in a natural rubber matrix. The samples were prepared for the different loadings of magnetic filler up to 120 phr in step of 30 phr. The tensile study indicated that the serviceability of the elastomer was not affected even for 120 phr loading of filler. The initial decrease in tensile strength was due to the reduction in the stress-induced crystallization of natural rubber matrix. The tensile was decreased then increased with the filler loading. Rubber ferrite composites with the filler composition 'x' being 0.6 showed the maximum tensile strength.

Makled *et al.,* (2004) studied barium ferrite powders which having the particle size in a range 45–200 μm. Barium ferrite powder was incorporated into a natural rubber with different loading levels up to 120 phr. The dynamic properties were more strongly dependent on the particles and particle–matrix characteristics than the magnetic and the mechanical properties. For further improvement detailed future works were needed to study the effects of size, shape and surface roughness of fillers on the magnetic and dynamic properties of barium ferrite–rubber composites. The results showed that the coercivity is improved and the saturation magnetization was linearly dependent on the mass fraction of the filler, while the tensile strength, strain at break and modules were highly influenced by the size, shape and volume fraction of ferrite particles. The BH_{max} was 1.18 MGOe and flexibility resilience of RFC was 0.844 at 120 phr.

Soloman *et al.,* (2004) studied rubber ferrite composites (RFC) containing of strontium ferrite ($SrFe_{12}O_{19}$) which synthesized by the ceramic techniques and then incorporated in natural rubber matrix according to a specific recipe. The rubber ferrite composites were prepared for various loadings of strontium ferrite, ranging from 40 to 120 phr in steps of 20. Hence, the 80 phr loading of strontium ferrite was taken as the control compound for further loadings of carbon black. RFCs containing carbon black were prepared for various loadings, namely 10 to 50 phr, in steps of 10. The mechanical properties of the RFCs studied showed that the ferrites behave as semi-reinforcing and the reinforcement was maximum in the presence of carbon black. The magnetization values increased with the loading of ferrite filler, but with the addition of carbon black, even though the values decreased, the RFCs containing carbon black still possessed appreciable magnetization values.

Soloman *et al.,* (2004) attemoted to incorporation pre-characterized hexagonal ferrites, namely barium ferrite ($BaFe_{12}O_{19}$) into natural rubber matrix. It was found that the processability was not much affected by filler incorporation. The physical properties indicated that the addition of magnetic fillers increased the modulus and hardness, with marginal decreased in the tensile strength. Study of the magnetic

properties indicated the formation of elastomer magnets with suitable value of saturation magnetization and retentivity. The magnetic properties of RFC can be controlled by the addition of appropriate amount of the ferrite filler.

Nontapat et al., (2005) studied the effect of paticle sizes of ferrite. On the physical properties of rubber ferrite composites (RFCs). The physical properties indicated that the addition of magnetic fillers increased the hardness, but decreased the tensile strength. The rubber ferrite composites at 60 phr was better shielding.

El-Nashar et al., (2006) investigated the mechanical, electrical and magnetic properties of natural rubber composites containing iron or nickel nanoparticles at different percentage varying from 0-120 phr. It was found that the optimum concentration of magnetic fillers in NR was 30 phr, which improved the rheometric characteristics and mechanical properties. Magnetic measurements showed superparamagnetic behavior for all Ni and Fe nanoparticles percentage. The electrical measurements showed a strong dependency of the conductivity on the percentage of magnetic nanoparticles.

El-Sabbagh et al., (2006) preparaed rubber composites based on natural rubber vulcanizates loaded with iron oxide aluminium oxide ($Fe_2O_3Al_2O_3$) fillers and investigated physical and magnetic properties. The prepared fillers were evalutated as reinforcing fillers with some magnetic properties, these properties were dependent on the ratio of iron oxide to aluminum oxide in each prepared ratio of these fillers. Rheological properties of rubber mixes containing ($1Fe_2O_3.3Al_2O_3$) and ($1Fe_2O_3:1Al_2O_3$) fillers exhibited better properties than mixes containing ($3Fe_2O_3.3Al_2O_3$) and (α-Fe_2O_3). Physical properties such as tensile strength, 100, 200% modulus, hardness increased by increasing with increasing the volume fraction of the investigated fillers concentration in the mixed vulcanizates.

Urogilova *et al.,* (2006) studied the influence of hard magnetic strontium ferrite filler content on the structure, vulcanization characteristics, magnetic and mechanical properties of rubber blends. The cure time was not influenced and both the remanence magnetization and the tensile strength linearly depended on the weight fraction of the magnetic fillers in the rubber-blends. Evaluation of influence of ferrite filler and carbon black on modulus 300% showed that the increase in the amount of carbon black in the mixture leaded to an increase of both characteristics.

MATERIALS AND METHODS

Materials

1. Natural Rubber (NR); STR5L, S.M.P. RUBBER, Thailand.
2. Fillers
   - Barium ferrite $(BaFe_{12}O_{19})$, commercial grade, Icelandic, Thailand
   - Barium ferrite $(BaFe_{12}O_{19})$, synthesized with Oxide One Pot Process (OOPS)
   - Carbon black (N 330)
3. Reagent
   - ZnO, an activator, Global Chemistry, Thailand.
   - Stearic acid, an activator, Imperial Industrial, Thailand.
   - Sulfur, crossling agent, Sahapaisal Industry, Thailand.
   - Monoalkoxy unsaturated fatty acid phosphate titanate, couplink TC 101, Behn Mayer, Thailand.
   - 2,2,4- Trimethyl-1,2-dihydroquinoline polymer (TMQ), an antioxidant, Eliokem, USA.
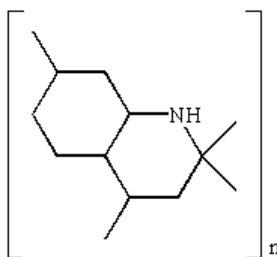
Figure 22 Structure of 2,2,4-Trimethyl-1,2-dihydroquinoline polymer (TMQ)

- N- cyclohexyl-2-benzothiazole Sulphenamide (CBS), an accelerator, Flexsys, Germany.
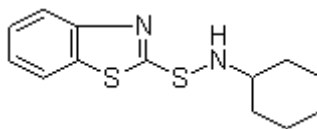
Figure 23 Structure of N-cyclohexyl-2-benzothiazole sulphenamide (CBS)

4. Equipments
   - Two Roll Mill
   - Moving Die Rheometer (MDR), Tech PRO
   - Compression molding, G30H-15-CX, Wabash, USA.
   - Hardness, Cogenix, Wallace
   - Tensile strength, Universal Testing Machine by Instron, USA
   - X-ray Diffraction (XRD), JEOL JDX-3530
   - Scanning Electron Microscopy, Phillips SEM XL30 & EDAX
   - Vibrating Sample Magnetometer (VSM), Lake Shore 7400 Series
   - BET Surface Area Analysis Quantachrome: Autosorb-1C
   - Oven

Methods

1. Preparation of rubber compounds and vulcanization

All ingredients were incorporated in a natural rubber matrix. The formulation of all rubber ferrite composites are shown in Table 4-6. The mixing was done in a two-roll mill at 70 ° C for 10-15 minutes. Finally, the curative were added and mixed with the compounds and after homogenization they were sheeted out and kept at room temperature for 24 hours before testing.

Prior to vulcanize the mixes, a vulcanization time was determined by means of Moving Die Rheometer (MDR). The Moving Die Rheometer measures the change in stiffness of a rubber sample, compressed between two heated platens, by an applied oscillating force. The degree of vulcanization determines the cure characteristic of the sample as it is heated and compressed. The test is known as a cure curve such as scorch time, time to percentage cure, maximum and minimum torque. The mixes were compression molded using a hydraulic hot press at 150 ° C, under pressure 15 MPa. The experiment was mainly divided into 3 factors.

Factor 1: Study the effect of commercial barium ferrite loading on the mechanical and magnetic properties of RFCs. The formulation are shown in Table 4.

Table 4 Formulation of rubber ferrite composites

Ingredients	phr.
Natural rubber	100
Stearic acid	1
Zinc Oxide	5
Accelerator (CBS)	0.6
Antioxidant (TMQ)	1
Sulphur	1.5
Barium ferrite commercial	0, 20, 40, 60, 80, 100, 120, 140

Factor 2: Comparison of the magnetic and mechanical properties between commercial and synthesized barium ferrites by OOPS method. The rubber formulation as shown in Table 5.

Table 5 Formulation of rubber ferrite composites

Ingredients	phr.	phr.
Natural rubber	100	100
Stearic acid	1	1
Zinc Oxide	5	5
Accelerator (CBS)	0.6	0.6
Antioxidant (TMQ)	1	1
Sulphur	1.5	1.5
Barium ferrite commercial	100	-
Barium ferrite (OOPS method)	-	100

Note: Barium ferrite (OOPS method) was received from Oxide One Pot Process.

Factor 3: Study the effect carbon black loading on mechanical properties of rubber ferrite composites that mix with commercial barium ferrite and synthesized barium ferrites by OOPS method. The formulation is shown in Table 6.

Table 6 Formulation of rubber ferrite composites

Ingredients	phr.	
Natural rubber	100	100
Stearic acid	1	1
Zinc Oxide	5	5
Accelerator (CBS)	0.6	0.6
Antioxidant (TMQ)	1	1
Sulphur	1.5	1.5
Barium ferrite commercial	100	-
Barium ferrite (OOPS method)	-	100
Carbon black (N 330)	10, 20, 30, 40	30

2. Cure Characteristics

The cure characteristics of rubber compound having sulfur as curing agent were assessed by Moving Die Rheometer (MDR). Vulcanization was performed using a compression-molding machine. The various rubber compounds were compression molded at 150°C according to their respective optimum cure times. Cure time was determined from the time to reach 90% (t_{c90}).

3. Characterization of Fillers

Physical properties and surface area of commercial barium ferrite and synthesized barium ferrite (OOPS) were determined by the Brunauer-Emmett-Teller (BET) on Autosorb-1 method. Particle size analyzer (wet sieve) was used to measure the particle size of the fillers. The information of structure and crystallographic orientation of barium ferrite was obtained from XRD measurement.

4. Mechanical Properties

4.1 Tensile strength

The vulcanized samples were cut into tensile specimens by using the punching machine. The cutting die punched the sample into dumbbell-shape. Testing was carried out on tensile testing machine in accordance with ASTM D412-92. The following tensile properties were measured: 100, 300, and 500% modulus, tensile strength (stress of rupture of specimen) and the elongation at break according to ASTM D 412-92 using the Universal Testing Machine with the load cell of 1 kN as shown in figure 24.

Figure 24 The Instron tensile tester

Tensile properties were calculated from the following equation

$$\sigma \quad = \quad F/A$$

where: σ = stress (N/mm^2)

F = force (N)

A = cross-sectional area of unstreched specimens (mm^2)

4.2 Hardness

Figure 25 Hardness Tester

Shore A hardness of the specimens was measured according to ASTM D 2240 using hardness tester. The specimens about 6 mm in thickness were placed on test platform. The durometer was held in a vertical position with point of the indenter

at least 12 mm from any edge of the specimens. An average of the five measurements was taken as the hardness value of the test sample.

4.3 Compression set

The origin thickness of the specimen was measured according to ASTM D 395-03. The test specimens were placed between the plates of the compression device with the spacers on each side, allowing sufficient clearance for the bulging of the rubber when compressed at 70° C for 22 hour. The specimens then rested on poor thermally conducting surface, such as wood, for 30 min before making the measurement of the final thickness.
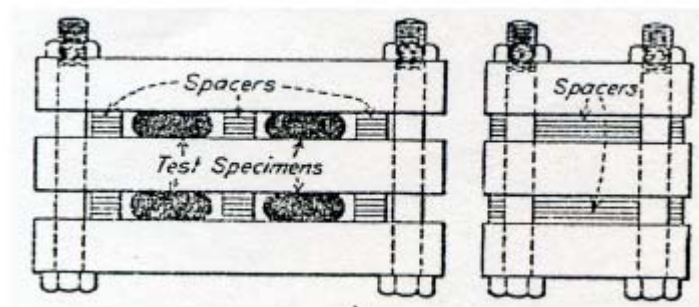
Figure 26 Device for compression set test under constant deflection.

The expression for the calculation of the compression set is:

$$C_B = [(t_o-t_i)/ (t_o-t_n)] \times 100$$

Where: C_B = compression set expressed as percentage of the original deflection

t_o = original thickness of specimen

t_i = final thickness of specimen

t_n = thickness of the spacer bar used (4.5mm)

4.4 Thermal Aging

Figure 27 Oven

Accelerated thermal-oxidative aging testing was followed in the present investigation. The thermal aging experiment was performed in an oven at temperature 100 ^{o} C for 3 days according to ASTM D573. The results are shown as the relative tensile strength of the specimens after thermal exposure.

4.5 Scanning Electron Microscope (SEM)

The phase morphology of the blend was studied by using scanning electron microscope (model JEOL-JSM-5410LV). The samples of the blends were broken in liquid nitrogen to avoid any possible deformation of phases. The samples were further dried. Then, the dried surfaces of the samples were gold coated and then examined by SEM.

5. Magnetic testing

A vibrating sample magnetometer (VSM) operates on Faraday's Law of Induction, which tells us that a changing magnetic field will produce an electric field. This electric field can be measured and can tell us information about the changing magnetic field. Magnetic Properties of the sample were examined at room temperture using Vibration Samples Magnetometer (VSM) up to 5 kOe. The magnetic parameters including coercivity (H_c), saturation magnetization (M_s), magnetic remanence (M_r) were obtained from these measurements.

System diagram of
Vibrating Sample Magnetometer
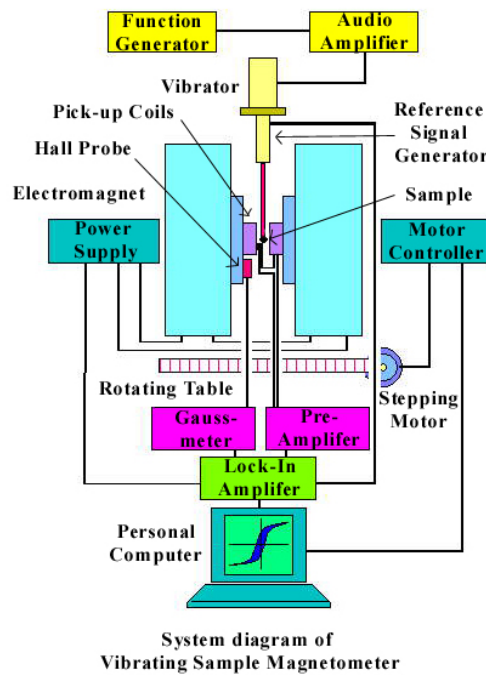
Figure 28 Vibration Sample Magnetometer

RESULTS AND DISCUSSION

1. Filler Characterization

Recently, the conventional way of producing barium ferrite ($BaFe_{12}O_{19}$) was the solid state reaction mixed with oxide/carbonate and calcined at high temperatures ($\geq 1200 \,^{\circ}$ C). The solid state reaction method has some inherent disadvantages: such as chemical inhomogeneity, coarser particle size and introduction of impurities during ball milling. Chemical methods such as co-precipitation, glass crystallization, microemulsion synthesis, hydrothermal reaction, and sol–gel method have overcome the above mentioned disadvantages and produced fine and homogeneous ferrite powders, but many of these methods lead to the formation of intermediate phases such as αFe_2O_3, $BaCO_3$, or $BaFe_2O_4$ together with barium ferrite.

Many researches have been focused on the improvement of the homogeneous ferrite powders. It provides several advantages, as compared to other chemical techniques. The oxide one pot synthesis (OOPS) process, is very simple and offers many advantages over traditional methods, including low processing temperature, high purity and homogeneous. The "One Pot" Process was successfully used to prepare the $MgAl_2O_4$ (Laobuthee *et al.,* 2000). Thus, it is of interest in this study to investigate the characteristics of barium ferrite powder synthesized by "The Oxide One Pot (OOPS) process" compared with those of the commercial grade of barium ferrite powder. The filler (barium ferrite powder) characteristics in terms of physical properties including particle size and surface area were determined by BET and particle size analyzer (Benito *et al*., 2001). The information of structure and crystallographic orientation of Barium Ferrite was also obtained from XRD measurements (Topal *et al*., 2007).

1.1 Physical Properties of barium ferrite powders
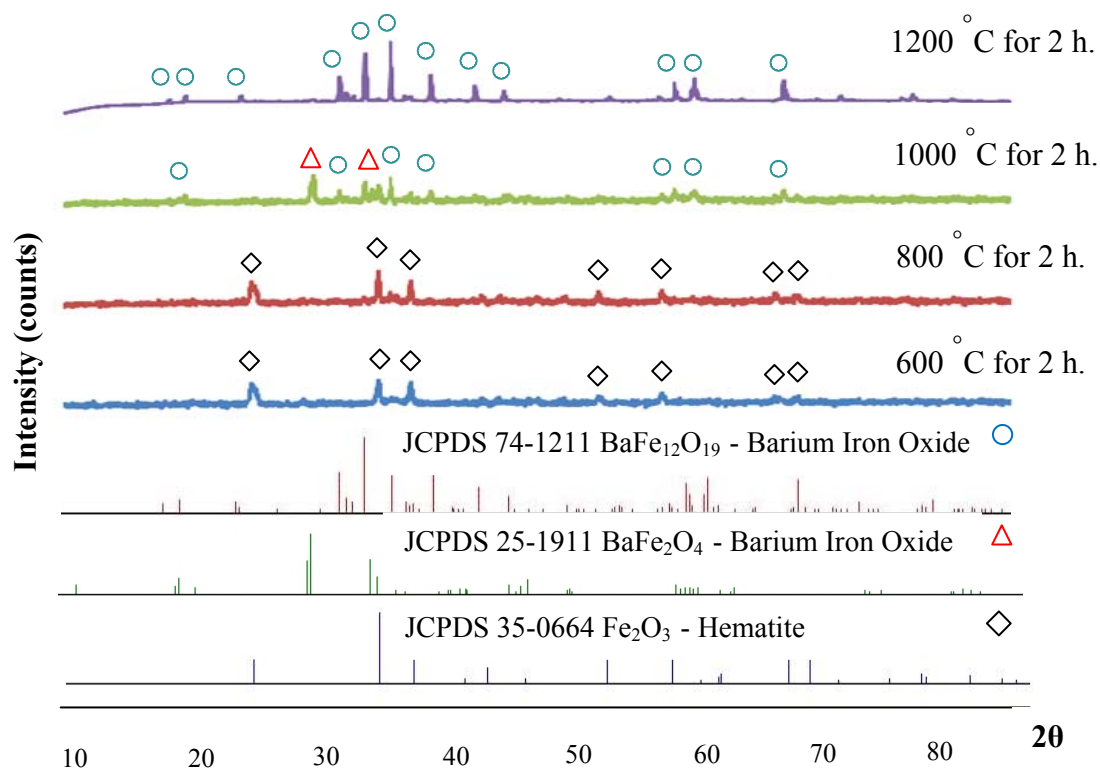
Figure 29 XRD patterns of barium ferrite powders calcined for 2 h at 600 °C,
800 °C, 1000 °C and 1200 °C

The determination of the crystalline phases was carried out by X-ray
diffraction (XRD) with CuKα radiation (λ = 1.5406 A ° and 2θ = 20–80 degrees).
From X-ray diffractograms obtained for the ceramic barium ferrite, Figure 29 shows
the XRD patterns of the samples calcined at 600 ° C, 800 ° C, 1000 ° C and 1200 ° C
for 2 h. The reference peaks obtained from XRD patterns of hematite (Fe_2O_3) and
barium iron oxide ($BaFe_2O_4$ and $BaFe_{12}O_{19}$) are seen from JCPDS 35-0664, JCPDS
25-1911 and JCPDS 74-1211, respectively. The XRD pattern of barium ferrites
calcined at 600 ° C and 800 ° C shows peak at the same positions as the reference
peak (JCPDS 35-0664). That is to say hematite phases of barium ferrite calcined at
lower temperatures (600 °C and 800 °C) were observed. The reference peak (JCPDS
74-1121), that shows 3 main peaks of hexagonal $BaFe_{12}O_{19}$ phase, can be seen in the
diffraction pattern at 30.31-34.10 of 2- theta degree. However, X-ray diffraction of

these samples calcined at 1000 ° C reveals that hexaferrite has been already formed at this temperature and therefore the reference of this peak seems to be the same as in the case of sample JCPDS 25-1911 showing antiferromagnetic $BaFe_2O_4$. However, it is clearly seen that the peaks of the samples calcined at 1000 ° C correspond to barium ferrite in both hematite phase and hexagonal phase. That is to say at this temperature (1000 ° C) we could not get the hexagonal phase of barium ferrite with high purity. It should be noted here that in order to receive high purity of hexagonal phase of barium ferrite, the precursor must be calcined at temperature of 1200 ° C for 2 h as can be seen from the XRD pattern showing the same peak as the reference JCPDS 74-1211 which is the peaks of hexaferrite phase ($BaFe_{12}O_{19}$). However, it has been known that the higher temperature to calcinate precursor, the more risk of safety and the lower cost of synthesis are the good advantage. In order to aviod the problem in the higer temperature (1200 ° C) to calcinate precursor, it is thus of our interest to calcinate the barium ferrite at lower temperature (1000 ° C), but increasing the calcination time (2, 5 and 8 h) instead.
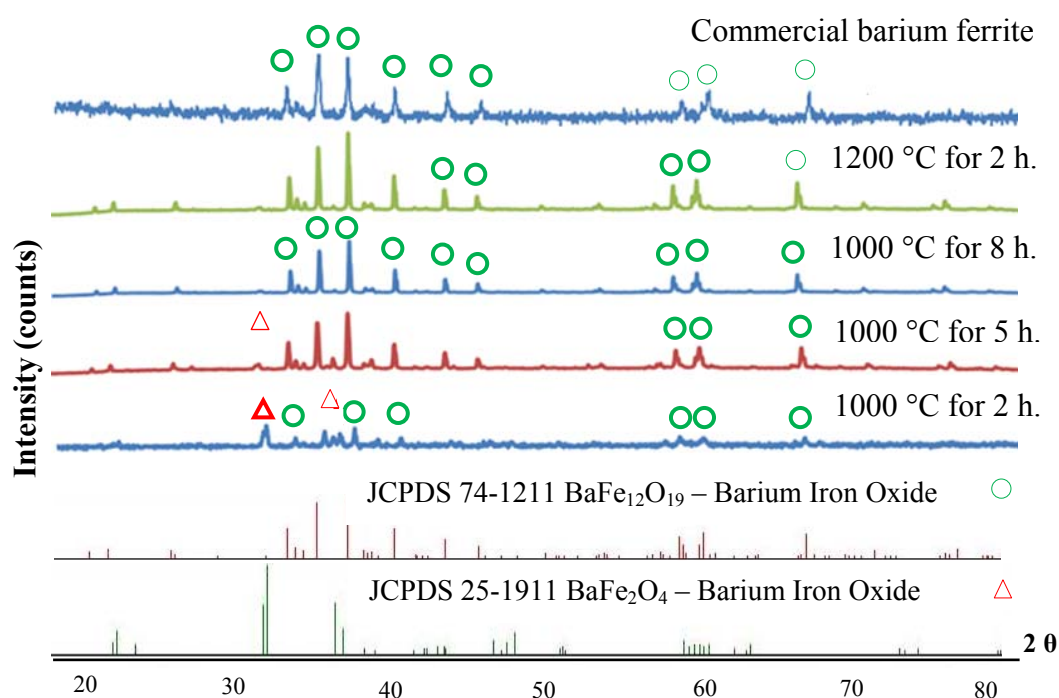
Figure 30 XRD patterns of barium ferrite powders calcined at different conditions

Figure 30 shows XRD patterns of samples calcined at 1000 ° C for 2, 5, and 8 h compared with the samples calcined at 1200 ° C for 2 h and commercial barium ferrite (with impurity phases less than 3% obtained well-defined sharp peaks and high intensity indicating the good crystalline quality of these samples). As seen from the JCPDS 74-1211, the main peak of barium ferrite phase was matched with the sample calcined at 1000 ° C for 5 and 8 h. A hexagonal phase with a small amount of hematite $BaFe_2O_4$ was observed after calcination at 1000 ° C for 2 h. That is to say in order to receive hexagonal phase of barium ferrite with high purity, the sample should be calcined at 1000 ° C for more than 2 h. The results confirm that the antiferromagnetic $BaFe_2O_4$ phases could be eliminated by the increase in sintering time. It was also observed that the intensity of XRD peak increases with increasing the sintering time from 2 to 8 h, indicating that hematite phase of precusor becomes hexaferrite phase after increasing sintering time.

Table 7 Physical properties of barium ferrite powders

	Condition of barium ferrite		Particle size (μm)	Surface area (m^2/g)
	Temperature (°C)	Time for precursor calcination (h.)		
OOPS 1	1000	2	19.86±0.69	2.38
OOPS 2	1000	5	20.10±0.20	3.99
OOPS 3	1000	8	27.38±2.73	4.59
OOPS 4	1200	2	23.63±1.42	3.07
commercial	-	-	16.72±0.98	6.06

The physical properties of barium ferrite powders such as surface area were accomplished by Quantachrome Automated Gas Sorption equipment, using N_2 as the adsorption/desorption gas. The particle average diameter was calculated using the BET method recorded in Table 7. The particle size and surface area of barium ferrite powders calcined at 1000 ° C for 2, 5 and 8 h were investigated compared with those

calcined at 1200 ° C for 2 h and commercial barium ferrite powders. Barium ferrites were found to have small mean agglomerates particle size between 17-28 μm. Also, it can be seen that barium ferrite calcined at 1000 ° C for 8 h gives larger particle size than those calcined at 1000 ° C for 2 and 5 h. It was found that the preferential grain growth of barium ferrite was observed with an increase in the time for sintering, probably due to the expandation of the grain boundaries, resulting in the increase in the particle size of barium ferrites after increasing sintering time. Moreover, it can be seen that precursor calcined at 1200 ° C for 2 h shows larger particle size than the one calcined at 1000 ° C for 2 h, Paul *et al.,* (2007) and Roy *et al.,* (n.d.).

Particle size and morphology of barium ferrite powders were examined by direct observation in Figure 31 showing SEM micrographs of these samples calcined at 1000 ° C for 2, 5 and 8 h. We have observed that the grains appear to stick each other and agglomerate in different masses throughout the micrograph. It was observed from SEM micrographs that the grains tend to require shape edges and some of them grain hexagonal shapes upon increasing time to calcinate for 8 h, Palla *et al.*, (1999) and David *et al.*, (2001). Increase of particle size of samples calcined at 1000 ° C for 2, 5, and 8 h means that the sample shows multidomain character, OlKhovih et al., (2000) and Kim *et al.*, (2007).

On the other hand, the increasing of surface area from the hematite precursor to the final hexaferrite particle can be explained by two main factors. First of all, a volume contraction is taking place due to the transformation precusor to hematite and secondly, there is a recrystallization process where the hexaferrite particles grow topotactically in the (0 0 1) direction from the (1 1 1) plane of hematite. A schematic representation of this transformation is shown in Figure 32 (Benito *et al.*, 2001).
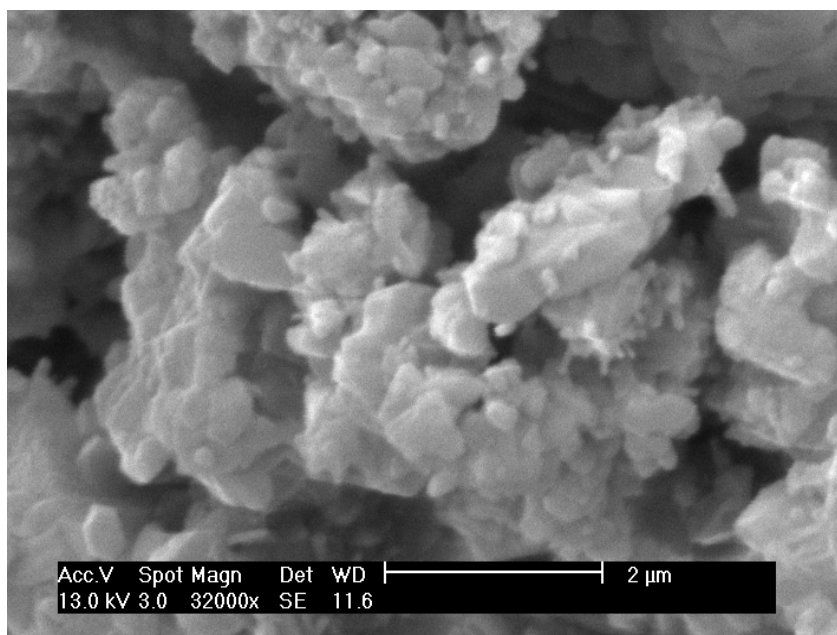
(a) BaFe$_{12}$O$_{19}$ calcined at 1000 ° C for 2 h
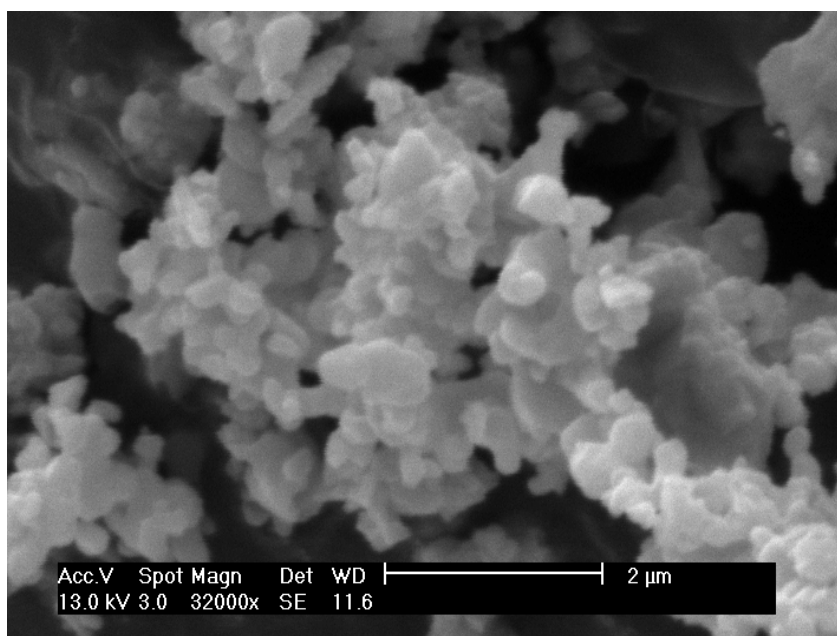
(b) BaFe$_{12}$O$_{19}$ calcined at 1000 ° C for 5 h

Figure 31 SEM images of barium ferrite powders
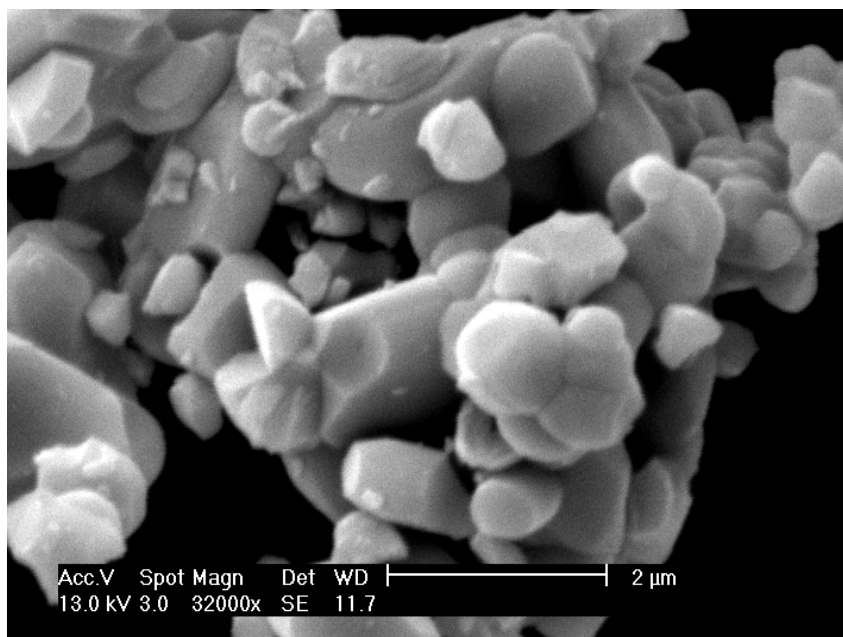
(C) BaFe$_{12}$O$_{19}$ calcined at 1000 ° C for 8 h

Figure 31 (continue) SEM images of barium ferrite powders
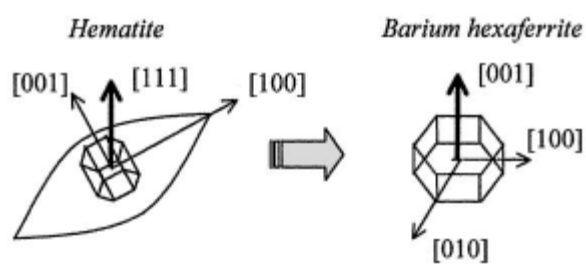
Figure 32 Schematic representation of the transformation from

hematite to barium hexaferrite.

1.2 Magnetic Properties of Barium Ferrite Powders

Table 8 Magnetic Properties of Barium Ferrite powders

Precursor condition		Coercivity (H_{ci}) (G)	Saturation Magnetization (M_s) (emu/g)	Magnetic Remanence (M_r) (emu/g)
Temperature (^{o}C)	Time (h)			
1000	2	3455.6	30.349	17.980
1000	5	4058.6	52.106	31.502
1000	8	4260.3	59.442	39.945
1200	2	2269.9	56.895	34.171
commercial	-	2393.7	59.741	45.111
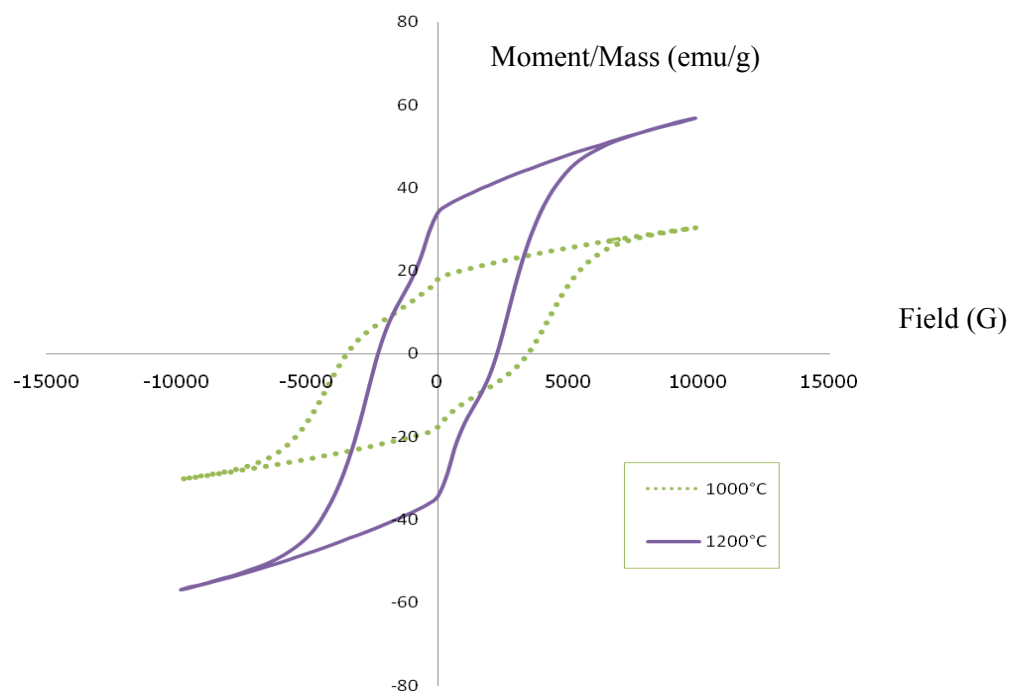
Figure 33 Hysteresis loop of barium ferrite powders calcined at 1000 ° C and
1200 ° C for 2 h.

Magnetic properties including saturation magnetization (M_s), magnetic remanence (M_r) and corecivity (H_c) were investigated at room temperature displaying in hysteresis loops. Hysteresis loops of the samples calcined at temperatures $1000 \degree$ C and $1200 \degree$ C for 2 h are shown in Figure 33. Table 8 summarizes the magnetic parameters of the samples calcined at $1000 \degree$ C for 2, 5 and 8 h including the ones calcined at $1200 \degree$ C for 2 h. The variation of the magnetic parameters with respect to temperature is presented, which indicates that by increasing the calcining temperature the values of saturation magnetization (M_s) and magnetic remanence (M_r) increased (Olkhovik *et al.*, 2001). However, magnetic remance (M_r) and corecivity (H_c) of barium ferrite powders calcined at $1000 \degree$ C for 8 h are greater than those of barium ferrite calcined at $1200 \degree$ C for 2 h. This can be due to grain growth, such as reduction in the number of surface atoms with respect to volume atoms and decrease in intra granular porosities. Also, variation of coercivity is dependent on not only calcined temperature but also time for calcination.

Also it is clear from these data (Table 8) that the change in magnetic remance (M_r) and corecivity (H_c) with field for the sample calcined at $1000 \degree$ C for 8 h is much steeper than the one calcined at the same temperature for shorter time (2 and 5 h). It means domain walls increase the strength of demagnetizing factor. This sample compared to others can be explained in terms of the demagnetizing-like interactions of neighboring domains. That can be associated to interparticle interactions which contribute constructively to the magnetization (magnetizing like effect). This kind of interaction is known to be a stabilizing one and it will enhance the remanence state, Xiang *et al.*, (1999) and Flavio (n.d.).

2. Effect of commercial barium ferrite loading on cure characteristics and mechanical properties of Rubber Ferrite Composites (RFCs)

Magnetic filler such as ferrites are one of the most useful magnetic materials ever discovered and cannot be easily replaced by any other magnetic material because they are inexpensive, stable and have a wide range of technological applications. So, they are still widely used wherever the product cost is a major consideration over magnetic performance although they have less magnetic strength than rare earth magnets. Recently strontium ferrite ($SrFe_{12}O_{19}$) has received a wide attention as a permanent magnet than barium ferrite ($BaFe_{12}O_{19}$) although they are relatively closed in magnetic properties and in addition the latter has a high chemical stability and low price than the former. The consideration that strontium ferrite is superior to barium ferrite may be owing to the accompaniment of little successes for the production of Barium Ferrite powders in a good form.

Barium ferrite in ceramic form find application in various devices such as magnetic memories, circulator, TV York and a variety of other modern devices. Rubber Ferrite Composites (RFCs) are increasingly used in the other devices where flexibility and mouldability is an important criterion. Natural rubber is selected as the matrix for mixing the magnetic filler, which required mechanical and magnetic properties. The evaluation of mechanical and magnetic properties of both the ceramic magnetic filler and rubber are also important since the interrelationship of the properties of the filler and the matrix will help in the design of devices for various applications. It is possible to gather valuable information regarding the matrix filler interaction, dispersion of filler and percolation threshold which are important in determining the physical properties of the composites (Soloman *et al*., 2004).

Recently, Rubber Ferrite Composites are used in the electronic devices and microwave absorber or anisotropic rubber magnets that are expensive. However, the barium ferrite powder, which is the most important raw material for producing such devices, has to import from aboard. Thus, the development of rubber ferrite

composite with the simple synthesized barium ferrite filler by OOPS method will be discussed in this study in order to receive the proper rubber formulation for producing such devices with reasonable prices. Generally, Rubber Ferrite Composites (RFCs) in the markets not only have quite low tensile strength (5-10 MPa) but also quite poor magnetic properties. Nevertheless, the study on the influence of barium ferrite loading on both the mechanical and magnetic properties of RFCs is necessary.

2.1 Effect of commercial barium ferrite loading on cure characteristics

In general, the crosslinking of polymer molecules such as curing is widely used to improve the physical properties of elastomeric materials. The processability and cure parameter were determined by using the Moving Die Rheometer (MDR) that evaluates viscosity, scorch and relaxation. The vulcanization characteristics were refered to a specific curing process of rubber compound involving high heat and the addition of sulfur. Cure characteristics reported of all vulcanization with sulfur system from parameters; namely minimum torque, maximum torque, scorch time and cure time were evaluated.

It has been known that the loading level of the fillers can affect the mooney viscosity, flow behavior, scorch time and cure rate of the rubber compounds (Karian *et al.*, 2003). Scorch time and cure time are also shorter when higher loading is employed. It is thus of interest in this thesis to study the effect of barium ferrite loading, which is a magnetic filler incorporated into natural rubber on cure characteristics in order to receive the proper rubber compound formulation for a wide range of applications.

Table 9 Cure characteristics of rubber compounds with different commercial barium ferrite loading (phr).

Rubber compounds	barium ferrite content (phr)	Cure Characteristics					
		M_L (lb-in)	M_H (lb-in)	ΔM (M_H-M_L)	t_{s2} (min:sec)	t_{c90} (min:sec)	CRI (min^{-1})
RFC 1	0	1.27	5.01	3.74	7.57	11.12	1.18
RFC 2	20	1.09	5.51	4.42	6.55	10.22	1.49
RFC 3	40	1.30	6.21	4.91	6.07	9.43	2.71
RFC 4	60	1.41	6.79	5.38	5.59	9.45	3.20
RFC 5	80	1.42	7.59	6.17	5.10	9.02	3.84
RFC 6	100	1.51	8.20	6.69	3.44	7.26	8.45
RFC 7	120	1.05	7.90	6.85	3.32	6.58	9.07
RFC 8	140	0.83	8.66	7.83	3.25	6.14	9.46

Table 9 summarizes the cure characteristics including minimum torque (M_L), maximum torque (M_H), delta torque (ΔM), scroch time (t_{s2}), optimum cure time (t_{c90}) and cure rate index (CRI) of rubber compounds with different magnetic filler content. The table shows that minimum torque, which is an indirect measure of the viscosity of compound, is slightly increased with increasing commercial Barium Ferrite loading. As well as, the maximum torque (M_H), which is given about the modulus of rubber compound, increased with increasing commercial barium ferrite loading up to 140 phr. The higher M_H with increasing barium ferrite loading was possibly due to high degree of filler-filler interaggregation. It can be noted that delta torque (ΔM) values were comparable with M_L and M_H, which depended mainly on the amount of free curative in the rubber compounds. It has been known that the higher the ΔM, the greater the crosslink formation would be obtained. It was also found from Table 9 that torque value (ΔM) increased with the increase in content of barium ferrite. These results can be explained by the effect of commercial barium ferrite filler which is the hard magnetic filler. When the barium ferrite was incorporated into natural rubber, it increased modulus of rubber compound, probably due to quite great compatibility between the barium ferrite and natural rubber matrix.

As can be seen, the increasing of filler loading contributed to viscosity of rubber compound, which the distance between barium ferrite particles is much closer when we increased the filler loading. The free volume that offers the space for mobility of rubber compound will decrease. The higher viscosity of rubber compound resulted in the increase in the torque values as a result of the increment M_L of rubber compound when barium ferrite was incorporated into natural rubber matrix.

Cure time is defined as the time required for optimum vulcanization of the rubber compound. This is an important parameter as long as the vulcanization is concerned. Evaluation of cure time is a prerequisite for molding the rubber compounds. It was observed from Table 9 as well as Figure 34 that samples loaded with barium ferrite at all contents exhibited shorter both scorch time (t_{S2}) and cure time (t_{C90}) than gum rubber. It can also be seen that scorch time and cure time slightly decreased with increasing barium ferrite loading. The reason for those results might be explained by the fact that barium ferrite powders, which are hard magnetic filler composed of iron particles, can transfer the generated heat during process to each other and might be resulted in the decrease in time for vulcanization (Lokande et $al.$, 2003). Moreover, the dilution effect of rubber when the barium ferrite loading was increased could be the cause of the reduction of scorch time (ts_2) and cure time (tc_{90}).
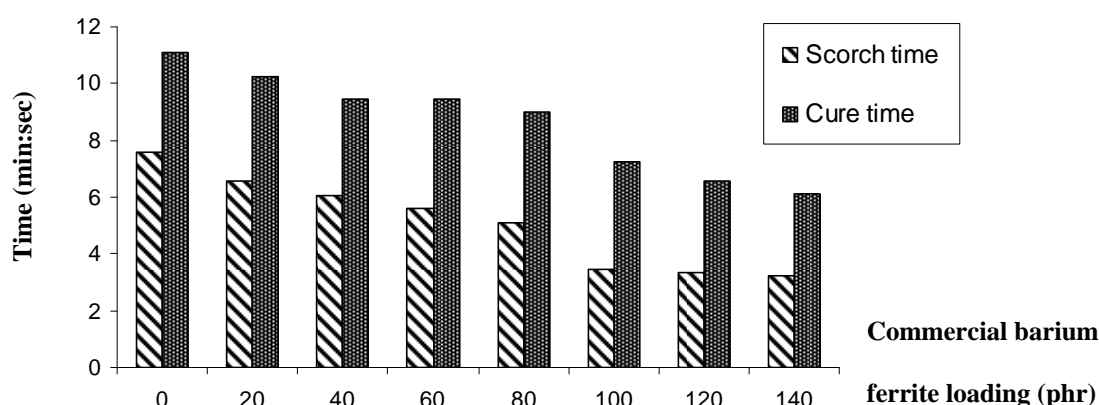
Figure 34 The scorch time (t_{S2}) and optimum cure time (t_{C90}) with different commercial barium ferrite loading.

It is in agreement with the cure rate index (CRI) determination, which is a measure of the rate of the curative reaction given by the following equation (El- Nashar *et al*., 2006):

$$CRI = 100 \, / \, t_{C90} \; x \; t_{S2}$$

It can be observed that CRI (Table 9) increased with increasing barium ferrite filler loading and it supported the activation of the curative reaction after adding barium ferrite, which is metal oxide acting as an accelerator, from 0 phr to 140 phr. As can be seen, CRI data were in good agreement with scorch time and cure time of rubber compounds as discussed earlier.

2.2 Effect of commercial barium ferrite loading on mechanical properties

In this section, the influence of different barium ferrite loading level has been investigated in terms of mechanical properties, morphology and their association. The mechanical properties including tensile properties, compression set and hardness of RFCs containing commercial barium ferrite with various loading, from 0 – 140 phr, in step of 20 are tabulated in Table 10.

Table 10 Mechanical properties of RFCs with different commercial barium ferrite
loading (phr)

Rubber compounds	barium ferrite content (phr)	Mechanical properties			
		Tensile strength (MPa)	100 % modulus (MPa)	300% Modulus (MPa)	Elongation at break (%)
RFC 1	0	15.30±2.40	0.52±0.03	1.02±0.08	691.26±61.30
RFC 2	20	15.59±1.48	0.59±0.02	1.20±0.08	699.37±56.30
RFC 3	40	13.44±1.52	0.70±0.05	1.70±0.17	685.48±33.71
RFC 4	60	16.90±1.85	0.85±0.06	2.26±0.21	656.30±17.58
RFC 5	80	18.53±0.50	0.92±0.03	2.47±0.19	679.03±29.18
RFC 6	100	18.98±1.17	1.05±0.08	2.99±0.34	661.70±35.56
RFC 7	120	16.40±0.70	0.99±0.04	2.85±0.16	639.00±22.00
RFC 8	140	16.40±1.30	1.01±0.06	2.61±0.19	695.00±10.00

From Table 10, it was obviously observed that the addition of magnetic
filler, barium ferrite, has strongly effect on the tensile properties including tensile
strength, modulus and elongation at break of the RFCs. It was found that tensile
strength and modulus of RFCs increased with increasing barium ferrite loading up to
100 phr and then decreased. The tensile strength will increase with increasing filler
loading until maximum point is reached since the filler particles are not adequately
separated or wetted in rubber phase. Furthermore, this could be because the
interaction between barium ferrite and natural rubber matrix was quite high and the
influence of the interaction increased by increasing loading. The high reinforcing
effect of barium ferrite was evident. In fact, the reinforcing effect of filler is more
noticeable at high tensile strength and modulus when it is perfectly dispersed in
matrix since the breakage depends on the amount of weak spot or inhomogeneities in
the vulcanized rubbers. As can be comfirmed by SEM (Figure 35), the dispersion of
reinforcing filler, barium ferrite, in the rubber matrix was quite good, resulting in the
increase in tensile strength when the addition of barium ferrite was increased.
However, tensile strength and modulus of RFCs started to decrease after adding
barium ferrite more than 100 phr as mentioned earlier. It might be explained by the

fact that at higher loading of barium ferrite, filler-filler interaction was responsible for the development of cracks confirmed by the fact that the dispersed particle having irregular shape showed agglomeration after loading of barium ferrite as seen in Figure 35. The SEM micrographs also showed that natural rubber matrix can not be able to hold all content of barium ferrite filler at higher loading (more than 100 phr) making less combination of matrix and filler at high filler loading resulting in the less tensile strength.
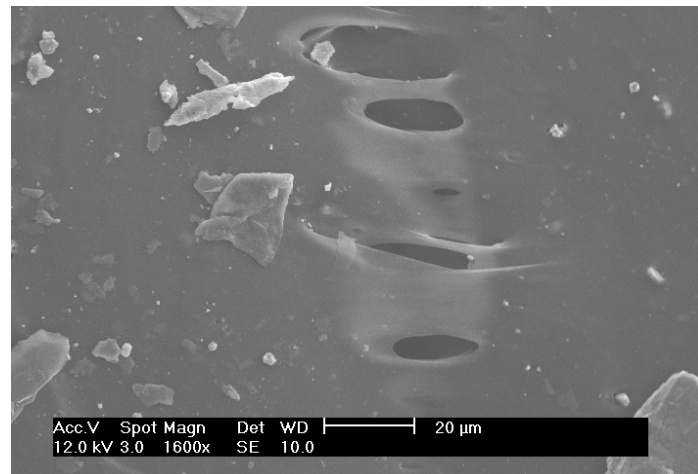
(a) NR without barium ferrite

Figure 35 SEM micrographs of RFCs with different commercial barium ferrite
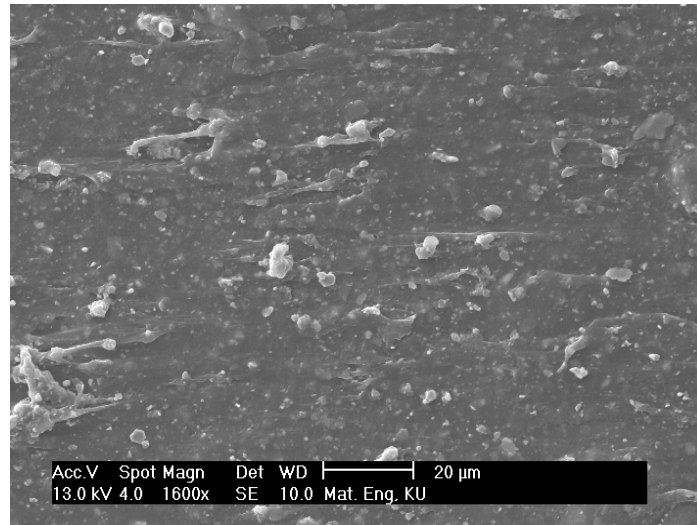
(b) RFC containing 40 phr barium ferrite
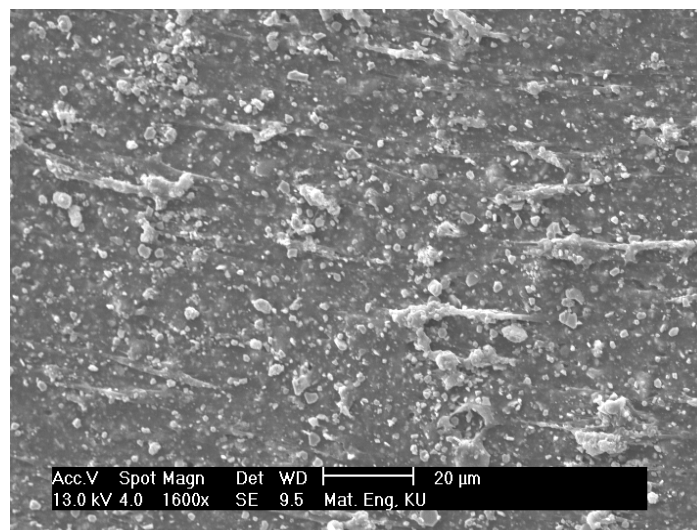
(c) RFC containing 100 phr barium ferrite

Figure 35 (continued) SEM micrographs of RFCs with different commercial

barium ferrite loading (phr)
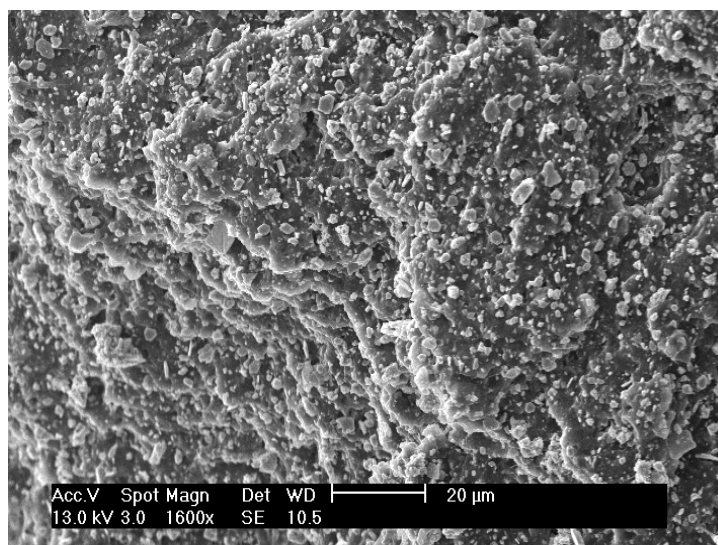
(d) RFC containing 120 phr barium ferrite

Figure 35 (continued) SEM micrographs of RFCs with different commercial barium ferrite loading (phr)
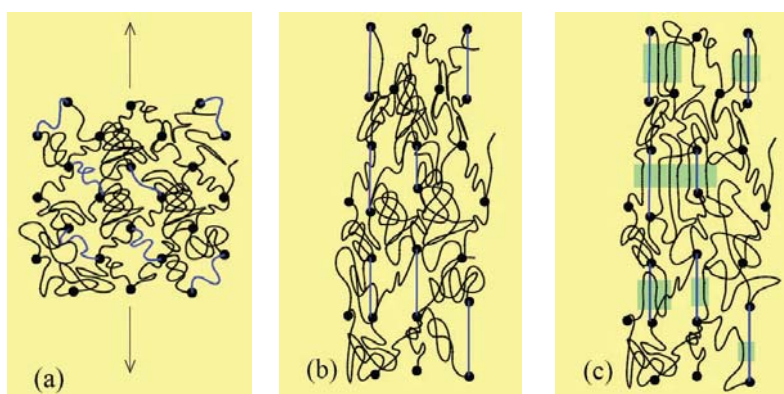
Figure 36 A model of the strain induced crystallization in vulcanized NR
(a) Before deformation. (b) After deformation: short chains are fully stretched. (c) Crystallites are grown from the stretched chains.

Another reason of the reduction in tensile strength when the filler loading of commercial barium ferrite is higher than 100 phr, might be the dilution effect, resulting in the decrease in strain induced crystallization in vulcanized NR as shown in Figure 36. It can be seen that pure NR showed relatively high tensile strength and high elasticity due to self-reinforcing effect caused by strain induced crystallization. Moreover, it should be noted here from the results in Table 10 that, elongation at break of RFCs decreased with increasing barium ferrite loading. It is possibly because the incorporation of filler particles into rubber could reduced the elasticity of the rubber chains due to the reduction of the strain-induced crystallization of NR matrix, leading to lower the elongation at break, Chipara *et al.,* (2004) and Dishovsky *et al.,* (2001).
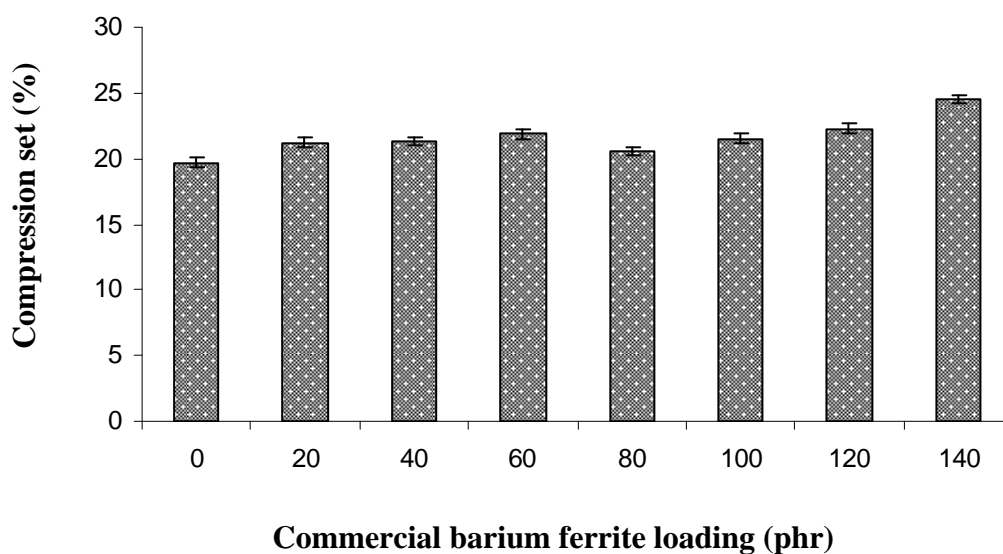
Figure 37 Compression set (%) of RFCs with different commercial barium ferrite loading (phr)

Compression set reflected the residual deformation due to the elastic of rubber under vulcanizate. Generally, the usual measurement of compression set is intended to evaluate delayed elastic recovery. Figure 37 shows the variation of % compression set of RFCs filled with various content of barium ferrite. It was found

that % compression set slightly increased as increasing loading of barium ferrite. The compression set relates with modulus where increasing of commercial barium ferrite diluted NR decreased elasticity (Nielsen, L.E., 1974). It is also expected that the dilution effect of rubber at higher loading of barium ferrite filler might be attributed to the diminishing elastic of composite.
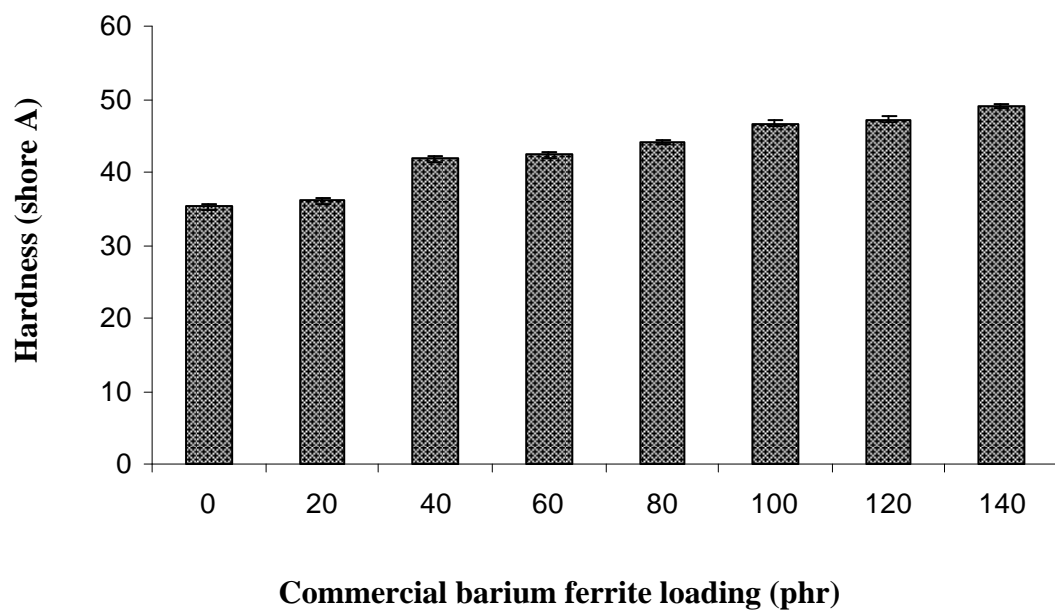
Figure 38 Hardness (Shore A) of RFCs with different commercial
barium ferrite loading (phr)

The hardness (Shore A) of these samples was also studied for different loading of the filler and the result is shown in Figure 38. It shows that the hardness increased with increasing filler loading. It can be explained by the fact that barium ferrite is rigid magnetic filler resulting in the improvement of hardness (Shore A). The result corresponded well with the increase in M_H and the decrease in the elasticity as a result of the increment of % compression set after increasing barium ferrite loading as discussed eariler in Table 9.

2.3 Effect of Thermal Aging on mechanical properties

In this experiment, the effect of thermal aging on the mechanical properties including tensile properties, compression set and hardness of the RFCs prepared from different content of commercial barium ferrite powders was also carried out. The results are shown as the mechanical properties and percentage change of the specimens after thermal aging in an oven at temperature of 100 $^{\circ}$ C for 3 days as represented in Table 11 and Figure 39.

Table 11 Mechanical properties of RFCs with different commercial barium ferrite loading (phr) after thermal aging at temperature of 100 $^{\circ}$ C for 3 days

Rubber compounds	barium ferrite content (phr)	Mechanical properties			
		Tensile strength (MPa)	100 % modulus (MPa)	300% Modulus (MPa)	Elongation at break (%)
Aging RFC 1	0	14.16±2.61 (-7.45%)	0.55±0.02 (5.77%)	1.25±0.07 (22.55%)	728.07±12 (5.35%)
Aging RFC 2	20	16.47±1.72 (5.64%)	0.64±0.04 (8.47%)	1.63±0.14 (35.83%)	713.12±20 (2.00%)
Aging RFC 3	40	17.13±0.89 (27.46%)	0.78±0.03 (11.42%)	2.18±0.11 (28.24%)	699.64±4 (2.04%)
Aging RFC 4	60	11.87±1.61 (-42.38%)	0.79±0.15 (-7.05%)	2.24±0.42 (-0.88%)	608.32±62 (-7.32%)
Aging RFC 5	80	15.17±1.73 (-18.13%)	1.01±0.01 (9.78%)	2.87±0.05 (16.19%)	593.35±23 (-12.67%)
Aging RFC 6	100	15.37±0.93 (-23.16%)	1.05±0.06 (0.00%)	2.89±0.15 (-3.34%)	613.46±9 (-7.83%)
Aging RFC 7	120	17.14±0.61 (4.51%)	1.22±0.06 (23.23%)	4.04±0.21 (41.75%)	598.62±46 (-6.41%)

Note: (….) the percentage change of the specimens after thermal aging

In general, oxidative of elastomers is accelerated by a number of factors including heat, heavy metal contamination, sulfur, light, moisture, swelling in oil and solvent, dynamic fatigue, oxygen, and ozone (Mattiar *et al.*, 2004).

In rubber compounds, temperature causes two competing reactions namely crosslink formation and scission of chains (Vinod *et al.*, 2002).

1. Crosslinking: A predominantly di- or polysulfidic crosslink network break down into monosulfidic crosslinks. The hardness increases, fatigue resistance decreases, and the compound become much stiffer.

2. Chain scission: The polymer chain breaks, causing a softening of the compound and decreased abrasion resistance. Natural rubber tends to show such degradation (James *et al.*,1994).

The effect of temperature on the performance of rubber (tensile strength and modulus) with various degradation reactions was observed in Figure 39. RFCs with barium ferrite filler loading up to 40 phr showed higher retention in tensile strength, after thermal aging at 100 $^{\circ}$ C for 3 days, possibly due to continuing chain vulcanization of the elastomer. Crosslinking of residual curative enhanced the tensile strength and modulus of RFC containing Barium Ferrite up to 40 phr shown as the positive percentage change of specimen after thermal aging seen in Table 11. One of the reasons of the reduction in tensile strength after adding more barium ferrite powders (greater than 40 phr) might be because barium ferrite powders, which are metal oxide, can transfer generated heat to each other causing the high iron concentrations may influence the long-term stability of the materials. Metal oxides, called barium ferrite powders in this study, are known to enhance the oxidation of rubber material. There are some possible explanations for influence the vulcanization reactions (Vinod *et al.*, 2001). Furthermore, the incorporation of barium ferrite particles into the rubber not only results in faster formation of the oxidized, but also in faster degradation within the sample, resulting in the decrease in tensile strength after thermal exposure. The elongation at break slightly decreased

with increasing filler loading due to dilution effect of NR matrix (Mohammed *et al*., 2002).
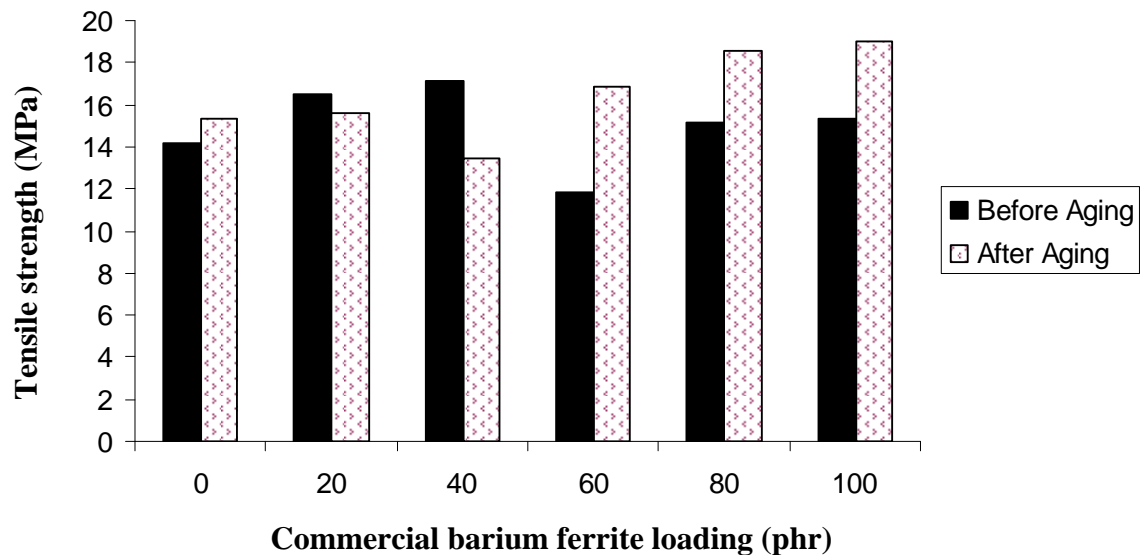
Figure 39 Tensile strength of RFCs with different commercial barium ferrite loading (phr) before and after thermal aging at temperature of 100 $^{\circ}$ C for 3 days

2.4 Magnetic Properties of Rubber Ferrite Composites

Hexagonal barium ferrite powders studied in this section are commercial grade. Prior to prepare RFCs by incorporated commercial barium ferrite powders in rubber matrix, fine powders less than 45 μm were removed by seiving in order to disaggregate the powders. Magnetic properties of RFCs filled with various content of commercial grade barium ferrite compared with the commercial barium ferrite were determined by means of a Vibration Sample Magnetometer (VSM). The values obtained from VSM measurements are shown in Table 12.

2.4.1 Effect of commercial barium ferrite loading on magnetic properties

Table 12 Magnetic properties of RFCs with different commercial

barium ferrite loading (phr)

Rubber Compound	barium ferrite loading (phr)	Coercivity (H_{ci}) (G)	Saturation Magnetization (M_s) (emu/g)	Magnetic Remanence (M_r) (emu/g)
RFC 1	0	769.54	7.7887×10^{-3}	362.37×10^{-6}
RFC 2	20	3179.3	11.369	6.6841
RFC 3	40	3225.3	15.273	9.4138
RFC 4	60	3141.2	27.186	15.881
RFC 5	80	3068.4	30.383	17.096
RFC 6	100	3208.9	30.447	18.487
$BaFe_{12}O_{19}$ powder	-	2393.7	59.442	45.111

Table 12 shows the variation of the magnetic properties for RFCs as a function of ferrite loading. It can be observed that the magnetic properties, including coercivity (H_{ci}), saturation magnetization (M_s) and magnetic remanence (M_r) of the RFCs dramatically increased compared with those of the gum rubber. Moreover, the commercial barium ferrite loading has considerably effect on the magnetic properties of RFCs, as a result of the magnetic properties of RFCs increased with increasing barium ferrite content incorporated in natural rubber matrix. Nevertheless, the saturation magnetization (M_s) and magnetic remanence (M_r) of RFCs filled with barium ferrite at all contents (from 20 to 100 phr) were lower than those of commercial barium ferrite powder.

Moment/mass (emu/g)
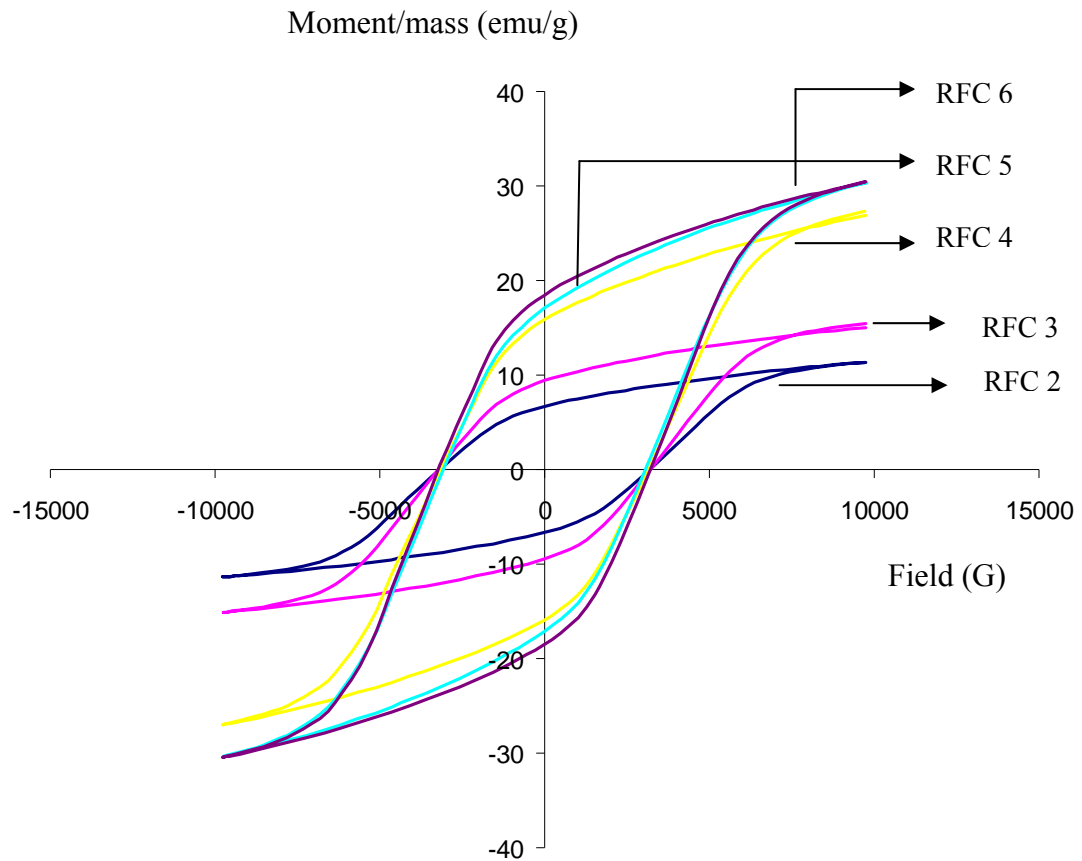
Figure 40 Magnetic Properties for RFCs with different commercial barium ferrite
filler loading (phr)

The increase in saturated magnetization (M_s) of RFCs with increasing
barium ferrite loading as shown in Figure 40, may be resulting from (1) the
desegregation of the filler caused by removing the fine powders prior to mixing, (2)
the high degree of mixing which is a critical factor in controlling the magnetic and
mechanical properties of polymers bonded magnets and (3) the fact that the present
magnetic particles as a filler are relatively large in size, randomly oriented,
uniformly dispersed and isolated from each other as seen from SEM in Figure 35.
The latter will lead to reduce the surface energy of the particles, which control the
mean distance between particles during a mixing process. So there is no tendency to
form agglomerates in the RFCs even at a relatively high loading level,
Lokander *et al.*, (2003) and Soloman *et al.*, (2004).

. The specific saturation magnetization, M_{rfc}, of RFCs is found to be linearly dependent on the mass fraction of ferrite and to obey a general relation as seen in equation.

$$M_{rfc} = M_f W_f$$

Where: M_f and W_f are the saturation magnetization and weight
fraction of the filler, respectively.

2.4.2 Effect of Thermal aging on magnetic properties

The influence of thermal aging (Aging RFC 6) on magnetic properties of Rubber Ferrite Composites filled with 100 phr commercial barium ferrite compared with the one without aging (RFC 6) is shown in Figure 41. The magnetic properties of saturation magnetization (M_s) and magnetic remanence (M_r) slightly increased after thermal aging. It might be explained by the fact that thermal aging influenced the defect of commercial powder in the perfect hexagonol shape, the randomly domain oriented in the order of change parallel to the phase of ferromagnetism (Makled *et al.*, 2004).
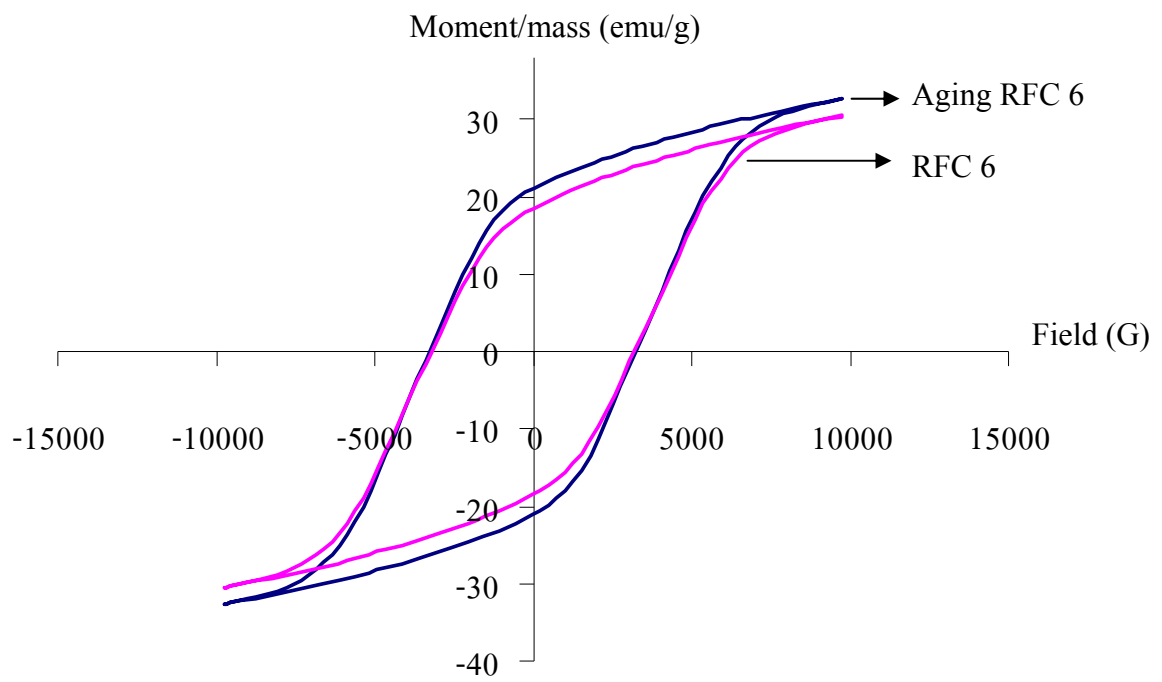
Figure 41 Comparison magnetic properties of RFCs with commercial barium ferrite
100 phr before and after thermal aging at temperature of 100 ^{o} C for 3 days

3. Comparison the magnetic and mechanical properties of RFCs filled with commercial and synthesized barium ferrites by OOPS method.

    3.1 Cure characteristics

        Cure characteristics of the filled rubber were significantly influenced by filler morphology such as particle size, microstructure and surface activity. That effects show the incorporation of filler in NR matrix. This section was aimed to investigate the cure characteristics of rubber compounds filled with synthesized barium ferrite calcined at 1000 $^\circ$ C for 2, 5, and 8 h compared with those filled with commercial grade barium ferrite at the same amount of loading (100 phr).

        Cure characteristics including minimum torque (M_L), maximum torque (M_H), delta torque (ΔM), scroch time (t_{s2}), optimum cure time (t_{c90}) of all rubbers containing 100 phr barium ferrite, are summarized in Table 14. It was found that rubber compound mixed with commercial grade of barium ferrite gave high values of both maximum and minimum torques compared to others. It can be said that because the commercial barium ferrite has small particle size and high surface area (Table 7), giving the better dispersion in NR matrix than others. The higher surface area of the filler, the greater rubber–filler interaction is expected. The influence of interaction between rubber-filler in rubber compound filled with commercial barium ferrite may be resulted in higher maximum and minimum torque than rubber compound mixed with synthesized barium ferrite.

Table 13 Cure characteristics of rubber compounds with different types of barium
ferrite (commercial grade and synthesized OOPS)

Rubber compounds	Time for precursor calcination (h)	Cure Characteristics				
		M_L (lb-in)	M_H (lb-in)	ΔM (M_H-M_L)	t_{s2} (min:sec)	t_{c90} (min:sec)
RFC 6_commercial	-	1.51	8.20	6.69	3.44	7.26
RFC 6_OOPS 2	2	1.08	7.81	6.73	3.39	7.05
RFC 6_OOPS 5	5	0.70	7.79	7.27	3.02	6.52
RFC 6_OOPS 8	8	0.53	7.51	6.98	2.49	6.13

However, it can be seen from Table 13 and Figure 42 that the
calcination time does not show signification effect on the cure characteristics of
rubber compounds.   It was found that the rubber compounds containing the
synthesized barium ferrite (OOPS method) calcined at 1000 ^{o} C for 2, 5, and 8 h
gave the comparable values of cure characteristics to one another.
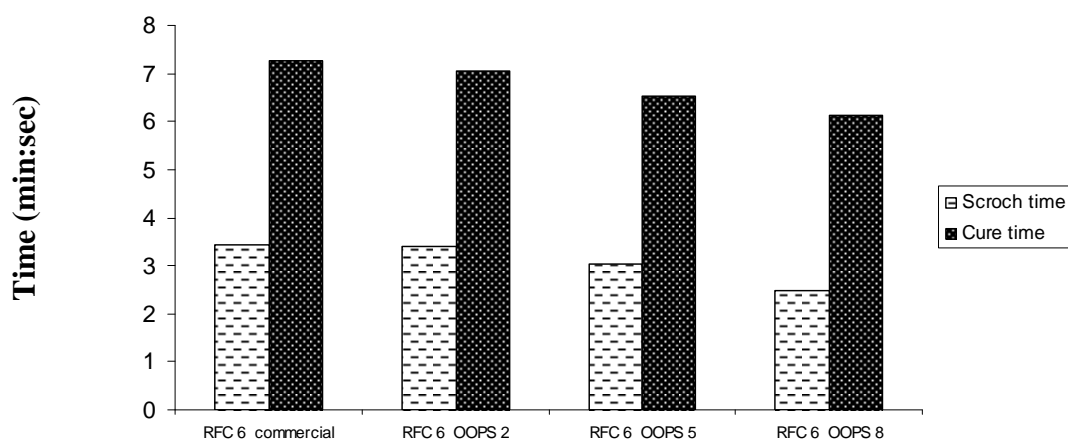
Figure 42 The scorch time (t_{s2}) and optimum cure time (t_{c90}) of rubber compound
with different types of barium ferrite

3.2 Mechanical properties RFCs with different types of barium ferrite (commercial grade and synthesized OOPS)

The mechanical properties including tensile properties and hardness of RFCs containing 100 phr of barium ferrite (commercial grade and synthesized OOPS) are shown in Table 14 and Figure 42. These properties were strongly influenced by the size, surface area, shape, loading and dispersion of the magnetic fillers, (Makled *et al.*, 2005) as well as the matrix properties and the interfacial adhesion between the filler and polymer matrix. The particle sizes of fillers in this study (barium ferrite) are relatively in the range of 17-28 μm (Table 7). Surface activity relates to the compatibility of the filler with a specific elastomer and the ability of the elastomer to adhere to the filler.

Table 14 100 % , 300% modulus, elongation at break (%) and hardness of RFCs with different types of barium ferrite (commercial grade and synthesized OOPS)

Compound rubber	barium ferrite loading (phr.)	100% modulus (MPa)	300% modulus (MPa)	Elongation at break (%)	Hardness (Shore A)
RFC 6	100	1.05±0.08	2.99±0.34	661.70±35.56	46.6±0.40
RFC 6-OOPS, 2h	100	1.02±0.07	2.07±0.22	550.48±25.24	36.5±0.30
RFC 6-OOPS, 5h	100	1.00±0.07	2.16±0.24	553.34±32.06	34.5±0.40
RFC 6-OOPS, 8h	100	0.96±0.02	2.54±0.26	564.73±16.92	34.6±0.02
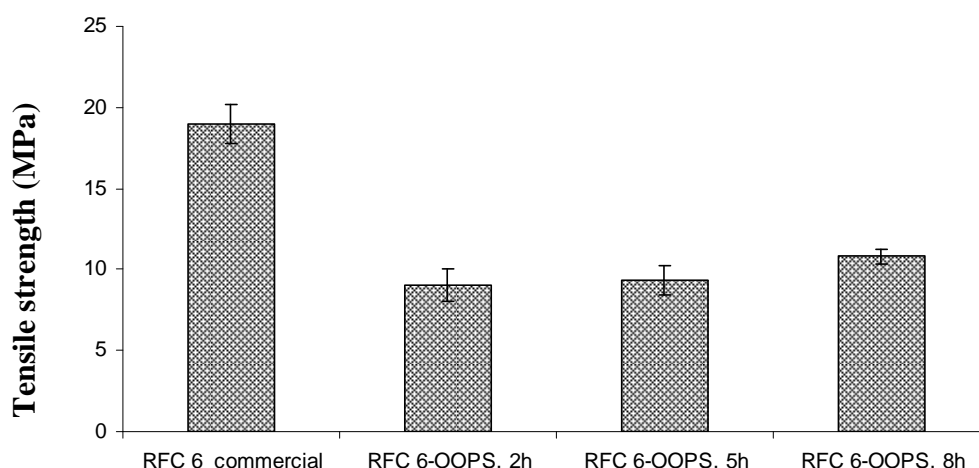
Figure 43 Tensile strength of RFCs with different types of barium ferrite
(commercial grade and synthesized OOPS)

It was found that mechanical properties including tensile strength, 100%, 300% modulus, elongation at break and hardness of RFCs mixed with commercial grade of barium ferrite were greater than those containing barium ferrite synthesized by OOPS calcined at 1000° C for all calcination time (2, 5 and 8 h) at the same loading (100 phr). The reason for that might be the fact that particle size of the barium ferrite powders synthesized by OOPS was larger than commercial barium ferrite, resulting in the weak interaction between the ferrite and rubber matrix. It seems reasonable then that this stress transfer will be better effected if the filler particles were smaller, because greater surface was thereby exposed for a given filler concentration. A compound's physical/mechanical properties can be strongly influenced by the surface activity of the filler, which is the ability of the filler's surface to bond with the matrix, for instance, an air gap between a filler particle and the matrix. The filler must make intimate contact with the elastomer chains if it is going to contribute to reinforcement of the rubber-filler composite. Fillers that have a high surface area have more contact area available, and therefore have a higher potential to reinforce the rubber chains. As can be seen from Figure 43, RFCs containing synthesized Barium Ferrite calcined for 8 h gave the highest tensile strength compared with those calcined for 2 and 5 h, as a result of the larger surface area as shown in Table 7.

However, it should be noted here that hardness of RFCs filled with synthesized barium ferrite calcined at 1000 $^{\circ}$C for all different calcination time was less than those filled with commercial grade of barium ferrite. It is thus of interest to further improve the hardness of RFCs containing synthesized barium ferrite. It will be discussed in the next section.

3.3 Magnetic properties of RFCs with different type of barium ferrite (commercial grade and synthesized OOPS)

Table 15 Magnetic properties of RFCs with different types of barium ferrite
(commercial grade and synthesized OOPS)

Compound rubber	barium ferrite (phr)	Coercivity (H_{ci}) (G)	Saturation Magnetization (M_s) (emu/g)	Magnetic Remanence (M_r) (emu/g)
RFC 6	100	3208.9	30.447	18.487
RFC 6-OOPS, 5h	100	3602.7	36.813	22.118
RFC 6-OOPS, 8h	100	3942.0	44.809	27.042

Table 15 displays the magnetic properties of RFCs containing synthesized barium ferrite calcined at 1000 $^{\circ}$C for 5 and 8 h compared with those of RFCs filled with commercial grade of barium ferrite at the same amount of filler loading (100 phr). It was obviously observed from Table 15 that RFCs with synthesized barium ferrite gave higher magnetic properties including saturation magnetization (M_s), magnetic remanence (M_r) and coercivity (H_{ci}) than RFCs with commercial barium ferrite. These results were consistent with the results obtained from the study of magnetic properties of barium ferrite powders synthesized by OOPS showing in Table 8 that the magnetic properties of barium ferrite were higher when increasing the calcination time from 2 to 8 h. The effect of calcination temperature on the magnetic properties was in a good agreement with the intensity of hexagonal $BaFe_{12}O_{19}$ phase at 30.31-34.10 of 2-theta degree of Barium Ferrite calcined at 1000 $^{\circ}$C for 2, 5 and 8 h seen from XRD pattern (Figure 30). It was

found that the high intensity of hexagonal $BaFe_{12}O_{19}$ phase related to the increase in the calcination time that required to yield hexagonal $BaFe_{12}O_{19}$ with high magnetic properties (Kim *et al.*, 2007).

4. The effect of carbon black loading in rubber composite incorporated with fixed commercial barium ferrite loading level at 100 phr

4.1 Effect of carbon black loading on cure characteristics

The development of rubber ferrite composite will be useable in devices for various applications. Generally, the rubber magnets are usually employed in a machine thus, the rubber ferrite composites (RFCs) must be durable and hard where the most important properties to use in primary application. Practically, reinforcing fillers, along with other essential chemicals, are incorporated into natural rubber prior to the vulcanization process. Recent studies (Soloman, M.A., 2004) have indicated that the addition of carbon black to RFCs enhanced cure characteristics and mechanical properties of the composites. In this section, the studies involve the incorporation of carbon black along with fixed commercial grade of Barium Ferrite fillers at 100 phr in rubber matrix. Hence, RFCs containing carbon black were prepared for various loading, namely 10, 20, 30 and 40 phr. The effect of carbon black loading on the cure characteristics and mechanical properties of RFCs containing 100 phr commercial grade of barium ferrite was then investigated.

Table 16 Cure characteristics of rubber compounds with different loading of carbon black mixed with fixed commercial barium ferrite in natural rubber

Rubber compounds	Content of filler (phr)		Cure Characteristics				
	barium Ferrite	carbon black	M_L (lb-in)	M_H (lb-in)	ΔM (M_H-M_L)	t_{s2} (min:sec)	t_{c90} (min:sec)
RFC 6_CB 0	100	-	1.51	8.20	6.69	3.44	7.26
RFC 6_CB 10	100	10	0.74	8.01	7.27	4.14	10.20
RFC 6_CB 20	100	20	0.63	8.14	7.51	3.41	9.44
RFC 6_CB 30	100	30	0.91	9.42	8.51	3.04	9.23
RFC 6_CB 40	100	40	1.36	10.43	9.07	2.58	8.58

Cure characteristics have a very important effect on healing time since the onset of crosslinking (scorch) or a time to cure of process (cure time) will limit the amount of healing that can move. The cure characteristics at different condition are shown in Table 16. Scorch times at different levels of torque rise were measured. Comparison of rubber compound incorporated with fixed content of commercial barium ferrite at 100 phr mixed with different carbon black loading (10, 20, 30 and 40 phr) was investigated. As expected, the M_H and ΔM of rubber compound without carbon black (RFC 6_CB 0) was less than rubber compounds mixed with carbon black at all loading (Eskandari *et al*., 2009 and Godin *et al*., 2009). This result indicated that carbon black influenced the maximum torque, in that the effective shear modulus of the composite increased steadily with the volume ratio of the filler added. Thus, the higher volume fraction of carbon black leads to a higher shear modulus, as indicated in this Table 16.
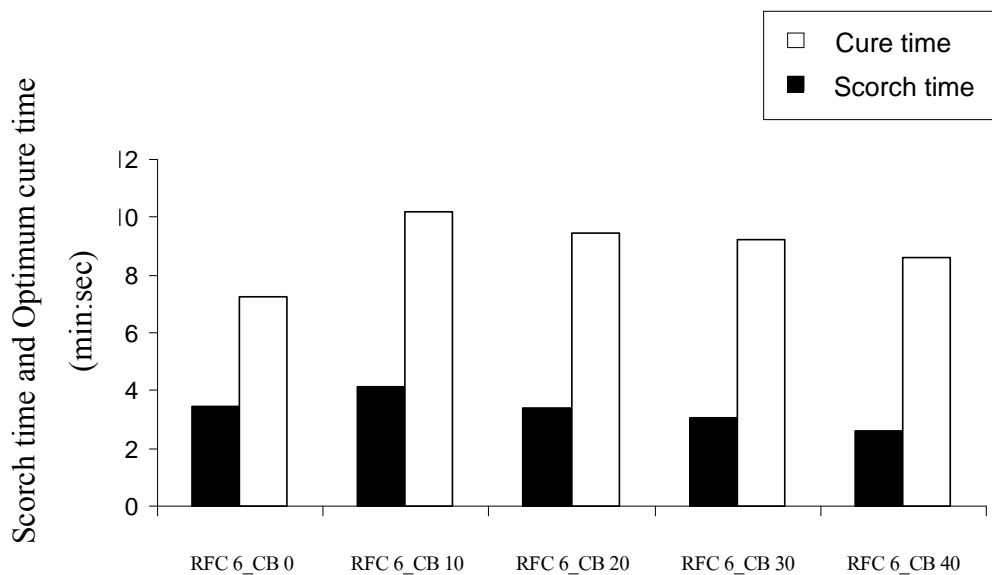
Figure 44 The effect of carbon black loading on scorch time (t_{s2}) and optimum cure time (t_{c90}) of rubber compounds with fixed commercial barium ferrite loading at 100 phr

From Table 16 and Figure 44, the incorporation of carbon black increased the mooney viscosity of rubber. The viscosity was increased with respect to the amount of carbon black. The high surface area of carbon black generates more heat buildup in the compounds under shear conditions in the kneader. When a higher amount of fillers is used, heat is also generated in the system since the compound tends to be more viscous. As a consequence, the vulcanization reaction can occur more readily so that the mooney viscosity increased while the scorch time and cure time were shortened. However, rubber compound mixed with 100 phr barium ferrite without carbon black showed less scorch time (t_{s2}) and cure time (t_{c90}) than the one mixed with carbon black. The reason for that might be because the sample including only magnetic particles without carbon black showed a poor bond between the magnetic particles and the rubber, with many voids existing between the two phases. When some carbon black was added, the bond is improved. When more carbon black was added, the magnetic particles were embedded in and well bound with the rubber matrix. Moreover, the decrease in scorch time and cure time with increasing carbon black content due to the dilution effect of NR that decreased the time to cure. That was found a decrease in scorch time with increasing carbon

black content. This is due to the restriction of mobility and deformability of the matrix with the introduction of mechanical restraint. It is widely known that the presence of CB reduces the scorch time; also its role as a basic catalyzed accelerating the curative. This observation is caused by the fact that the carbon black (N330) is reinforcing filler which has good surface activity, chemical properties and non-uniform of porous surface which contribute to maximum interphase interaction between polymer chain and filler, Accorsi *et al.*, (1999) and Chen *et al.*, (2008)

4.2 Effect of carbon black loading on mechanical properties

Soloman *et al.*, (2004) and Kurian *et al.*, (2003) indicated that the addition of carbon black to RFCs enhanced mechanical properties of the composites. It is thus aimed in this study to improve the mechanical properties of RFCs by the incorporation of carbon black at different loading. The influence of carbon black loading level on the mechanical properties, namely tensile strength, 100 and 300% modulus and elongation at break of RFCs with fixed barium ferrite loading at 100 phr has been conducted by varying the amount of carbon black from 10-40 phr in step of 10. The results are displayed in Table 17.

Table 17 Mechanical Properties RFCs incorporated with 100 phr of commercial grade barium ferrite and mixed with different carbon black loading (phr)

Rubber compounds	Content of filler (phr)		Mechanical properties			
	barium ferrite	carbon black	Tensile strength (MPa)	100 % modulus (MPa)	300% Modulus (MPa)	Elongation at break (%)
RFC 6_CB 0	100	-	18.98±1.17	1.05±0.08	2.99±0.34	661.70±35.56
RFC 6_CB 10	100	10	14.71±0.60	1.29±0.08	4.75±0.32	553.45±19.33
RFC 6_CB 20	100	20	15.51±1.31	1.05±0.02	3.57±0.11	677.34±82.38
RFC 6_CB 30	100	30	16.92±0.63	2.01±0.12	7.65±0.60	494.84±12.60
RFC 6_CB 40	100	40	16.02±0.70	1.85±0.09	6.94±0.35	492.53±12.84

It was found from Table 17 that the addition of carbon black deteriorated tensile strength of RFCs, as a result of the reduction in tensile strength of RFCs containing carbon black at all loading compared with RFC without carbon black. It might be explained by the poor interaction between barium ferrite filler and carbon black. This is because inner voids occupy the place of magnetic particles and lead to a decrease in the volume of magnetic particles. Moreover, the decrease of tensile strength is due to the reduction of the stress-induced crystallization of the NR matrix by the initial loading of the filler and the maximum loading of filler loading of carbon black at 30 phr.

However, it can be seen that tensile strength of rubber ferrite composite slightly increased with increasing carbon black loading up to 30 phr and then tensile strength decreased. The reduction of tensile strength after adding high amount of carbon black at 40 phr can be attributed to the fact that the network of forked crack branches, direction of crack propagation influenced tensile strength was dropped. The explanation can be confirmed by SEM micrographs as shown in Figure 45. The dilution effect of NR was one of the reasons of the reduction in tensile strength since the filler particles are not wetted in rubber matrix resulting in the agglomeration between ferrite-ferrite interaction rather than rubber-ferrite interaction.
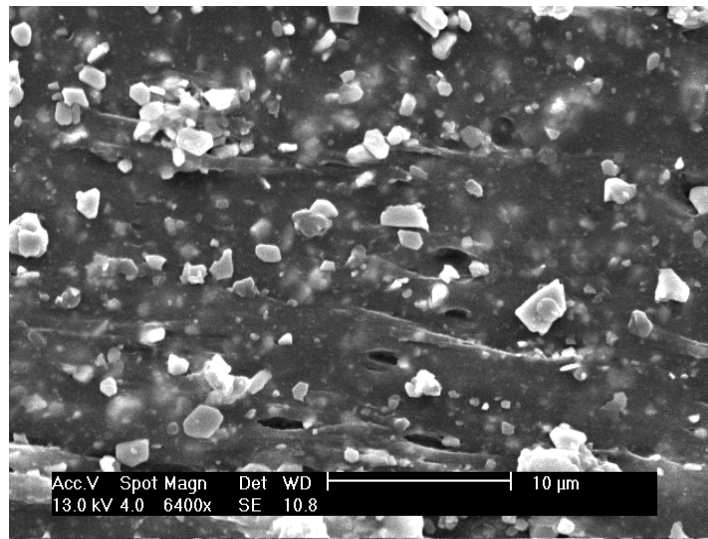
(a) RFC (100 phr of commercial barium ferrite) containing 10 phr of carbon black
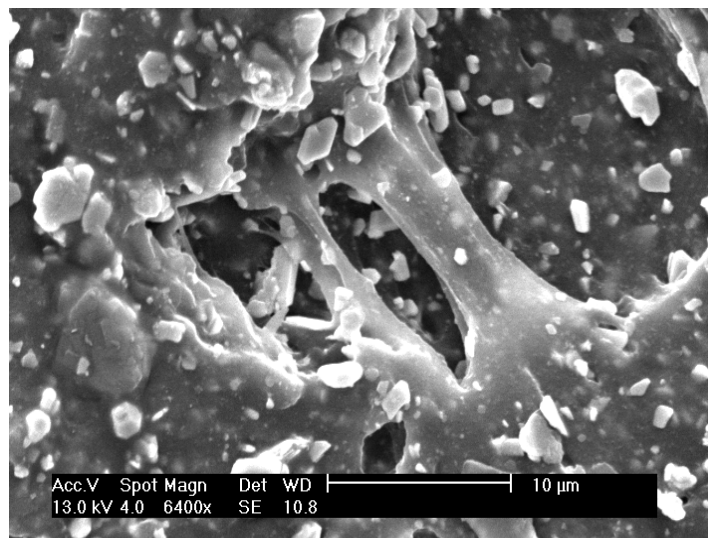
(b) RFC (100 phr of commercial barium ferrite) containing 20 phr of carbon black

Figure 45 SEM micrographs of RFCs incorporated with 100 phr of commercial
barium ferrite loading and mixed with different loading of carbon black

(c) RFC (100 phr of commercial barium ferrite) containing 30 phr carbon black
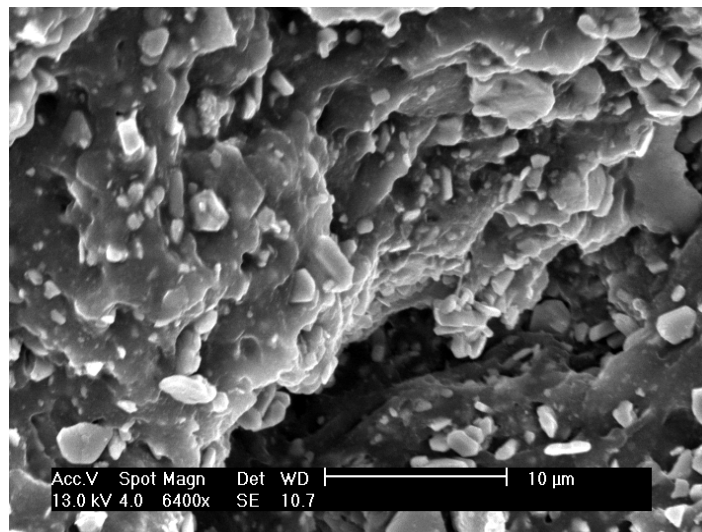
(d) RFC (100 phr of commercial barium ferrite) containing 40 phr carbon black

Figure 45 (continued) SEM micrographs of RFCs incorporated with 100 phr of commercial barium ferrite loading and mixed with different loading of carbon black (phr)
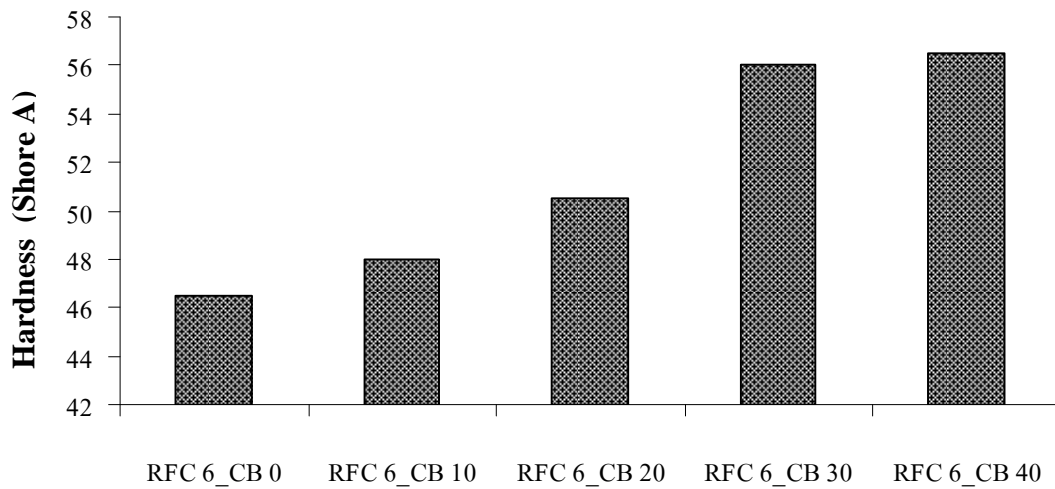
Figure 46 Hardness (Shore A) of RFCs incorporated with 100 phr of commercial grade barium ferrite and mixed with different carbon black loading (phr)

As can be seen in Table 17 and Figure 46, modulus and hardness (Figure 46) of RFCs increased with increasing of carbon black loading. It can be explained that carbon black is reinforcement filler and can disperse quite well in natural rubber matrix resulting in an enhancement of shear modulus of RFCs giving the increase in 100% and 300% modulus after the increment of carbon black loading. The results were consistent quite well with the increase in the maximum torques (M_H) discussed earlier in Table 15. It was found that the Einstein – Guth – Gold equation could be explained to the filled vulcanizates over wide range of strains if the effective volume of the filler was introduced (El-Sabbagh et al., 2006).

$$\sigma_f = \sigma_0(1 + 2.5f\,\Phi + 14.2\,f^2\Phi^2)$$

with $\qquad \Phi_{\text{eff}} = f\,\Phi$

Where : σ_f =   the modulus of the filled vulcanizate

σ_0 =   the modulus of gum

Φ =   the volume fraction of the filler

Φ_{eff} =   the effective volume fraction of filler

f =   the effectiveness factor for transforming Φ into Φ_{eff}

However, in terms of elongation at break of RFCs, it was found that elongation at break decreased with increasing carbon black loading as shown in Table 16. It is believed that it might be because of the dilution effect of NR matrix, resulting in the decrease in elasticity with increasing filler loading. It should be noted here that the decrease in elongation at break as a result of a reduction of elasticity after the increase in carbon black loading was in good agreement with the increase in modulus and hardness of RFCs as discussed earlier.

As mentioned earlier, RFCs with barium ferrite synthesized by OOPS method gave lower mechanical properties, including tensile properties and hardness than RFCs filled with commercial grade of barium ferrite. It is thus our purposed to further improve those properties of the RFCs containing barium ferrite synthesized by OOPS method by the addition of carbon black into the natural rubber matrix filled with fixed amount of synthesized barium ferrite at 100 phr. In this case, the amount of incorporated carbon black was fixed at 30 phr. The influence of incorporation carbon black at 30 phr on the cure characteristics and mechanical properties of RFCs filled with synthesized Barium Ferrite has been obtained.

Table 18 Cure characteristics of rubber compounds with containing 30 phr of carbon black mixed with 100 phr loading of synthesized barium ferrite (OOPS)

Rubber compounds	filler loading (phr)		Cure Characteristics				
	barium ferrite	carbon black	M_L (lb-in)	M_H (lb-in)	ΔM (M_H-M_L)	t_{s2} (min:sec)	t_{c90} (min:sec)
RFC 6-OOPS, 8h	100	-	0.53	7.51	6.98	2.49	6.13
RFC 6_OOPS, 8h+CB	100	30	0.96	10.07	9.11	2.54	8.54

The cure characteristics including M_L, M_H, ΔM, scorch time and optimum cure time of rubber compound filled with 30 phr carbon black were compared with those of the one without carbon black loading (Table 18). As expected, the M_H and ΔM of RFCs (mixed with synthesized OOPS barium ferrite powders) containing 30 phr of carbon black were greater than those of rubber compounds without carbon black. This result indicated that carbon black influenced the maximum torque, and the effective shear modulus of the composite increased.

Moreover, it was found that the incorporation of carbon black into the RFCs filled with 100 phr barium ferrite synthesized by OOPS method gave prolong scorch time (t_{s2}) and optimum cure time (t_{c90}) compared with RFCs without carbon black loading.

Table 19 Mechanical properties of RFCs containing 30 phr of carbon black mixed with 100 phr loading of synthesized barium ferrite (OOPS)

Rubber compounds	carbon black content (phr)	Mechanical properties			
		Tensile strength (MPa)	100 % modulus (MPa)	300% Modulus (MPa)	Elongation at break (%)
RFC 6-OOPS, 8h	0	10.82±1.03	0.96±0.02	2.54±0.26	564.73±16.92
RFC 6-OOPS, 8h+CB 30	30	11.02±0.53	1.80±0.03	6.20±0.75	417.32±44.53

The incorporation of carbon black into the natural rubber matrix filled with synthesized barium ferrite influenced not only on the cure characteristics of rubber compounds as shown previously, but also on the tensile properties as well as hardness of the RFCs as seen in Table 19 and Figure 47. It was found that the incorporation of carbon black is known to reinforce the matrixes that can be enhanced the 100 % and 300 % modulus and stiffness of RFCs. Also, it was observed that there was the decrease in the elongation at break of RFCs containing 30 phr of carbon black compared with RFCs without carbon black. It is probably due to the dilution effect because the addition of carbon black diluted volume fraction of NR matrix. It should be noted here that the addition of carbon black showed no significant effect on tensile strength. Nevertheless, it was successfully improved hardness of RFCs by the incorporation of 30 phr carbon black into rubber matrix as shown in Figure 47.
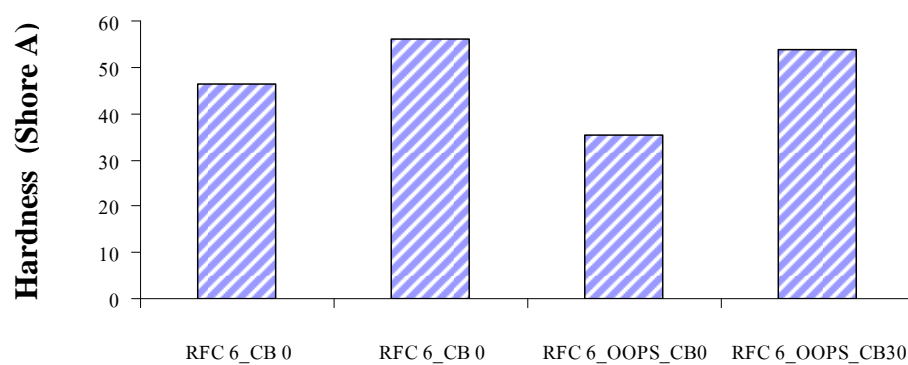
Figure 47 Hardness (Shore A) of RFCs containing 30 phr of carbon black
mixed with 100 phr loading of synthesized barium ferrite (OOPS)

CONCLUSION

The purpose of this study was to prepare the Rubber Ferrite Composites (RFCs) from barium ferrite synthesized by the Oxide One Pot Process (OOPS) method compared with RFCs containing commercial grade of barium ferrite for selected application, especially in magnet sheet. The effect of barium ferrite (commercial grade) on the cure characteristics, mechanical and magnetic properties of RFCs was investigated. It was observed that commercial barium ferrite loading has strongly influenced on cure characteristics of rubber compounds. The scorch time and optimum cure time increase with increasing barium ferrite content. It was also found that tensile strength of RFCs show the optimum value at 100 phr barium ferrite loading. However, the incorporation of higher barium ferrite loading (more than 100 phr) into rubber matrix has decreased tensile properties of the RFCs because agglomeration of filler might be appeared and the incorporation of filler particles into rubber could reduce the elasticity of the rubber chains due to the reduction of the stress- induced crystallization of NR matrix. Moreover, elongation at break of RFCs decreases, whereas compression set of RFCs increases with increasing filler loading as a result of the reduction in the elasticity of the rubber chains. The influence of thermal aging on the mechanical properties of RFCs was also undertaken. It was found that at barium ferrite loading up to 40 phr, crosslinking phenomenon is dominant for causing the change in mechanical properties of RFCs, whereas at higher barium ferrite loading the change in mechanical properties was predominantly due to chain scission. In addition, it was observed that magnetic properties including Saturation Magnetization (M_s) and Magnetic Remanence (M_r) obviously increase with increasing barium ferrite loading.

Barium ferrite synthesized by OOPS method was prepared at different calcined temperatures from $600\,^{\circ}$C to $1200\,^{\circ}$C for 2 h. It was found that the higher calcined temperature, the better magnetic properties. Even though, barium ferrite calcined at $1000\,^{\circ}$C gives hexaferrite phase along with hematite phase, making hexagonal barium ferrite with lower purity than the one calcined at $1200\,^{\circ}$C, the temperature for calcination of interest in this study was still at $1000\,^{\circ}$C. The effect of

calcination time (2, 5 and 8 h) on the barium ferrite calcined at $1000\,^{\circ}C$ on the mechanical and magnetic properties was studied. It was found that the higher the time for calcination, the greater the tensile strength of RFCs filled with barium ferrite calcined at $1000\,^{\circ}C$. However, the calcination time does not show significant effect on the hardness of RFCs. It was also found that tensile properties and hardness of RFCs mixed with commercial grade barium ferrite are greater than those of RFCs containing synthesized OOPS barium ferrite. In order to improve the mechanical properties of RFCs with OOPS barium ferrite, the incorporation of carbon black into the rubber matrix filled with 100 phr of commercial grade of barium ferrite was investigated. It was found that the incorporation of 30 phr carbon black considerably improves the hardness of RFCs. In terms of magnetic properties, as expected it was observed that the higher the calcination time from 2 to 8 h, the greater the magnetic properties of RFCs are. It should be noted here that the magnetic properties of RFCs with OOPS barium ferrite is obviously higher than those of RFCs with commercial grade of barium ferrite. That is to say there is the high possibility of replacing the commercial barium ferrite with the one synthesized by OOPS method for producing the rubber magnet sheet.

LITERATURE CITED

Accorsi, J.V. 1999. The Impact of Carbon Black morphology and dispersion on The weather ability of Polyethylene. n.p. **Symposium on the International Wire & Cable.** Cabot Corporation Billerica, Massachusetts, United State of America

Akiba, M. and D. Chakravorty. 1997. Nanocrystalline magnetic alloys and ceramics. **J. Sadhana.** 28:283-297

Benito, G., M.P. Morales, J. Requena, V. Raposo, M. Vazquez and J.S. Moy**.** 2001. Barium hexaferrite monodispersed nanoparticles prepared by the ceramic method**. Journal of Magnetism and Magnetic Materials .** 234:65-72

Brannen, C.L. 2006. Donor-Acceptor Contributions to Ferromagnetic Exchange Coupling within Heterospin Biradicals. **University of North Carolina State.** North Carolina. n.p.

Chen, L., X.L. Gong and W.H. Lib**.** 2008. Effect of carbon black on the mechanical performances of magnetorheological elastomers**. Journal of Polymer Testing.** 27:340-345

Chipara, M., D. Hui, J. Sankar, D. Leslie-Pelecky, A. Bender, L. Yue, R. Skomski and D.J. Sellmyer. 2004. On styrene–butadiene–styrene–barium ferrite nanocomposites**. J. Composites: Part B.** 35:235-243

Dishovsky, N., K. Ruskova and I. Radulov. 2001. "In situ" Magnetic Modification of Polar Elastomers. **Journal Materials Research Bulletin.** 36: 34-45.

El-Nashr, D.E., S.H. Mansour and E. Girgis. 2006. Nikel and Iron nano particles in Natural Rubber Composites. **J. Journal Mater Sci**. 41: 5359-5364.

El-Sabbagh, S.H., N.M. Ahmed, and W.M. Daoush. 2006. Colored Rubber
Vulcanizates with Some Magnetic Properties. **Journal of Applied Polymer
Science**. 102: 494-505

Eskandari, M.and H. Arastoopour. 2009. Studying the pulverization mechanisms of
low-cross-link-density Natural Rubber with and without Carbon black.
Journal of Powder Technology. 189:454-461

Flavio de Campos, M. n.d. Effect of Grain Size and Crystalline Orientation on the
Coercivity of Sintered Magnets. **Instituto Nacional de Metrologia.** Duque
de Caxias. RJ. Brasil

Godin, N., S. Chaki, J. Courbon, S. Deschanel, S. Gillet and B. Gautier. 2009.
Acoustic Emission Potentialities for Characterization of Mullins Effect in
Natural Rubber Materials filled with Carbon Black. **Journal of Polymer
Testing**. 28: 103-105

Harry S.K. 1987. **Handbook of Fillers for plastics,** Van Nostrand Reinhold, New
York.

Hoffman, W. 1965. **Vulcanization and Vulcanizing Agents.** J. Eur. Polym.
92:98-104.

Jame E. M. 1994. **The science and technology of rubber**. John Wiley & Sons,Inc.,
United State of America.

Kim, S.G., W.N. Wang, T. Iwaki, A. Yabuki and K. Okuyama.   2007. Low-
Temperature Crystallization of Barium Ferrite Nanoparticles by a Sodium
Citrate-Aided Synthetic Process. **Journal Phys. Chem.** 111:10175-10180.

Kingery, W.D., H.K. Bowen and D.R. Uhlmann. 1975. **Introduction to ceramic.** Wiley Interscience, Newyork.

Kurian, P., K.A. Malini. and M.R. Anantharaman. 2003. Loading dependence similarities on the Cure time and Mechanical Properties of Rubber Ferrite Composites containing Nickel Zinc Ferrite. **Journal of Material Latter.** 57:3381-3386

————, ————, M.A. Soloman, M.R. Anantharaman and P.A. Joy. 2003. Effect of Carbon Black on the Mechanical and Dielectric Properties of Rubber Ferrite Composites containing Barium Ferrite. **Journal of Applied Polymer Science.** 89:769-778.

Laobuthee, A., S. Wongkasemjit, E. Traversa and R.M. Laine. 2000. MgAl2O4 spinel powders from oxide one pot synthesis (OOPS) process from ceramic humidity sensors. **Journal of the European Ceramic Society**. 20:19-97

Lee, J.Y., S.H. Lee and S.W. Kim. 2000. Polymer-Particle Filler Systems. **Materials Chemistry and Physics**. 63(3):251-255.

Lokander, M and B. Stenberg. 2003. Performance of Isotropic Magnetorheological Rubber Materials. **Journal of Polymer Testing**. 22:245-251.

————, ————, and ————, ————. 2003. Improving the Magnetorheological Effect in Isotropic Magnetorheological Rubber Materials. **Journal of Polymer Testing**. 677-680.

Lopez-Manchado, M.A., J.L. Valentin, J. Carretero, F. Barroso and M. Arroyo. 2007. Rubber network in elastomer nanocomposites. **Journal of European Polymer**. 43:4143-4150.

Makled, M.H., T. Matsui, H. Mabuchi, M.K. El-Mansy and K. Morii. 2005. Magnetic and Dynamic Mechanical Properties of Barium Ferrite-Natural Rubber Composites. **Journal of Material Processing Technology.** 160:229-233.

Mali, A and A. Ataie. 2005. Structural characterization of nano-crystalline $BaFe_{12}O_{19}$ powders synthesized by sol–gel combustion route. **J. Scripta Materialia.** 53:1065-1070

Malini, K.A., E.M. Mohammed, S. Sindhu, P.A. Joy, K. Date, D. Kulkarni, P. Kurian, and M.R. Anantharaman. 2001. Magnetic and Processibility studied on Rubber Ferrite Composites based on Natural Rubber and mixed Ferrite. **Journal of Material Science.** 36:5551-5557.

Mattias, L., T. Reitberger and B. Stenberg. 2004. Oxidation of Natural Rubber-based Magnetorheological Elastomers. **Journal Polymer Degradation and Stability**. 86:476-471.

Mohammed, E.M., K.A. Malini, P. Kurian and M.R. Anantharaman. 2002. Modification of Dielectric and Mechanical Properties of Rubber Ferrite Composites containing Manganese Zinc Ferrite. **Material Research Bukketin**. 37: 753-768.

Morton, M. 1959. **Introduction to Rubber Technology**. Reinhold Publisher Corporation, New York.

Mozaffari, M., M.Taheri and J.Amighian. 2009. Preparation of barium hexaferrite nanopowders by the sol–gel method, using goethite**. Journal of Magnetism and Magnetic Materials.** 321:1285-1289.

Nontapan, S., K. Kalayanee, L. Sikong, T. Bhongsuwan. n.d. EMI Shielding
Materials Made from Natural Rubber Blended with Magnetic Ferrite Powder.
Department of Mining and Materials Engineering. Faculty of Engineering.
Prince of Songkhla University. Hat Yai. Songkhla. n.p.

Nowosielski, R., R. Babilas and J. Wrona. 2007. Microstructure and Magnetic
Properties of Commercial Barium Ferrite Powders. **Journal of Acheivement
in Material and Manufacturing Engineering**. 20: 307-310.

Ol'khovik, L.P., Z. I. Sizova, E. V. Shurinova, and A. S. Kamzin. 2005.
Determination of the Surface Anisotropy Contribution to the Magnetic
Anisotropy Field of a Nanocrystalline Barium Ferrite Powder at Various
Temperatures. **J. Physics of the Solid State.** 47:1261-1264.

Paul, K.M. 2007. Magnetic and structural properties of Ba M-type ferrite-composite
powders. **J. Physica B.** 388:337-343

Radwan, M., M.M. Rashad and M.M. Hessien. 2007. Synthesis and characterization
of barium hexaferrite nanoparticles**. Journal of Materials Processing
Technology.** 181:106-109

Roy, D., C. Shivakumara and P.S. Anil Kumar. n.d. Observation of the exchange
spring behavior in hard-soft-ferrite nanocomposite. **Journal of Magnetism and
Magnetic Materials.** n.p.

Saito, S. 1988. **Advance Ceramics.** Oxford University, OHMSHA Ltd. England.

Soloman, M.A., P. Kurian, M.A. Anantharaman and P.A. Joy. 2004. Evaluation of
the Magnetic and Mechanical Properties of Rubber Ferrite Composites
Containing Strontium Ferrite. **Journal of Polymer –Plastics Technology
and Engineering.** 43:1013-1028.

Sung, W.F. and C. Rudowicz. n.d. **A closer look at the hysteresis loop for ferromagnets.** Department of Physics and Material science, The university of Hong Kong, Hong Kong, China.

Topal, U. 2008. Factors influencing the remanent properties of hard magnetic barium ferrites: Impurity phases and grain sizes**. Journal of Magnetism and Magnetic Materials.** 320:331-335**.**

Urogiova, E., I. Hudec, D. Bellusova and P. Suri. 2007. Structure and properties of Rubber Blends with Ferromagnetic Fillers. **Polym. Adv. Technol**. 18: 128-134

Vinod, V.S., S. Varghese and B. Kuriakose. 2002. Degradation behavior of Natural Rubber-Aluminium powder Composites: Effect of Heat, Ozone and High Energy Radiation. **Journal of Polymer Degradation and Stability.** 75:405-412.

Xanthos, M. 2005. **Functional Fillers for Plastics.** Wiley-VCH Verlag GmbH&Co. KgaA, Waeinheim

Xiangyuan, L., J. Wang, L. Ming Gan and S. Choon Ng. 1999. Improving the magnetic properties of hydrothermally synthesized barium ferrite. **Journal of Magnetism and Magnetic Materials.** 195:452-459

Yang, Y., Y. Hu, L. Chen, X. Gong, W. Jiang, P. Zhang and Z. Chen. 2006. Effects of Rubber/Magnetic Particle interactions on the performance of Magnetorheological Elastomers. **Polymer Testing.** 25:262-267.

APPENDIX

Appendix Table 1 Report on Particle size of commercial Barium Ferrite

Particle size distribution of BaFe$_{12}$O$_{19}$

Particle size (μm)	Amount of residue (%)
> 150	19.27
75-150	12.67
45-74	2.33
< 45	65.73

Quantachrome Corporation
Quantachrome Autosorb Automated Gas Sorption System Report
Autosorb for Windows® Version 1.19   Page 2 of 5

Sample ID   BaFe12O19
Description   TISTR
Comments
Sample Weight   0.2691 g
Adsorbate   NITROGEN   Outgas Temp   300.0 °C   Operator   Rungrueng
Cross-Sec Area   16.2 Å²/molecule Outgas Time   3.0 hrs   Analysis Time   58.5 min
NonIdeality   6.580E-05   P/Po Toler   0   End of Run   01/03/1980 0!
Molecular Wt   28.0134 g/mol   Equil Time   3   File Name   AS7B1216.RAW
Station #   1   Bath Temp.   77.40

AREA-VOLUME-PORE SIZE SUMMARY

SURFACE AREA DATA

Multipoint BET... 2.920E+00 m²/g
Single Point BET... 2.928E+00 m²/g
Langmuir Surface Area.................................... 4.307E+00 m²/g
t-Method External Surface Area........................... 5.702E-01 m²/g
t-Method Micro Pore Surface Area......................... 2.350E+00 m²/g
DR Method Micro Pore Area................................ 4.471E+00 m²/g

PORE VOLUME DATA

t-Method Micro Pore Volume............................... 1.245E-03 cc/g
DR Method Micro Pore Volume.............................. 1.589E-03 cc/g
HK Method Cumulative Pore Volume......................... 1.503E-03 cc/g
SF Method Cumulative Pore Volume......................... 1.508E-03 cc/g

PORE SIZE DATA

DR Method Micro Pore Width   .... 6.260E+01 Å
DA Method Pore Diameter (Mode)......................... 1.480E+01 Å
HK Method Pore Width   (Mode)......................... 1.367E+01 Å
SF Method Pore Diameter (Mode)......................... 2.565E+01 Å

DATA REDUCTION PARAMETERS

Thermal Transpiration : ON
Effective Molecule Diameter (D) 3.5400 Å
Effective Cell Stem Inner Diameter (d) 4.0000 mm
Last Po Acquired 798.20 mm Hg
Additional Initialization Information Not Recorded

BJH/DH Moving Average Size 4

Interaction Constant (K) 2.9600 nm

TISTR
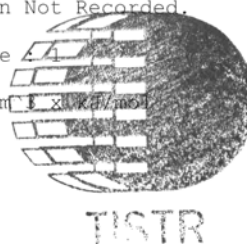
**Appendix Figure 1** Report on surface area of commercial Barium Ferrite

*** Multi Plot ***

```
File Name    : Service\BaF
Sample Name  : BaF                    Comment : 20/9/50
Date & Time  : 09-20-07 10:26:42
Condition
 X-ray Tube : Cu(1.54060 A)    Voltage : 40.0 kV    Current : 30.0 mA
 Scan Range : 2.0000 <-> 80.0000 deg    Step Size : 0.0200 deg
 Count Time : 0.60 sec    Slit  DS : 1.00 deg  SS : 1.00 deg  RS : 0.15 mm
```

[Group:Service. Data:BaF] BaF

O = Barium Iron Oxide (BaFe$_{12}$O$_{19}$)
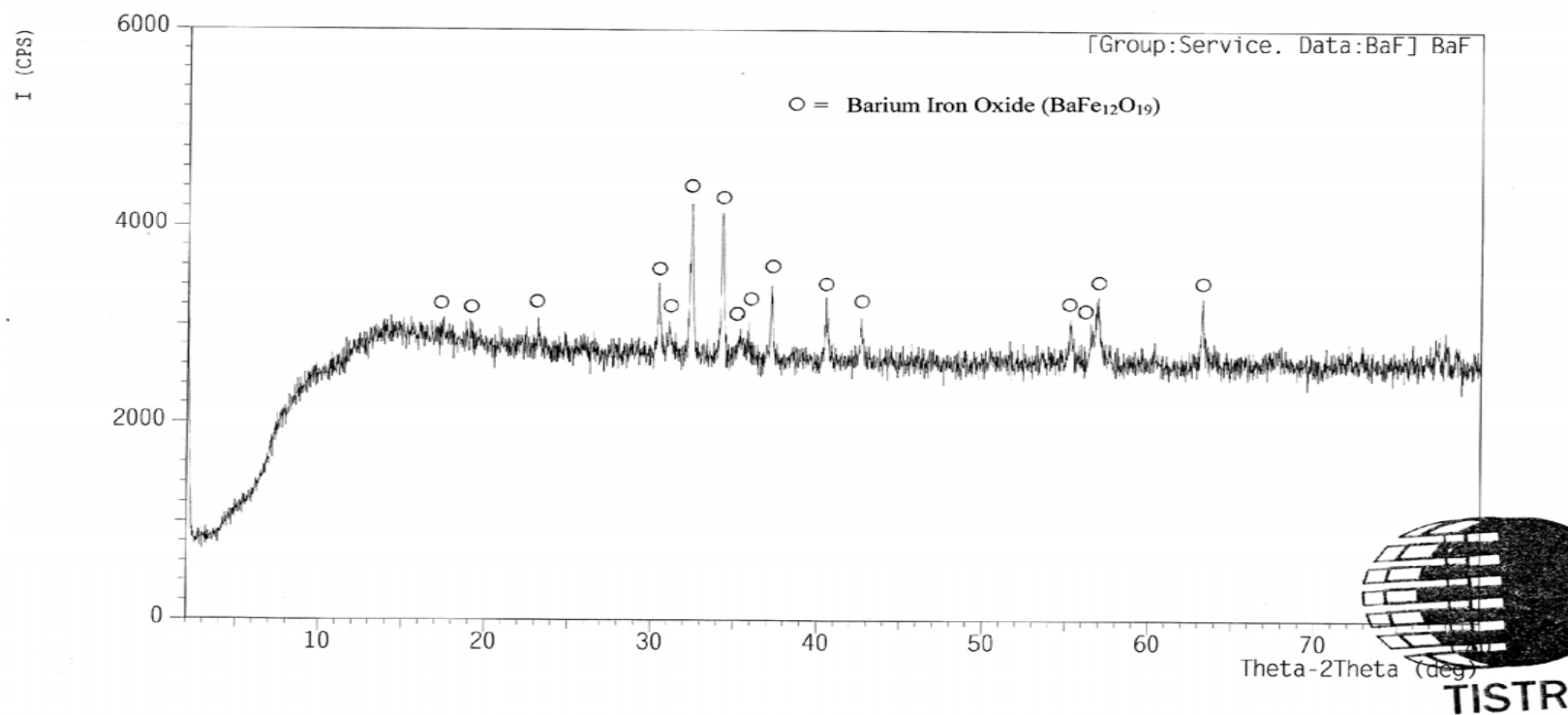
Appendix Figure 2 Report on XRD pattern of ceramic

CIRRICULUM VITAE

NAME	: Miss Lalita Kantiyong	
BIRTHDAY	: November 28, 1984	
BIRTHDAY PLACE	: Phichit, Thailand	

EDUCATION : **YEAR** **INSTITUTE** **DEGREE/DIPLOMA**

        2006   Nareasuan Univ.   B.Sc.(Chemistry)

SCHOLARSHIP : Thai Research Fund (TRF) 2006-2008

Kasetsart University Research and Development
Institute (KURDI) 2007-2009

Postgraduate Education and Research Program in
Physical Chemistry (ADB KU-Chem) 2008